

**Key Words:**

**Retention:  
#Permanent#**

**Key WTP R&T References:  
Test Specification:  
24590-PTF-TSP-RT-01-006 Rev. 0**

**Task Technical Plan  
WSRC-TR-2002-00083 Rev. 0  
SRT-RPP-2002-00036 Rev. 0**

**Test Scoping Statement:  
S89**

## **WASTE FEED EVAPORATION PHYSICAL PROPERTIES MODELING (U)**

**C. D. Barnes  
W. E. Daniel  
J. E. Laurinat**

**Issue Date: JULY, 2003**

Westinghouse Savannah River Company  
Savannah River Site  
Aiken, SC 29808

---

Prepared for the U.S. Department of Energy Under Contract Number DE-AC09-96SR18500



**This document was prepared in conjunction with work accomplished under Contract No. DE-AC09-96SR18500 with the U. S. Department of Energy.**

#### **DISCLAIMER**

**This report was prepared as an account of work sponsored by an agency of the United States Government. Neither the United States Government nor any agency thereof, nor any of their employees, makes any warranty, express or implied, or assumes any legal liability or responsibility for the accuracy, completeness, or usefulness of any information, apparatus, product or process disclosed, or represents that its use would not infringe privately owned rights. Reference herein to any specific commercial product, process or service by trade name, trademark, manufacturer, or otherwise does not necessarily constitute or imply its endorsement, recommendation, or favoring by the United States Government or any agency thereof. The views and opinions of authors expressed herein do not necessarily state or reflect those of the United States Government or any agency thereof.**

**This report has been reproduced directly from the best available copy.**

**Available for sale to the public, in paper, from: U.S. Department of Commerce, National Technical Information Service, 5285 Port Royal Road, Springfield, VA 22161,  
phone: (800) 553-6847,  
fax: (703) 605-6900  
email: [orders@ntis.fedworld.gov](mailto:orders@ntis.fedworld.gov)  
online ordering: <http://www.ntis.gov/help/index.asp>**

**Available electronically at <http://www.osti.gov/bridge>  
Available for a processing fee to U.S. Department of Energy and its contractors, in paper, from: U.S. Department of Energy, Office of Scientific and Technical Information, P.O. Box 62, Oak Ridge, TN 37831-0062,  
phone: (865)576-8401,  
fax: (865)576-5728  
email: [reports@adonis.osti.gov](mailto:reports@adonis.osti.gov)**

## TABLE OF CONTENTS

|  |           |
|--|-----------|
| <b>LIST OF FIGURES .....</b>   | <b>iv</b> |
| <b>LIST OF TABLES .....</b>  | <b>v</b>  |
| <b>LIST OF ACRONYMS .....</b>  | <b>v</b>  |
| <b>1.0 SUMMARY OF TESTING.....</b>   | <b>1</b>  |
| <b>1.1 Objectives .....</b>  | <b>1</b>  |
| <b>1.2 Conduct of Testing.....</b>   | <b>1</b>  |
| <b>1.3 Results and Performance Against Objectives .....</b>  | <b>3</b>  |
| <b>1.4 Quality Requirements .....</b>  | <b>5</b>  |
| <b>1.5 Issues .....</b>  | <b>5</b>  |
| <b>2.0 Discussion.....</b>   | <b>5</b>  |
| <b>2.1 Introduction and Background.....</b>  | <b>5</b>  |
| <b>2.2 Development of the OLI Database “ZEOLITE” .....</b>   | <b>6</b>  |
| <b>2.3 Description of Pre-Treatment Process.....</b>   | <b>8</b>  |
| <b>2.4 OLI/ESP Model Flowsheet and Chemistry Model .....</b>   | <b>10</b> |
| <b>2.5 Determination of the Factor Space for the Designs of Experiment .....</b>   | <b>13</b> |
| <b>2.6 Results.....</b>  | <b>16</b> |
| <b>2.6.1 Predictive Models with Model vs. Simulation Plots .....</b>   | <b>17</b> |
| <b>2.6.1.1 Sub-Envelope A-a Predictive Models.....</b>   | <b>17</b> |
| <b>2.6.1.2 Envelope B/D Predictive Models .....</b>  | <b>21</b> |
| <b>2.6.1.3 Envelope C Predictive Models .....</b>  | <b>24</b> |
| <b>2.6.2 Comparison of Simulation with Experimental Results .....</b>  | <b>28</b> |
| <b>2.6.3 Fate of Aluminum, Strontium, Sodium and NAS gel Through the Pre-Treatment Process for Three Waste Feed Compositions .....</b> | <b>33</b> |
| <b>3.0 Future Work.....</b>  | <b>39</b> |
| <b>4.0 REFERENCES.....</b>   | <b>40</b> |
| <b>APPENDIX A. Example Model Calculation .....</b>   | <b>42</b> |
| <b>APPENDIX B. Design Matrices for Envelopes A, B/D, and C .....</b>   | <b>45</b> |
| <b>APPENDIX C. Undissolved Solids Predicted by OLI/ESP for Envelopes A-a, B/D, and C.....</b>  | <b>54</b> |
| <b>APPENDIX D. OLI Prediction of Heat Capacity for Simple NaOH-H<sub>2</sub>O and NaNO<sub>3</sub>-H<sub>2</sub>O Systems.....</b>     | <b>63</b> |
| <b>APPENDIX E. Results of Trial Simulations for which the Number of Wash Stages was Varied.....</b>                                    | <b>64</b> |

## **LIST OF FIGURES**

|   |    |
|---|----|
| Figure 1. Simplified Model Flow Diagram for Envelopes A and B/D .....   | 2  |
| Figure 2. Simplified Model Flow Diagram for Envelope C .....  | 11 |
| Figure 3. Sub-envelope A-a Volume Reduction Factor.....   | 18 |
| Figure 4. Sub-envelope A-a Slurry Heat Capacity .....   | 19 |
| Figure 5. Sub-envelope A-a Supernate Viscosity .....  | 20 |
| Figure 6. Envelope A Evaporator Bottoms Slurry Density .....  | 21 |
| Figure 7. Envelope B/D Volume Reduction Factor.....   | 22 |
| Figure 8. Envelope B/D Slurry Heat Capacity.....  | 22 |
| Figure 9. Envelope B/D Supernate Viscosity .....  | 23 |
| Figure 10. Envelope B/D Evaporator Bottoms Slurry Density.....  | 24 |
| Figure 11. Envelope C Volume Reduction Factor.....  | 25 |
| Figure 12. Envelope C Slurry Heat Capacity.....   | 26 |
| Figure 13. Envelope C Supernate Viscosity .....   | 26 |
| Figure 14. Envelope C Evaporator Bottoms Slurry Density.....  | 27 |
| Figure 15. Evaporator Temperature at Bubble Point Pressure .....  | 28 |
| Figure 16. Fate of Aluminum Through Pre-Treatment Process for AN-104.....   | 33 |
| Figure 17. Fate of Aluminum Through Pre-Treatment Process for AZ-102 .....  | 34 |
| Figure 18. Fate of Aluminum Through Pre-Treatment Process for AN-107.....   | 34 |
| Figure 19. Fate of Strontium Through Pre-Treatment Process for AN-107 .....   | 35 |
| Figure 20. Fate of Sodium Through Pre-Treatment Process for AN-104.....   | 36 |
| Figure 21. Fate of Sodium Through Pre-Treatment Process for AZ-102 .....  | 36 |
| Figure 22. Fate of Sodium Through Pre-Treatment Process for AN-107 .....  | 37 |
| Figure 23. Fate of NAS gel Through Pre-Treatment Process for AN-104 .....   | 38 |
| Figure 24. Fate of NAS gel Through Pre-Treatment Process for AZ-102.....  | 38 |
| Figure 25. OLI/ESP Prediction of Cp Compared to Published Values for NaNO <sub>3</sub> -H <sub>2</sub> O System<br>at 20°C and Various Concentrations ..... | 63 |
| Figure 26. OLI/ESP Prediction of Cp Compared to Published Values for NaOH-H <sub>2</sub> O System<br>at 20°C and Various Concentrations .....               | 63 |
| Figure 27. UF1 Slurry .....   | 64 |
| Figure 28. UF Recycle .....   | 64 |
| Figure 29. UF2 Slurry .....   | 65 |
| Figure 30. Slurry to HLW .....  | 65 |
| Figure 31. Evaporator Overhead.....   | 65 |

## **LIST OF TABLES**

|   |    |
|---|----|
| Table 1. Distinctions in the Pre-Treatment Process for each Envelope .....                        | 9  |
| Table 2. Definition for Sub-envelope A-a Factor Space.....  | 15 |
| Table 3. Definition for Envelope B/D Factor Space.....  | 15 |
| Table 4. Definition for Envelope C Factor Space.....  | 16 |
| Table 5 Valid Variable Ranges for Sub-Envelope A-a Models.....                                    | 18 |
| Table 6 Valid Variable Ranges for Envelope B/D Models.....  | 21 |
| Table 7 Valid Variable Ranges for Envelope C Models.....  | 24 |
| Table 8. Comparison of Experimental with Simulation Supernate Compositions .....                  | 29 |
| Table 9. Comparison of Experimental with Simulation Na Molarity, Density and Viscosity            | 30 |
| Table 10. Comparison of Experimental with Simulation Heat Capacity and Thermal Conductivity ..... | 31 |
| Table 11. Comparison of Experimental with Simulation Dissolved and Undissolved Solids             | 31 |
| Table 12. Comparison of Experimental with Simulation Precipitated Solid Species.....              | 32 |
| Table 13. Experimental Slurry Composition .....   | 32 |
| Table 14. Sub-envelope A-a Computer Simulation Design Matrix.....                                 | 45 |
| Table 15. Envelope B/D Computer Simulation Design Matrix.....                                     | 48 |
| Table 16. Envelope C Computer Simulation Design Matrix.....                                       | 51 |
| Table 17. Sub-Envelope A-a Solids.....  | 54 |
| Table 18. Envelope B/D Solids.....  | 57 |
| Table 19. Envelope C Solids.....  | 60 |

## **LIST OF ACRONYMS**

|         |   |
|---------|---|
| FEP     | Hanford RPP-WTP Waste Feed Evaporator Process         |
| GCWB    | The Geochemist's Workbench                            |
| IX      | Ion Exchange  |
| HLW     | High Level Waste                                      |
| LAW     | Low Activity Waste                                    |
| NAS gel | Sodium Aluminosilicate gelatin                        |
| OLH     | Orthogonal Latin Hypercube                            |
| OLI/ESP | OLI Environmental Simulation Package Software         |
| TF-COUP | Tank Farm - Contractor Operation and Utilization Plan |
| SBS     | Submerged Bed Scrubber                                |
| Sr/TRU  | Strontium/Transuranic                                 |
| UF      | Ultra-Filtration                                      |
| VRF     | Volume Reduction Factor                               |
| XRD     | X-Ray Diffraction                                     |

## **1.0 SUMMARY OF TESTING**

### **1.1 OBJECTIVES**

This document describes the waste feed evaporator (FEP) modeling work done as requested in the Waste Feed Evaporation and Physical Properties Modeling<sup>[1]</sup> test specification and specified in the Task Technical and Quality Assurance Plan for Waste Feed Evaporation and Physical Property Modeling<sup>[2]</sup> (items C, E, F, G, and H) for the R&T Test Scoping Statement S-89 in support of the Hanford River Protection Project (RPP) Waste Treatment Plant (WTP) project. A private OLI database (ZEOLITE) was developed and used in this work in order to include the behavior of aluminosilicates such a NAS-gel in the OLI/ESP simulations, in addition to the development of the mathematical models.

Mathematical models were developed that describe certain physical properties in the Hanford RPP-WTP waste feed evaporator process (FEP) for envelopes A, B/D, and C. In particular, models were developed for the feed stream to the first ultra-filtration step characterizing it's heat capacity, thermal conductivity, and viscosity (items E, F, and G respectively of the task plan), as well as the density of the evaporator contents (item C of the task plan). The scope of the task was expanded to include the volume reduction factor across the waste feed evaporator (total evaporator feed volume / evaporator bottoms volume). All the physical properties were modeled as functions of the waste feed composition, temperature, and the HLW SBS recycle volumetric flow rate relative to that of the waste feed. The goal for the mathematical models was to predict the physical property to within ±15% of the predicted simulation value with a confidence of 80%.

The simulation model approximating the FEP process used to develop the correlations was relatively complex, and not possible to duplicate within the scope of the bench scale evaporation experiments. Therefore, simulants were made of 13 design points (a subset of the points used in the model fits) using the compositions of the ultra-filtration feed streams as predicted by the simulation model. The chemistry and physical properties of the supernate (the modeled stream) as predicted by the simulation were compared with the analytical results of experimental simulant work as a method of validating the simulation software (item H of the task plan).

Although the task plan calls for the derivation of additional physical property models (items A, B and D of the task plan), the nature of the pre-treatment process made it either unnecessary or irrelevant, and is discussed in section 2.1. Composition data for AY-102 did not exist following the transfer of C106 to AY-102, which was being characterized at the time of this report. Because this tank composition will be used in the upcoming integrated pilot test, a decision was made to include the AY-102 modeling work as part of the pilot test.

### **1.2 CONDUCT OF TESTING**

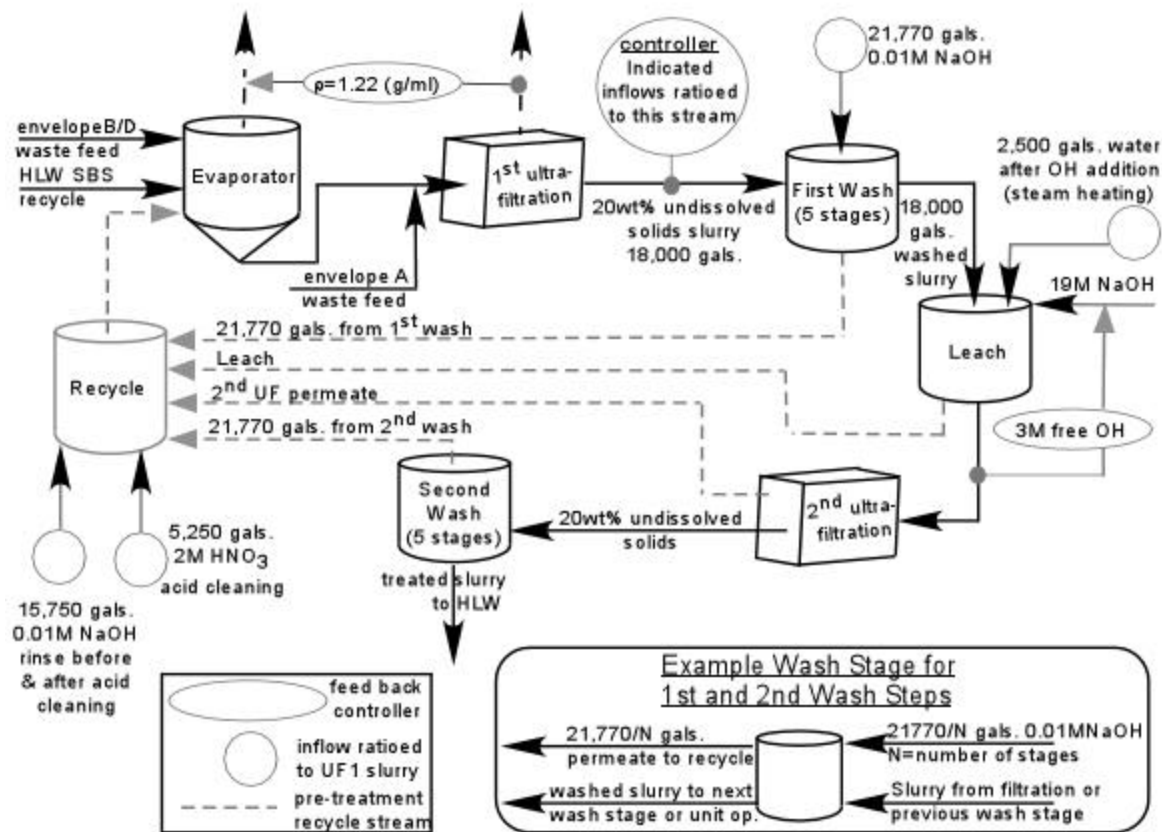
A different set of physical property models were developed for each of the three envelopes. The model variables are the waste feed composition, ultra-filtration feed stream temperature

(20 – 70°C), and the volumetric flow ratio of HLW SBS recycle relative to the waste feed (0 – 2). The matrices were generated assuming that the physical properties could be modeled using polynomials that are linear in composition, and up to second order with respect to the process variables (i.e. temperature, etc.). However, nonlinear (exponential) fits proved better for the viscosity.

Envelope A was divided into what we designate here as sub-envelope A-a (represented by tanks AP-101, AN-104, AN-105, SY-101, AN-103, AW-101, and AW-104) and sub-envelope A-b (represented by tank AY-102, the modeling for this envelope was originally part of this work, but was moved to the integrated pilot testing). Models were also developed for envelope B/D (represented by tanks AZ-101 and AZ-102) and envelope C (represented by tanks AN-102 and AN-107).

The model flow-sheet for the waste feed evaporator varies slightly depending on the envelope being simulated. The simulation flow-sheet for envelopes A and B/D is shown in Figure 1. The flow-sheet for envelope C excludes leach and second wash steps and includes the Sr/TRU precipitation steps.

**Figure 1. Simplified Model Flow Diagram for Envelopes A and B/D**



The waste feed evaporator process was simulated using the OLI Environmental Simulation Program (OLI/ESP) version 6.6 using the CARBONAT, HNO3DB, SILICA, and ZEOLITE private databases, along with the public database.

The model fits were done using JMP<sup>®</sup> version 5.0.1<sup>[3]</sup> using the linear platform (least squares linear regression) for the polynomials and the non-linear platform for the exponential forms of viscosity.

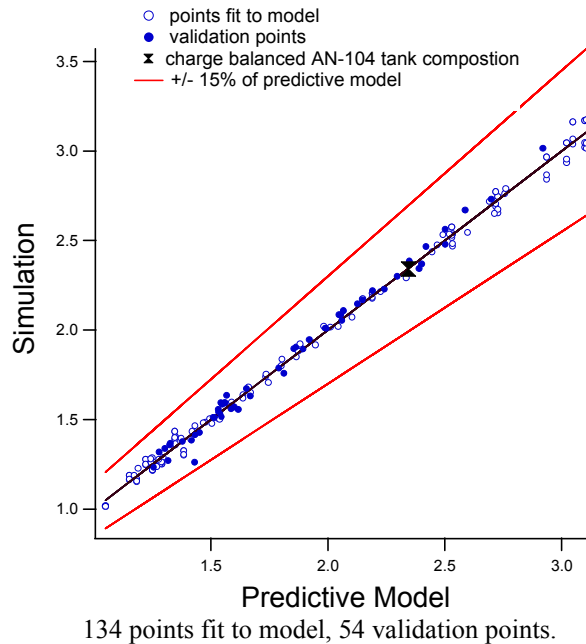
Validation of the models was done in two parts; the physical property model predictions were compared to those of the simulation software for design points not included in the model fit, and the chemistry and physical properties predicted by the simulation software was compared to experimental results for selected simulation design points.

### **1.3 RESULTS AND PERFORMANCE AGAINST OBJECTIVES**

The following figure is an example of the type of plot used to validate the physical property models against the simulation results, showing the viscosity as predicted by the model vs. the simulation viscosity. The plot shows three types of data: the open circles represent data points included in the model fit, the filled circles represent the validation data points (which were not included in the model fit), and the bow-tie represents a simulation based on a actual tank composition using an expanded OLI/ESP chemistry model to include all the minor/trace species (to verify these minor species have, at best, a minor effect on the physical properties being determined). The two red curves are at  $\pm 15\%$  of the model prediction as a measure of the model's success at predicting the simulation results. The complete set of results can be found in section 2.6.

As shown in the figure below all the validation points (filled circles) fall between the red curves, showing that the model meets the  $\pm 15\%$  with 80% confidence acceptance criteria. In addition, the simulation using the expanded model falls within the curves indicating the variables selected for the correlations are adequate. The model equation is shown immediately following the figure.

### Sub-envelope A-a Supernate Viscosity (cP)



$$\text{viscosity(cP)} = 0.0544[\text{NO}_2] + 0.0608[\text{NO}_3] - 0.149[\text{OH}]$$

$$+ \exp \left( \frac{219}{77.4 + [\text{Temp}]} - 0.947 - 0.0678[[\text{NO}_2] - 0.134[\text{NO}_3]] + 0.0611[\text{OH}] - 0.0826[\text{NO}_3][\text{NO}_2] \right)$$

All the physical property models meet the acceptance criteria of  $\pm 15\%$  with a confidence of 80%, therefore the physical property models meet the objectives as stated in the task plan, with the exception of the envelope A volume reduction factor, where 68% of the validation points are within  $\pm 15\%$ .

The physical properties of the ultra-filtration feed stream supernate showed, in general, good agreement between simulation predictions and analytical results. Three simulants overshot the target sodium molarity (defined as the composition predicted by OLI/ESP) somewhat (by more than 7%) and comparisons with simulation results were consistent with the “higher than target” sodium content of the simulant. The remaining points were generally within 5% of the target sodium molarity. For these points, the difference between the simulation and experimental physical property results were less than 2% for density, 9% for viscosity, and 16% for heat capacity (although the simulation heat capacities were based on the slurry with the experimental was based on the supernate). Both simulation and experimental data predicted a thermal conductivity equal to that of water within the error of experimental measurements and the error of the trial model fits of the simulation data.

The compositions of the ultra-filtration supernate were also in relatively good agreement. The values given below include the three high sodium points mentioned above. The Ca and Fe concentrations were on the order of  $1xE^{-5}$  M and  $1xE^{-4}$  M respectively for both the simulation and experimental results. S, P and Si were on the order of 0.05, 0.02, and 0.07M respectively for both the experimental and simulation results, with average differences of 8, 34 and 34% respectively. From a chemical point of view, these differences are minor at these small concentrations. Al was on the order of 0.4M for both simulation and experimental results, with an average difference of 16%. This concentration is high enough to suggest that OLI/ESP is under predicting the solubility of Al (by 16%), resulting in a conservative estimate for the formation of NASGel.

## **1.4 QUALITY REQUIREMENTS**

This work was conducted under the applicable requirements of NQA-1, 1989 and NQA-2a 1990, Part 2.7 as described in the technical task plan.

The quality requirements pertaining to OLI/ESP simulation software have been addressed in the document “Software Quality Assurance Plan for Hanford RPP-WTP Evaporator Modeling”<sup>[5]</sup>. OLI/ESP version 6.6 was used with the private databases CARBONAT, HNO3DB, SILICA, and ZEOLITE. JMP version 5.0.1 was used to fit the simulation physical property data to the mathematical forms.

## **1.5 ISSUES**

None.

# **2.0 DISCUSSION**

## **2.1 INTRODUCTION AND BACKGROUND**

This document describes the waste feed evaporator (FEP) modeling work done as requested in the Waste Feed Evaporation and Physical Properties Modeling<sup>[1]</sup> test specification and specified in the Task Technical and Quality Assurance Plan for Waste Feed Evaporation and Physical Property Modeling<sup>[2]</sup> (items C, E, F, G, and H) for the R&T Test Scoping Statement S-89 in support of the Hanford River Protection Project (RPP) Waste Treatment Plant (WTP) project.

Waste currently stored in underground tanks at Hanford is to be pre-treated in preparation for vitrification and permanent storage. Pre-treatment, the first step in separating the HLW from the LAW waste, includes evaporation to reduce the volume sent to the HLW and LAW melters, ultra-filtration to concentrate the slurry sent to HLW, caustic wash steps to reduce the sodium content of the slurry solids, and can include a caustic leach step to reduce the aluminum content of the HLW slurry solids. The wash, leach, and second ultra-filtration steps generate recycle streams which will be returned to the Waste Feed Evaporator along

with recycle streams from other WTP processes, the most significant of these being the HLW SBS recycle stream. The permeate from the first ultra-filtration step will be sent to the LAW process for treatment by the cesium ion-exchange column and eventual vitrification. The treated/concentrated slurry will be sent to HLW for the addition of glass formers in preparation for vitrification.

Savannah River Technology Center personnel have been asked to develop mathematical models for the viscosity, Cp, and thermal conductivity of the feed stream to the first ultra-filtration step as a function of waste feed composition, HLW SBS recycle flow rate, and the ultra-filtration feed stream temperature. The scope of the project was expanded to include modeling of the volume reduction factor across the waste feed evaporator (total evaporator feed volume / evaporator bottoms volume) as a function of the same variables.

Although the task plan calls for the derivation of additional physical property models (items A, B and D of the task plan), the nature of the pre-treatment process made it either unnecessary or irrelevant. These properties include sodium molarity (as a function of density) and bulk solubility of the ultra-filtration feed stream. Because the evaporation was controlled to achieve a filtrate density of 1.22 (g/ml), the density was constant. Also, modeling of the solubility point was unnecessary because the flow-sheet calls for the filtration step to concentrate the stream to 20wt% insoluble/precipitated solids, which presumes solids are already present. Thermal conductivity values were calculated for all the design points and none deviated significantly from that of water (within the error of the trial model fit), therefore, thermal conductivity was not modeled.

Also, models were not developed for a sub-set of envelope A consisting of tank AY-102. This tank was being characterized at the time of this report, and no other data was available since C106 was combined with AY-102. Because this tank composition will be used in the upcoming integrated pilot test, a decision was made to include the AY-102 modeling work as part of the pilot test.

In addition to the flowsheet models just described, this task required a new solubility database for aluminosilicates. Recent operation of the Savannah River Site waste evaporators demonstrated that aluminosilicate minerals can precipitate from caustic waste solutions if aluminum and silicon concentrations are sufficiently high. To model deposition of aluminosilicates in the RPP evaporators, SRTC/ITP contracted OLI Systems, Inc., to create a database to calculate the solubilities of zeolites and related aluminosilicate species in caustic solutions. A version of this database, called ZEOLITE, was used in conjunction with other OLI public and private databases to perform the modeling calculations for this study.

## **2.2 DEVELOPMENT OF THE OLI DATABASE “ZEOLITE”**

The ZEOLITE database contains solubility models for four aluminosilicate species, three of which are crystalline solids and one which is an amorphous gel. The amorphous gel, called sodium aluminosilicate gel or NAS gel, forms as a precursor to the crystallization and

precipitation of zeolite A. The aluminosilicate solid transforms into the three crystalline phases, zeolite A, hydroxysodalite, and cancrinite, in the stated order as it ages.

In the ZEOLITE database, the solubility models for NAS gel and zeolite A are based on data from Ejaz, Jones, and Graham<sup>[6]</sup>. Ejaz et al. measured solubilities for the dissolution of NAS gel and zeolite A in 3.0 to 4.4 molar NaOH solutions. Temperatures for these measurements ranged from 30°C to 80°C. Solubility models for hydroxysodalite and cancrinite are based on data from Barnes, Addai-Mensah, and Gerson<sup>[7]</sup>. Barnes et al. precipitated hydroxysodalite and cancrinite by seeding crystals in supersaturated solutions containing approximately 4.3 molal NaOH, 0.4 molal Na<sub>2</sub>CO<sub>3</sub>, and 1.8 molal Al(OH)<sub>3</sub>. Temperatures for the Barnes et al. measurements varied from 90°C to 220°C. OLI assigned the stoichiometries given by these date sources to all four modeled species.

OLI developed its solubility models using activity coefficient parameters and standard state Gibbs free energies and entropies to fit these two sets of solubility data. The model for cancrinite solubility is based on simultaneous regression of activity coefficient parameters and standard state properties. Subsequent regression of standard state free energies and entropies with the activity coefficient parameters derived for cancrinite then gave the solubility models for hydroxysodalite, zeolite A, and NAS gel. OLI selected cancrinite as the basis for its correlation of activity coefficients because cancrinite solubility data covered a wider temperature range than the data for the other phases. A regression package embedded in the OLI calculation engine performed the model calculations. OLI included models for the solubilities of both hydrated and anhydrous forms, but recommends that only the hydrated forms be used in solubility calculations.

To improve the solubility models, OLI added an ionic species and several ion-ion interactions to the default set contained in the PUBLIC database and modified properties for other species. The added species is AlSiO<sub>3</sub>(OH)<sub>4</sub><sup>3-</sup>. Properties for this species were derived by fitting the solubility data. Spectroscopic evidence presented by Kinrade and Swaddle<sup>[8]</sup>, Swaddle et al.<sup>[9]</sup>, and Gout et al.<sup>[10]</sup> attest to the existence of this ion and hence support its addition to the database.

Helgeson-Kirkham-Flowers (HKF) parameters<sup>[11]</sup> were altered for several species, namely, Al(OH)<sub>3</sub>, Al(OH)<sub>4</sub><sup>-</sup>, NaAl(OH)<sub>4</sub>, and H<sub>4</sub>SiO<sub>4</sub>. Diakanov et al.<sup>[12]</sup> provided HKF parameters for the first three of these species, and Stefansson<sup>[13]</sup> gave values for these parameters for H<sub>4</sub>SiO<sub>4</sub>.

OLI added three pairs of ion-ion interactions to the ZEOLITE database: Al(OH)<sub>4</sub><sup>-</sup>/AlSiO<sub>3</sub>(OH)<sub>4</sub><sup>3-</sup>, AlSiO<sub>3</sub>(OH)<sub>4</sub><sup>3-</sup>/Na<sup>+</sup>, and NaCO<sub>3</sub><sup>-</sup>/OH<sup>-</sup>. These interactions are modeled using Bromley activity coefficient parameters<sup>[14]</sup>.

Before the OLI database was used, it was verified by comparing measured and calculated solubilities<sup>[15]</sup>. Solubilities were compared for the data used to generate the OLI model and for two independent sets of data. Not surprisingly, calculated solubilities agreed closely with most of the Ejaz et al. and Barnes et al. data. The only exceptions were the Ejaz et al. data for NAS gel at 80°C and zeolite A at 30°C, and the Barnes et al. data at 220°C. Calculated

NAS gel solubilities exceeded measured values at 80°C; Ejaz et al. attribute this apparent discrepancy to rapid crystallization of the NAS gel to the much less soluble zeolite A at this temperature. At 30°C, the calculated solubilities for zeolite A were greater than measured values; apparently, at this temperature, crystallization was too slow to achieve equilibrium saturation during the measurement interval. Calculated solubilities also exceeded measured values for the Barnes et al. data at 220°C.

In addition to these comparisons, the OLI model was benchmarked against independent data from Breuer et al. and Park and Englezos<sup>[16]</sup>. Breuer et al. measured solubilities of zeolite A and hydroxysodalite for simulants of solutions used to process aluminum from ore. For zeolite A, calculated solubilities were an order of magnitude lower than measured solubilities. For hydroxysodalite, agreement between calculated and measured solubilities was close within the range of concentrations for which OLI fit its model, but calculated solubilities were significantly higher as the caustic concentrations dropped. Park and Englezos<sup>[17]</sup> measured hydroxysodalite solubilities for surrogates of paper pulp liquors. Calculated solubilities significantly exceeded measured values for the Park and Englezos data. This last comparison probably should be given less consideration than the other comparisons, because Park and Englezos did not seed their solutions and in several cases failed to obtain a precipitate with the correct stoichiometric aluminum-to-silicon ratio.

The results of an OLI/ESP simulation using the ZEOLITE database were compared with those from Geochemist's Workbench (GCWB). The GCWB database did not have some of the species used in the OLI simulation ( $\text{NO}_2$  was treated as  $\text{NO}_3$ , and oxalate as  $\text{CO}_2$  and  $\text{CO}_3$ ), otherwise the systems were identical. OLI predicted the precipitation of 98 moles of gibbsite and 0.12 moles of NAS gel, where GCWB predicted 184 moles gibbsite and 0.54 moles of NAS gel. While not exact, the values are of the same order of magnitude. Only gibbsite and NAS gel were allowed to precipitate in both simulations (zeolite A, cancrinite, etc. were not allowed to precipitate).

## **2.3 DESCRIPTION OF PRE-TREATMENT PROCESS**

Much of the description below is based on information from the document “WTP Material Balance and Process Flowsheet Bases, Requirements, and Results”<sup>[18]</sup>. Table 1 outlines the differences the in pre-treatment process for each envelope.

**Table 1. Distinctions in the Pre-Treatment Process for each Envelope**

| Envelope  | A-a   | B/D   | C  |
|---|---|---|--|
| Insoluble/precipitated solids concentration in the 1 <sup>st</sup> ultra-filtration feed stream | 20wt%   | 20wt%   | 15wt%  |
| Point of introduction of waste feed stream to process   | Fed to 1 <sup>st</sup> ultra-filtration step (after evaporator) | Fed directly to evaporator with recycle streams | Fed to SR/TRU precipitation, which in turn feeds the 1 <sup>st</sup> ultra-filtration step |
| 1 <sup>st</sup> wash  | Yes   | Yes   | Yes  |
| Leach   | Yes   | Yes   | No   |
| 2 <sup>nd</sup> wash  | Yes   | Yes   | No   |
| Sr/TRU precipitation  | No  | No  | Yes  |

The tank wastes are categorized into three envelopes, A, B, C and D, based on their general composition and the various processes from which the wastes were generated. A, B, and C represent supernates, and D represents the solids of envelope B. Envelope B/D wastes contain higher levels of halides and sulfur, reducing the amount of waste loading possible in the glass, and envelope C wastes contain relatively larger amounts of complexants and Sr/TRU. Because of these variations in composition, the pre-treatment process differs somewhat for each envelope. The process for envelopes A and B/D are described first, then the process for envelope C.

The pre-treatment of envelopes A and B/D are identical except for the point of introduction of the waste feed stream to the pre-treatment process. Envelope A waste will be fed to the pre-treatment process at a sodium concentration greater than 5M. Because the permeate from the first ultra-filtration step has a target density of 1.22 (g/ml) to prevent floatation of the cesium IX resin, and since experience has shown that waste at a concentration of 5M Na has a density in this neighborhood, there is no need to concentrate envelope A waste. In fact, it must be diluted with the evaporator bottoms (HLW SBS and pre-treatment recycles concentrated to less than 5M Na) to achieve the target permeate density. Therefore envelope A tank waste will not be feed to the evaporator, but blended with the evaporator bottoms in the ultra-filtration holding tank following the evaporator. Envelope B/D tank wastes will be sent to the process at less than 5M Na, and therefore combined with the recycle streams prior to evaporation and then concentrated to a supernate density of 1.22 (g/ml).

The contents of the ultra-filtration holding tank will be cycled through the filter until the slurry is concentrated to 20wt% undissolved solids, with the resulting permeate being fed to the LAW for processing by the cesium IX column. The slurry will then be washed with 0.01M NaOH to reduce the sodium content. This is to be done in 22 batches, where one batch consists of adding a volume of 0.01M NaOH, mixing the tank, then filtering an equal volume of supernate to be forwarded to a pre-treatment recycle holding tank and eventually fed to the waste feed evaporator. 21,770 gallons of 0.01M NaOH will be used for every 18,000 gallons of slurry to be washed (~1000 gallons of caustic for each wash batch), generating 21,770 gallons of decanted supernate.

Following the first caustic wash, the envelope A and B/D slurry solids are leached of aluminum by adding sufficient 19M NaOH to achieve a concentration of 3M free OH, followed by heating of the slurry to 50°C with a steam lance. The leached slurry will then be cycled through the second ultra-filtration step to a concentration of 20wt% undissolved solids and the permeate sent to a recycle holding tank and eventually fed to the waste feed evaporator. Finally, the slurry will be washed a second time in a manner identical to the first wash step, with a volume (equal to the wash addition) of filtered supernate being sent to the waste feed evaporator recycle holding tank (as feed to the waste feed evaporator), and the treated slurry sent to HLW in preparation for vitrification.

By definition, envelope C contains higher levels of Sr/TRU than the other envelopes. The tank waste for this envelope will be fed to the Sr/TRU precipitation step where 0.1M SrNO<sub>3</sub> and 0.1M NaMnO<sub>4</sub> solutions are added to achieve a slurry concentration of 0.01M Sr and 0.075M MnO<sub>4</sub>. In addition, 19M NaOH will be added to achieve a concentration of 1M free OH to enhance the precipitation. The resulting slurry will then be fed to the ultra-filtration holding tank where it will be combined with the evaporator bottoms and then concentrated to 15wt% undissolved solids by ultra-filtration and the permeate sent to LAW for processing by the cesium IX columns. Unlike envelopes A and B/D, the concentrated slurry is processed through the first wash step only, and will not go through the leach, 2<sup>nd</sup> filtration, nor the 2<sup>nd</sup> caustic wash steps. The first wash step is identical to that for envelopes A and B/D. The slurry from the single wash step will be sent to HLW for eventual vitrification.

For every 18,000 gallons of concentrated slurry produced by the first ultra-filtration step, the filters will be cleaned with 5,250 gallons of 2M HNO<sub>3</sub> (acid cleaning) and 15,750 gallons of 0.01M NaOH (caustic rinse). This is based on two acid cleaning cycles and pre/post acid cleaning caustic washes (verbal communication from Ivan Papp, Aug. 2002 quarterly meeting). These resulting streams are then sent to a waste feed evaporator recycle holding tank and eventually fed to the waste feed evaporator.

19M NaOH is added to the recycle generated from the pre-treatment process (by the wash, leach, and acid cleaning steps) to adjust the pH to 13 prior to being fed to the waste feed evaporator.

Additional recycle streams are sent to pre-treatment from other processes. The most significant of these is the HLW SBS recycle which has been included in the simulation model. Other recycle streams are either extremely dilute or relatively small, and were not included in the simulation flow-sheet described in the following.

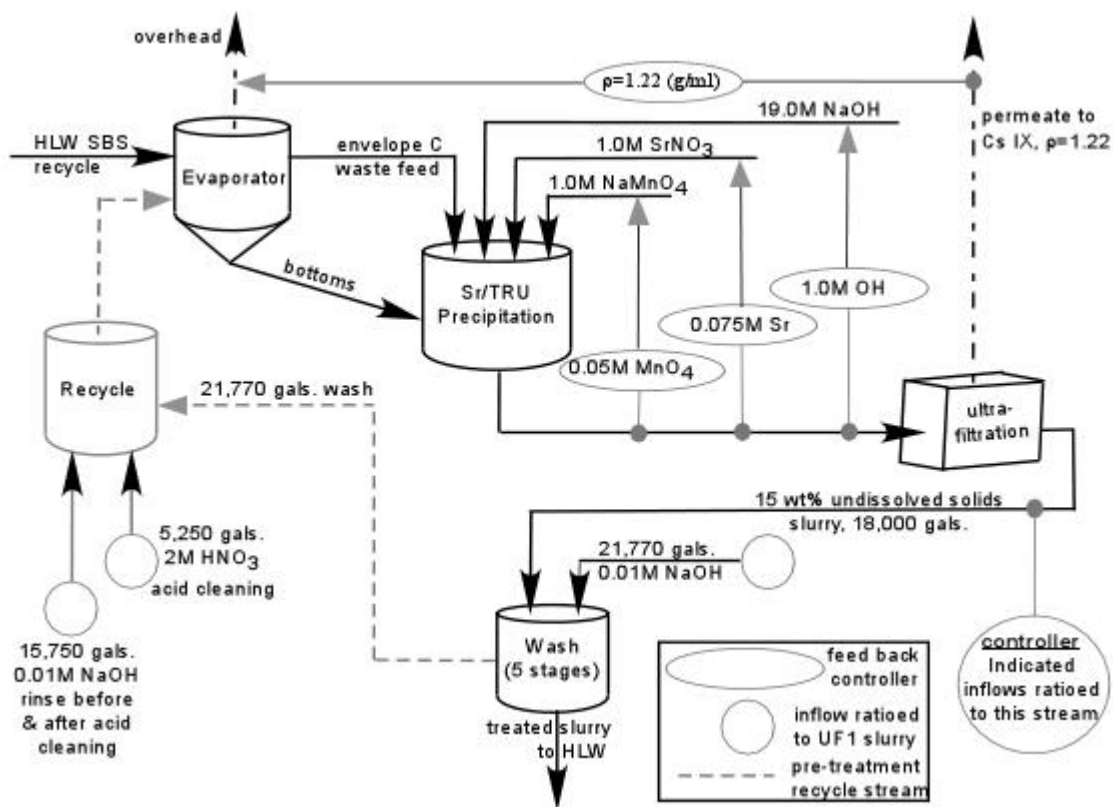
## **2.4 OLI/ESP MODEL FLOWSHEET AND CHEMISTRY MODEL**

The RPP pre-treatment process was simulated using the OLI Environmental Simulation Program (OLI/ESP) version 6.6 using the CARBONAT, HNO3DB, SILICA, and ZEOLITE private databases, along with the public database. The simulation was set up as a steady-state process, and included iterations on the recycle streams generated by the pre-treatment process from the wash, leach, and acid cleaning steps until the entire flow-sheet converged.

The evaporator was modeled as a flash calculation [19] (as opposed to a dynamic simulation) since the overhead is essentially water and its composition does not vary with bottoms composition. The evaporation rate was controlled such that the density of the 1<sup>st</sup> ultra-filtration permeate (sent to LAW) was 1.22(g/ml) at the design point temperature. The evaporator was operated at 50°C at the bubble point pressure, and the 1<sup>st</sup> filter was operated at 1 atm. and the design point temperature. All other unit operations and streams were set to 1 atm. and 25°C.

The actual pre-treatment process described in Section 2.3 is approximated in the OLI/ESP simulation flowsheet by using a series of unit operations to represent each of the steps as shown in Figure 1 and Figure 2.

**Figure 2. Simplified Model Flow Diagram for Envelope C**



To reduce the simulation execution time, the number of stages simulated for each of the two wash steps was reduced from 22 to 5. The actual process will use about 22,000 gallons of 0.01M NaOH for every 18,000 gallons of concentrated slurry (or about 1000 gallons per wash stage). For the purpose of the simulation, the 22,000 gallons of wash was divided by the number of stages simulated in order to keep the volume of wash used per 18000 gallons of concentrated slurry constant, e.g. for five stages, 4,400 gallons of 0.01M NaOH were used in each wash stage. Trial simulations in which the number of stages was varied showed 5 stages to give the best combination of reduced execution time with a minimum of error due

to approximating the 22 wash stages of the actual process with fewer stages in the simulation, with less than a 5% difference in a number of measurements (such as Na molarity, flow rates, etc.) as compared to the full 22 stage model (see Appendix E).

The waste feed flow rates used in the simulations were based on a LAW glass production rate of 30 metric tons per day at a Na<sub>2</sub>O loading of 19.5, 7.5, and 17.0wt% for envelope A, B/D, and C respectively (from Table A-15 of the TF COUP document<sup>[20]</sup>), where only the sodium content of the waste stream was used to calculate the Na<sub>2</sub>O loading. This was not necessary for the model (any flow rate could have been used), but was a choice of convenience.

The HLW SBS flow rate is not tied directly to the pre-treatment process, and therefore treated as an independent variable for the physical property models developed here. It is expressed in terms of its volumetric flow relative to that of the waste feed stream, having a range of 0 – 2 (i.e. up to twice the volumetric flow rate of the waste feed stream). The composition was fixed for all simulations, and based on the analytical results from the VSL melter pilot testing.

The remaining inflows are set to the rates/flow ratios as described in Section 2.3, that is, 19M NaOH is added at the leach step to achieve 3M OH, and for every 18,000 gallons of concentrated slurry from the first filter, 1) 2,500 gallons of water is added to represent the steam heating during the leach step, 2) 21,770 gallons of caustic wash for each of the 1<sup>st</sup> and 2<sup>nd</sup> wash steps, and 3), 15,750 gallons of caustic wash and 5,250 gallons of acid for cleaning of the filters.

For all the design points simulated, the recycle stream generated from the pre-treatment process had a pH of 13 or greater, so no pH adjustment was done.

Because OLI/ESP does not yet have the capability to calculate the heat capacity of a stream directly, this was done for the ultra-filtration feed stream using the OLI Scratch Pad tool in OLI/Express to generate an enthalpy vs. temperature plot at the calculated steady-state composition. This was done from 15 – 75°C in one degree increments.

The chemistry models used for all simulations include the species given in Table 2, Table 3, and Table 4 of the next section. Additional simulations (beyond those of the design points) were done based on actual tank compositions which used an expanded chemistry model to include the very minor species. (In both cases a patch was required from OLI to increase the number of allowed anion-cation interactions due to the large chemistry models).

Because NAS gel is a necessary precursor to crystalline aluminosilicates (zeolite A, hydroxysodalite, and cancrinite), only the precipitation of NAS gel was modeled. The residence time of the evaporator bottoms is short relative to the kinetics of crystalline aluminosilicate formation; it is not anticipated that these will form to a significant degree in the evaporator. However, when NAS gel is predicted, the crystalline forms will eventually form, possibly in holding tanks and downstream processes if conditions are not significantly different.

## **2.5 DETERMINATION OF THE FACTOR SPACE FOR THE DESIGNS OF EXPERIMENT**

The simulation design matrix was derived from the model factor space, which in turn is defined by model variables and their ranges. The design matrices are given in Appendix C and described briefly below. Their derivation is more fully described in other documents<sup>[21-23]</sup>.

The design matrices consist of two types of design points. One type is used exclusively in the model fits, and consist only of the extreme (minimum and maximum) values of the variable ranges (this assumes a linear response). The second type is generated using the Orthogonal Latin Hypercube (OLH) technique<sup>[24]</sup>, which produces points uniformly distributed over the linear factor space. These points are used to either improve the model fit if the response is found to be non-linear, or (when not included in the model fit) to validate the property model prediction against the simulation results. The model variables and corresponding factor spaces and constraints from which these matrices were derived are described in the following.

The physical property models are given in terms of two types of variables, 1) mixture variables which define the composition of the waste feed stream, and 2) process variables which define the “state” of the stream, these being the temperature, SBS/Feed ratio, and a waste feed dilution factor (expressed in terms of Na molarity as described below). The dilution of the waste feed stream was included as a variable since the volume reduction factor (VRF) is a strong function of this, and the tank waste may be diluted prior to being sent to the pre-treatment process.

For all envelopes, the temperature range was given to be 20-70°C and the range for the HLW SBS volumetric flow rate was chosen to be 0-2 times that of the waste feed stream. The ranges for the waste feed stream sodium molarity (the “dilution factor”) were based on the tank waste analysis and the sodium molarities of the diluted waste feed sent to pre-treatment as specified in the “WTP Mass Balance and Process flow-sheet”<sup>[18]</sup>.

Given the broad range in composition, attempting to capture the behavior of all three envelopes in a single model would likely result in models with unacceptably large error. Therefore, a separate set of physical property models was developed for each of the three envelopes. The significant species and corresponding concentration ranges for each of the envelopes were determined using various sources of tank characterization data.

Envelope A was divided into what we designate here as sub-envelope A-a (represented by tanks AP-101, AP-104, AN-104, AN-105, SY-101, AN-103, AW-101, and AW-104) and sub-envelope A-b (represented by tank AY-102), the composition of AY-102 being distinct (much older waste) from the other A tanks. The factor space of envelope B/D is represented by the compositions of tanks AZ-101 and AZ-102, and envelope C by tanks AN-102 and AN-107.

In order to derive the composition (mixture variable) ranges for each envelope, it was necessary to “normalize” the concentrations by some common value. This is because the models predict properties of the filtration feed stream based, in large part, on the composition of the waste feed stream, and the feed is either directly or indirectly (via pre-treatment recycle) concentrated through the evaporator. The models should predict very similar physical property value for waste feeds of identical compositions but different dilutions, since in each case enough water will be evaporated to achieve a permeate density of 1.22 (g/ml), resulting in identical permeates. (The prediction would be identical except for the difference in the SBS flow rate relative to the amount of waste feed solids at different waste feed dilutions). Therefore, the models should not be a function of the amount of water present in the feed. Normalizing the concentrations removes this water dependence from the models. This was born out in the model fits in that only the VRF models included the “dilution factor” variable (described below) since it is of course a strong function of the dilution of the waste feed stream. For all other models, this “dilution factor” was determined to be a statistically insignificant by the JMP software, and not included as a variable.

Normalization of the mixture variable concentrations was done using two different approaches (either approach would have been satisfactory for all envelopes, but this was not apparent to the author at the time the factor spaces were being developed). The analytical tank compositions (expressed in molarities) for envelopes A and C were adjusted to an otherwise identical stream at 5M Na. That is, all molar concentrations were multiplied by the ratio of 5 divided by the analytical sodium molarity value. The choice of normalizing to a value of 5M Na stream was somewhat arbitrary; it is roughly the mid-point of the streams fed to the pre-treatment process and corresponds to the target permeate density. These “normalized” mixture values defined the factor space used to generate the design matrix. For envelope B/D models, a mixture variable is expressed in terms of its mass fraction relative the total mass of the model’s mixture variables

(e.g.  $[AlO_2] = \frac{mass_{AlO_2}}{mass_{AlO_2} + mass_{CO_3} + mass_{Fe} + mass_{NO_3} + mass_{OH} + mass_{SO_4}}$  ), and these values defined the factor space used to generate the design matrix. Given these forms of expression, the species to be included as mixture variables were determined.

The significant species of sub-envelope A-a, their corresponding concentration ranges, and constraints had already been determined based on the tank waste compositions as given in the TF-COUP<sup>[20]</sup> document as part of the experimental simulant work<sup>[25, 26]</sup>. With minor modifications (fixing SO<sub>4</sub> and oxalate concentration to the maximum value of the range, 0.0554M and 0.02M respectively), the same factor space was used for this modeling work and is given in Table 2. The constraints were defined such that  $[AlO_2]/[OH] \leq 0.7$ ,  $[PO_4] + 0.07[F] \leq 0.05$ , and the sum of the molar charge of the mixture variables must be equal 4.73648. The concentrations are in terms of a 5M Na solution (i.e. a concentration of 0.1M OH in a 7M Na solution is adjusted to  $0.1 \times 5/7 = 0.0714$  M OH).

**Table 2. Definition for Sub-envelope A-a Factor Space**

| Variable                   | Mixture Variable Molar Ranges<br>Normalized to equivalent molarity at 5M Na |   |                            |   |   |                             |   | Process Variables |                            |              |
|----------------------------|---|---|----------------------------|---|---|-----------------------------|---|-------------------|----------------------------|--------------|
|                            | [AlO <sub>2</sub> ]<br>(molar at<br>5M Na)                                  | [CO <sub>3</sub> ]<br>(molar at<br>5M Na)         | [F]<br>(molar at<br>5M Na) | [NO <sub>2</sub> ]<br>(molar at<br>5M Na) | [NO <sub>3</sub> ]<br>(molar at<br>5M Na) | [OH]<br>(molar at<br>5M Na) | [PO <sub>4</sub> ]<br>(molar at<br>5M Na)   | [Na]<br>(molar)   | SBS / Feed<br>(volumetric) | Temp<br>(°C) |
| minimum                    | 0.207   | 0.326   | 0.00927                    | 0.731                                     | 0.991                                     | 0.983                       | 0.00632   | 5.6               | 0.0                        | 20           |
| maximum                    | 1.12  | 0.686   | 0.236                      | 1.59                                      | 2.08                                      | 2.89                        | 0.0436  | 7.0               | 2.0                        | 70           |
| constraints                | [AlO <sub>2</sub> ]/[OH]≤0.7  | [PO <sub>4</sub> ]+0.07[F]≤0.05                   |                            |   |   |                             | charge equivalent: [AlO <sub>2</sub> ]+2[CO <sub>3</sub> ]+[F]+[NO <sub>3</sub> ]+[NO <sub>2</sub> ]+[OH]+3[PO <sub>4</sub> ]=4.73648 |                   |                            |              |
| Fixed Molar Concentrations |   |   |                            |   |   |                             |   |                   |                            |              |
|                            | [SO <sub>4</sub> ] (molar at 5M Na)   | [C <sub>2</sub> O <sub>4</sub> ] (molar at 5M Na) |                            | [Cl] (molar at 5M Na)                     |   |                             | [SiO <sub>3</sub> ] (molar at 5M Na)  |                   |                            |              |
|                            | 0.0544  |   | 0.02                       |   |   | 0.102                       |   | 0.00636           |                            |              |

The composition factor space for envelope B/D was based on tank characterization reports for AZ-101<sup>[27]</sup> and AZ-102<sup>[28]</sup>. Analytical data of both dissolved and undissolved solids were combined to represent the total solids in the slurry. Because the undissolved solids are in equilibrium with the supernate and calculated by the simulation, the factor space must be in terms of the total slurry solids. Therefore, the mixture variables for the envelope B/D physical property models are in terms of the total slurry solids. However, the “dilution factor, expressed as the process variable “sodium molarity”, is the molarity of the supernate. A constraint was imposed on the net charge of the mixture variables based on the ranges observed in the data. These ranges are in Table 3, along with the concentration of several species that were fixed relative to that of sodium, either because they were relatively small or showed little variation in the analytical data.

**Table 3. Definition for Envelope B/D Factor Space**

| Variable                              | Mixture Variable Mass Fraction Ranges<br>Mass fraction relative to total mass of mixture variables  |  |                            |  |                            |  | Process Variables |                            |              |
|---------------------------------------|---|--|----------------------------|--|----------------------------|--|-------------------|----------------------------|--------------|
|                                       | [AlO <sub>2</sub> ]<br>(mass<br>fraction)   | [CO <sub>3</sub> ]<br>(mass<br>fraction) | [Fe]<br>(mass<br>fraction) | [NO <sub>3</sub> ]<br>(mass<br>fraction) | [OH]<br>(mass<br>fraction) | [SO <sub>4</sub> ]<br>(mass<br>fraction) | [Na]<br>(molar)   | SBS / Feed<br>(volumetric) | Temp<br>(°C) |
| minimum                               | 0.129   | 0.284                                    | 0.0411                     | 0.115                                    | 0.0508                     | 0.0952                                   | 2.33              | 0.0                        | 20           |
| maximum                               | 0.161   | 0.500                                    | 0.080                      | 0.306                                    | 0.113                      | 0.183                                    | 4.48              | 2.0                        | 70           |
| charge<br>constraint                  | -0.02355 ≤ -0.016955[AlO <sub>2</sub> ]+0.053718[Fe]-0.016128[NO <sub>3</sub> ]-0.020820[SO <sub>4</sub> ]-0.058798[OH]-0.033328[CO <sub>3</sub> ] ≤ -0.02094 |  |                            |  |                            |  |                   |                            |              |
| Molar Ratios Fixed Relative to Sodium |   |  |                            |  |                            |  |                   |                            |              |
| [NO <sub>2</sub> ]                    | [K]   | [F]                                      | [Zr]                       | [CrO <sub>4</sub> ]                      | [SiO <sub>3</sub> ]        | [C <sub>2</sub> O <sub>4</sub> ]         |                   |                            |              |
| 0.27                                  | 0.027   | 0.018                                    | 0.005                      | 0.0044                                   | 0.0041                     | 0.008                                    |                   |                            |              |

The composition factor space for envelope C was based on tank waste characterization reports for tanks AN-102<sup>[29, 30]</sup> and AN-107<sup>[31-33]</sup>. Only one ionic form of EDTA (ethylenediaminetetraacetic acid) – dihydrogen EDTA – was available for the purpose of the simulations, hence all reported forms of EDTA in the analytical data were input as this single

anion. Table 4 shows the mixture and process variable ranges, the mixture variable charge constraint, and the species whose concentration was fixed relative to Na due to their small or relatively consistent concentration in the analytical data.

**Table 4. Definition for Envelope C Factor Space**

| Variable                       | Mixture Variable Molar Ranges<br>Normalized to equivalent molarity at 5M Na |   |   |  |  |   | Process Variables                  |                                  |                                  |  |
|--------------------------------|---|---|---|--|--|---|------------------------------------|----------------------------------|----------------------------------|--|
|                                | [AlO <sub>2</sub> ]<br>(molar at<br>5M Na)                                  | [CO <sub>3</sub> ]<br>(molar at<br>5M Na) | [NO <sub>2</sub> ]<br>(molar at<br>5M Na)               | [NO <sub>3</sub> ]<br>(molar at<br>5M Na)  | [OH]<br>(molar at<br>5M Na)                | [SO <sub>4</sub> ]<br>(molar at<br>5M Na) | [Na]<br>(molar)                    | SBS / Feed<br>(volumetric)       | Temp<br>(°C)                     |  |
| minimum                        | 0.015   | 0.560                                     | 0.780   | 1.50                                       | 0.138                                      | 0.051                                     | 7.0                                | 0.0                              | 20                               |  |
| maximum                        | 0.290   | 0.940                                     | 1.19  | 2.30                                       | 0.295                                      | 0.112                                     | 8.5                                | 2.0                              | 70                               |  |
| charge<br>constraint           | $4.27 \leq [AlO_2] + [NO_2] + [NO_3] + [OH] + 2[CO_3] + 2[SO_4] \leq 5.33$  |   |   |  |  |   |                                    |                                  |                                  |  |
| Fixed Molar Concentrations     |   |   |   |  |  |   |                                    |                                  |                                  |  |
| [Cl]<br>(molar<br>at 5M<br>Na) | [F]<br>(molar at<br>5M Na)  | [PO <sub>4</sub> ]<br>(molar at<br>5M Na) | [C <sub>2</sub> O <sub>4</sub> ]<br>(molar at<br>5M Na) | [CrO <sub>4</sub> ]<br>(molar at<br>5M Na) | [SiO <sub>3</sub> ]<br>(molar at<br>5M Na) | [formate]<br>(molar at<br>5M Na)          | [glycolate]<br>(molar at 5M<br>Na) | [acetate]<br>(molar at<br>5M Na) | [citrate]<br>(molar at<br>5M Na) | [H <sub>2</sub> EDTA]<br>(molar at 5M<br>Na) |
| 0.052                          | 0.0016  | 0.022                                     | 0.0033  | 0.0011                                     | 0.002                                      | 0.091                                     | 0.01                               | 0.024                            | 0.015                            | 0.025  |

## 2.6 RESULTS

The results are given below in three sections, 1) the model fits with plots comparing model predictions with simulation results, 2) comparison of simulation with experimental simulant results of 13 selected design points, and 3) a snapshot of the progression of aluminum and sodium concentrations through the pre-treatment process for each of the envelopes, in addition to the Sr concentrations for envelope C. Included with the model/simulation plots are the results of simulations based on actual tank compositions for each of the three envelopes (AN-104, AZ-102, and AN-107 for A, B/D, and C respectively) which used an expanded chemistry model to include a majority of the constituents given in the analytical reports. This was a measure of the combined effect of the “minor” constituents on the property models.

Because computer experiments have no random error associated with the results, statistics that are normally used to measure the success of a model from a typical lab experiment could not be used here. Also, it is not feasible to run lab experiments duplicating the complicated pre-treatment process being simulated. Therefore, the physical property models were validated in two stages, one to test whether the derived property models give a reasonable representation of the simulation software predictions, and the other comparing the chemistry predicted by the software with results from experimental simulant work.

Validation of the physical property models against the simulation predictions was done using design points generated by the Orthogonal Latin Hypercube technique<sup>[24]</sup>, which produces points uniformly distributed over the linear factor space. If the physical property models

adequately predict a majority of the OLH points which were not included in the model fit, the model is considered to be a fair representation of the simulation software.

Validation of the simulation software was done by making simulants of 13 selected simulation design points based on the composition of the ultra-filtration feed stream predicted by OLI/ESP. The solids and supernate compositions and physical properties of these simulants were compared with the simulation prediction.

It was not possible to predict how certain simulation design points would behave prior to running the simulations. In very few cases, the concentration of the feed stream was such that it was not possible to dilute it to the target 1.22 (g/ml) supernate density with the generated pre-treatment recycle (none of these cases has HLW SBS). In these situations the simulation was modified so that the pre-treatment recycle by-passed the evaporator and the feed stream diluted with water. There were also very few cases where the feed stream was dilute and the evaporator bottoms flow rate too small for the combined streams to achieve the target 1.22 (g/ml) density. In these situations the evaporator bottoms were concentrated to 30wt% total solids, and the initial dilution of the waste feed reduced. These are considered reasonable adjustments as these cases represent extremes in the operating conditions, and waste streams would not be sent to the pre-treatment process in a state of dilution that would make it impossible reach the target density.

For envelope C, 10 points (2, 6, 10, 14, 18, 22, 26, 30, 34, 38) were removed from the design matrix for which the sodium molarity of the waste feed was given at the high value of the factor space. The sodium molarity of these points had to be adjusted to the minimum factor space value to achieve the target permeate density. The matrix already contained these points at the low sodium value. Because this is a process variable, it does not effect the design as these points represent a combination of conditions (no SBS flow and high sodium waste feed) which would not occur under normal operating conditions.

### **2.6.1 Predictive Models with Model vs. Simulation Plots**

Plots of the simulation results vs. the model prediction are shown for each of the models, with curves indicating  $\pm 15\%$  (or  $\pm 5\%$ ) of the model prediction as a measure of the model's success relative to the simulation results.

The heat capacity models were very successful relative to the simulation predictions, and the viscosity models are well within 15% of the simulation predictions. The volume reduction factor (VRF) models for envelopes B/D and C are, with few exceptions, within  $\pm 15\%$  of the simulation predictions. The VRF model for sub envelope A-a shows a definite correlation between the model prediction and simulation results, but there is some scatter beyond  $\pm 15\%$  of the simulation prediction (note that the VRF range for this envelope is by far the greatest).

#### **2.6.1.1 Sub-Envelope A-a Predictive Models**

All concentrations are in terms of molarity. The concentrations of the mixture variables (all species except Na) are expressed relative to a stream at a 5M Na concentration. (e.g. an

$[AlO_2]$  concentration of 2M in an 8M Na stream is first adjusted to an equivalent concentration in a 5M stream:  $2M AlO_2 * (5M Na / 8M Na) = 1.25M AlO_2$ ) and then applied to the equation.  $[Na]$  is used as a process variable to adjust the water content of the feed stream while keeping the amount of solids relative to each other constant. An example calculation is given in Appendix A. Temperature is in  $^{\circ}C$ , and the SBS/Feed ratio is a volumetric flow ratio of the HLW SBS relative to the waste feed.

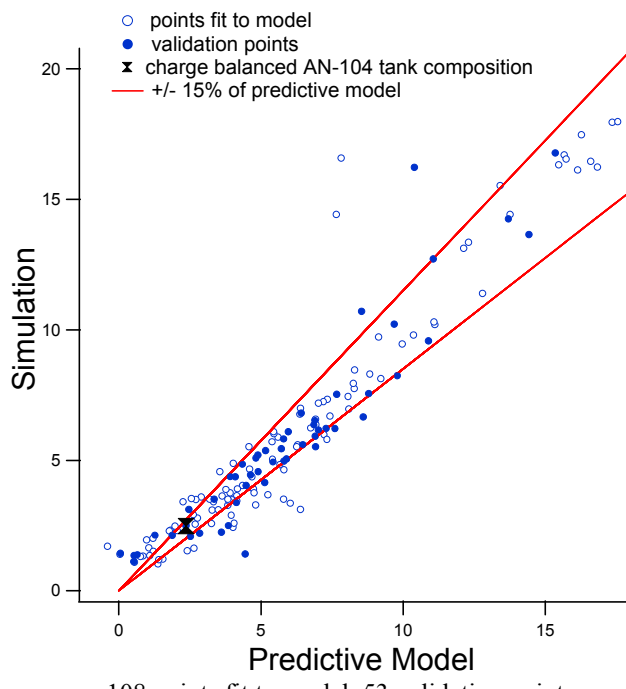
**Table 5 Valid Variable Ranges for Sub-Envelope A-a Models**

| Variable | Mixture Variable Molar Ranges<br>Normalized to equivalent molarity at 5M Na |                                 |                              |                                 |                                 |                               |                                 | Process Variables |                            |                         |
|----------|---|---------------------------------|------------------------------|---------------------------------|---------------------------------|-------------------------------|---------------------------------|-------------------|----------------------------|-------------------------|
|          | $[AlO_2]$<br>(molar at<br>5M Na)  | $[CO_3]$<br>(molar at<br>5M Na) | $[F]$<br>(molar at<br>5M Na) | $[NO_2]$<br>(molar at<br>5M Na) | $[NO_3]$<br>(molar at<br>5M Na) | $[OH]$<br>(molar at<br>5M Na) | $[PO_4]$<br>(molar at<br>5M Na) | $[Na]$<br>(molar) | SBS / Feed<br>(volumetric) | Temp<br>( $^{\circ}C$ ) |
| minimum  | 0.207   | 0.326                           | 0.00927                      | 0.731                           | 0.991                           | 0.983                         | 0.00632                         | 5.6               | 0.0                        | 20                      |
| maximum  | 1.12  | 0.686                           | 0.236                        | 1.59                            | 2.08                            | 2.89                          | 0.0436                          | 7.0               | 2.0                        | 70                      |

The sub-envelope A-a volume reduction factor (VRF: volume of total evaporator feed / volume of evaporator bottoms) at endpoint – steady state conditions is given as:

$$\begin{aligned}
 VRF = & -35.7 + 7.32[AlO_2] + 37.3[CO_3] + 6.21[F] - 10.1[Na] + 19.1[NO_2] \\
 & + 16.5[NO_3] + 28.8[OH] + 2.06[PO_4] + 12.6[SBS] + 0.781[Temp] \\
 & - 3.84[CO_3][Na] - 1.92[NO_2][Na] - 1.68[NO_3][Na] - 3.52[OH][Na] \\
 & + 1.80[Na]^2 - 2.01[AlO_2][SBS] - 1.17[Na][SBS] - 1.78[SBS]^2 \\
 & - 0.165[Na][Temp] + 0.0465[OH][Temp] + 0.0740[SBS][Temp] + 0.00266[Temp]^2
 \end{aligned} \quad (1)$$

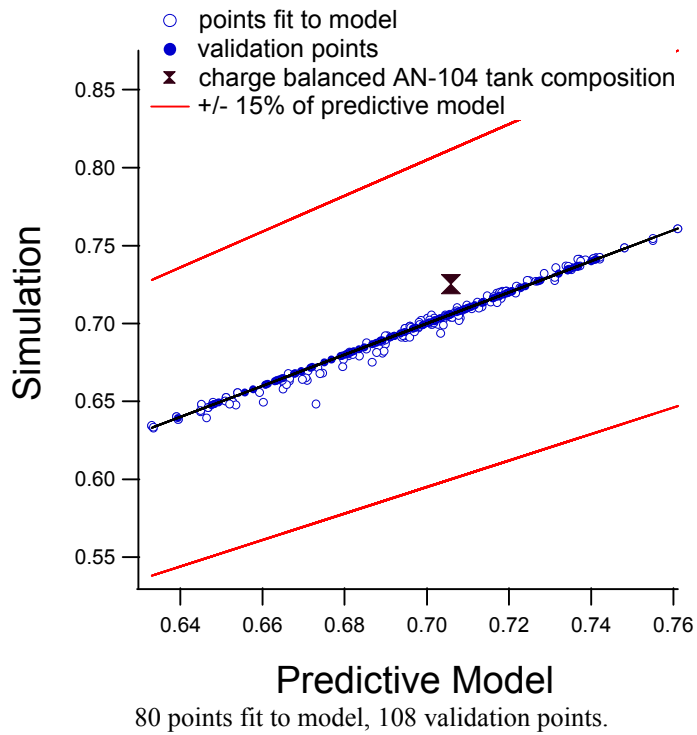
**Figure 3. Sub-envelope A-a Volume Reduction Factor**



The sub-envelope A-a slurry heat capacity at endpoint – steady state conditions is given as:

$$\text{Cp} \left( \frac{\text{cal}}{\text{gram } {}^\circ\text{C}} \right) = 0.0460 + 0.191[AlO_2] + 0.311[CO_3] + 0.135[F] + 0.140[NO_2] \\ + 0.144[NO_3] + 0.141[OH] + 0.426[PO_4] - 0.00300[SBS] \\ - 0.00206[Temp] + 0.000857[AlO_2][Temp] + 0.000406[F][Temp] \\ + 0.000185[NO_3][Temp] + 0.000231[OH][Temp] \quad (2)$$

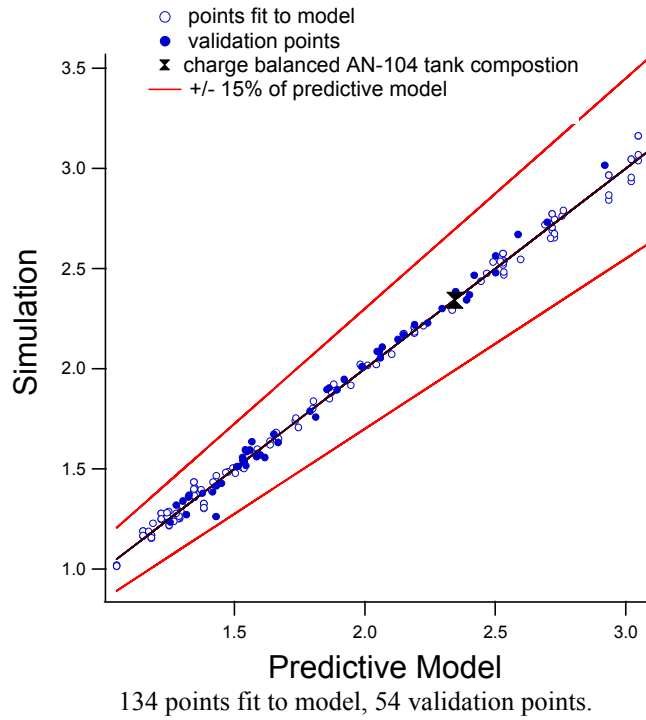
**Figure 4. Sub-envelope A-a Slurry Heat Capacity  $(\text{cal}/(\text{gram } {}^\circ\text{C}))$**



The sub-envelope A-a supernate viscosity at endpoint – steady state conditions is given as:

$$\text{viscosity(cP)} = 0.0544[NO_2] + 0.0608[NO_3] - 0.149[OH] \\ + \exp \left( \frac{219}{77.4 + [\text{Temp}]} - 0.947 - 0.0678[[NO_2] - 0.134[NO_3]] \right. \\ \left. + 0.0611[OH] - 0.0826[NO_3][NO_2] \right) \quad (3)$$

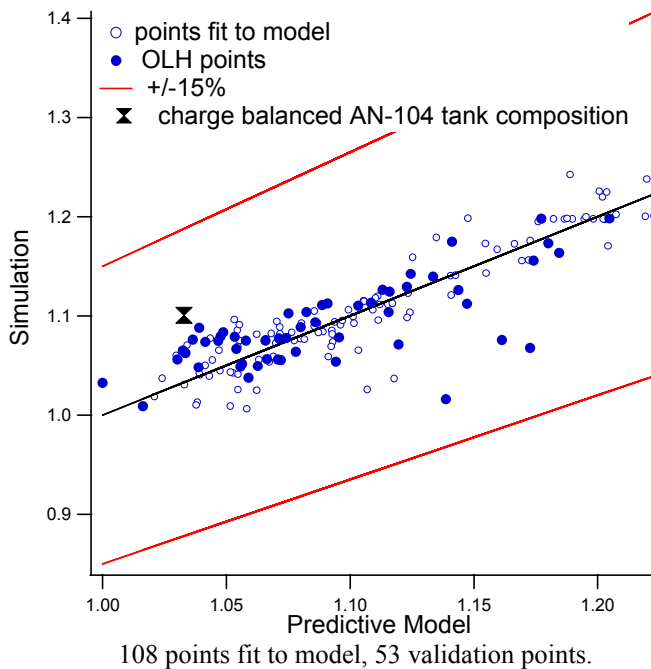
**Figure 5. Sub-envelope A-a Supernate Viscosity (cP)**



The envelope A evaporator slurry density at 50°C, endpoint – steady state conditions is given as:

$$\begin{aligned}
 \text{density} \left( \frac{\text{g}}{\text{ml}} \right) = & 2.14 + 0.363[\text{ALO}_3] + 0.372[\text{CO}_3] + 0.132[\text{F}] + 0.187[\text{NO}_2] \\
 & + 0.201[\text{NO}_3] + 0.377[\text{OH}] + 0.810[\text{PO}_4] - 0.686[\text{Na}] \\
 & + 0.0639[\text{SBS}] - 0.00424[\text{Temp}] - 0.0251[\text{OH}][\text{Na}] \\
 & + 0.00669[\text{CO}_3][\text{Temp}] + 0.00323[\text{F}][\text{Temp}] \quad (4) \\
 & + 0.00340[\text{NO}_2][\text{Temp}] + 0.00258[\text{NO}_3][\text{Temp}] \\
 & + 0.00310[\text{OH}][\text{Temp}] - 0.00243[\text{Na}][\text{Temp}] \\
 & + 0.0579[\text{Na}]^2 - 0.0241[\text{SBS}]^2 + 0.0000945[\text{Temp}]^2
 \end{aligned}$$

**Figure 6. Envelope A Evaporator Bottoms Slurry Density**



### 2.6.1.2 Envelope B/D Predictive Models

All concentrations for the envelope B/D model mixture variables listed in Table 6 are in terms of weight fraction relative to the total mass of all the mixture variables. [Na] is used as a process variable to, in effect, adjust the water content of the feed stream while keeping the amount of solids relative to each other constant. An example calculation is given in Appendix A. Temperature is in °C, and the SBS/Feed ratio is a volumetric flow ratio of the HLW SBS relative to the waste feed.

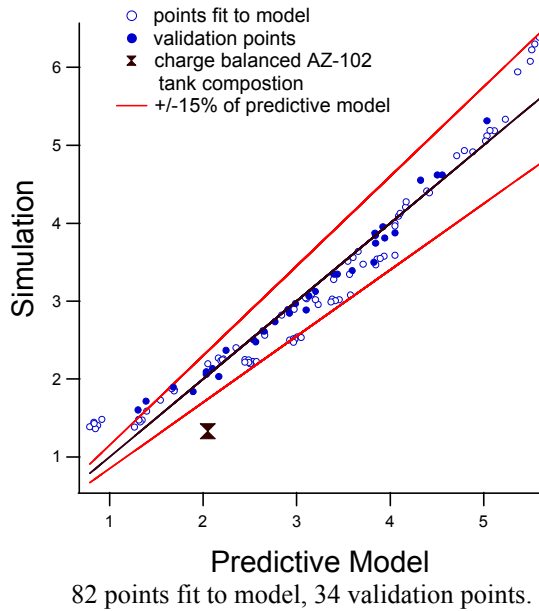
**Table 6 Valid Variable Ranges for Envelope B/D Models**

| Variable | Mixture Variable Mass Fraction Ranges<br>Mass fraction relative to total mass of mixture variables |                                       |                         |                                       |                         |                                       | Process Variables |                            |              |
|----------|--|---------------------------------------|-------------------------|---------------------------------------|-------------------------|---------------------------------------|-------------------|----------------------------|--------------|
|          | [AlO <sub>2</sub> ]<br>(mass fraction)   | [CO <sub>3</sub> ]<br>(mass fraction) | [Fe]<br>(mass fraction) | [NO <sub>3</sub> ]<br>(mass fraction) | [OH]<br>(mass fraction) | [SO <sub>4</sub> ]<br>(mass fraction) | [Na]<br>(molar)   | SBS / Feed<br>(volumetric) | Temp<br>(°C) |
| minimum  | 0.129  | 0.284                                 | 0.0411                  | 0.115                                 | 0.0508                  | 0.0952                                | 2.33              | 0.0                        | 20           |
| maximum  | 0.161  | 0.500                                 | 0.080                   | 0.306                                 | 0.113                   | 0.183                                 | 4.48              | 2.0                        | 70           |

The envelope B/D volume reduction factor (VRF: volume of total evaporator feed / volume of evaporator bottoms) at endpoint – steady state conditions is given as:

$$\begin{aligned}
 VRF = & 1.98 + 3.76[AlO_2] + 4.03[CO_3] + 4.74[Fe] + 3.72[NO_3] + 3.56[OH] \\
 & + 3.96[SO_4] - 2.06[Na] + 1.33[SBS] + 0.00958[Temp] + 0.195[Na]^2 \\
 & - 3.23[Fe][SBS] + 1.78[OH][SBS]
 \end{aligned} \quad (5)$$

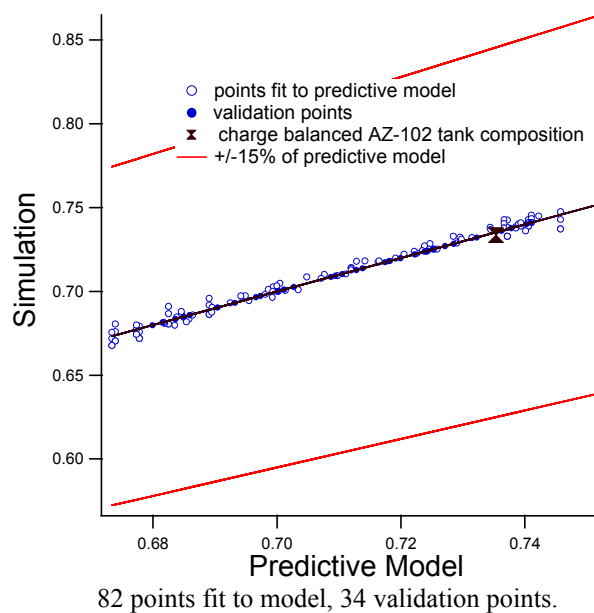
**Figure 7. Envelope B/D Volume Reduction Factor**



The envelope B/D slurry heat capacity at endpoint – steady state conditions is given as:

$$C_p \left( \frac{\text{cal}}{\text{gram } {}^\circ\text{C}} \right) = 0.855[AlO_2] + 0.758[CO_3] + 0.602[Fe] + 0.701[NO_3] + 0.913[OH] + 0.798[SO_4] - 0.00127[\text{Temp}] \quad (6)$$

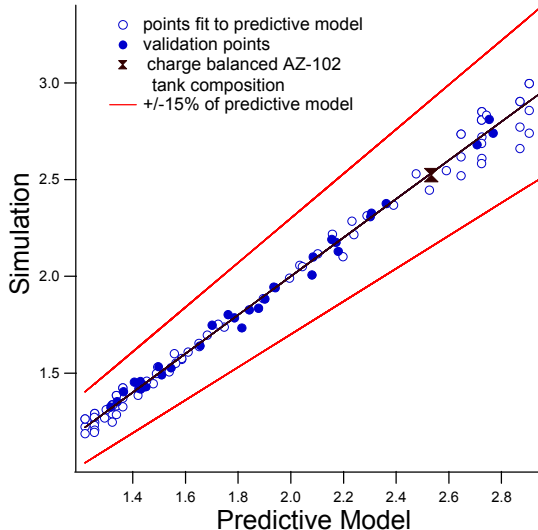
**Figure 8. Envelope B/D Slurry Heat Capacity  $(\text{cal}/(\text{gram } {}^\circ\text{C}))$**



The envelope B/D supernate viscosity at endpoint – steady state conditions is given as:

$$\text{viscosity(cP)} = \exp\left(\frac{333}{104 + [\text{Temp}]} - 1.86 + 0.435[\text{CO}_3] + 1.63[\text{CO}_3][\text{OH}]\right) \quad (7)$$

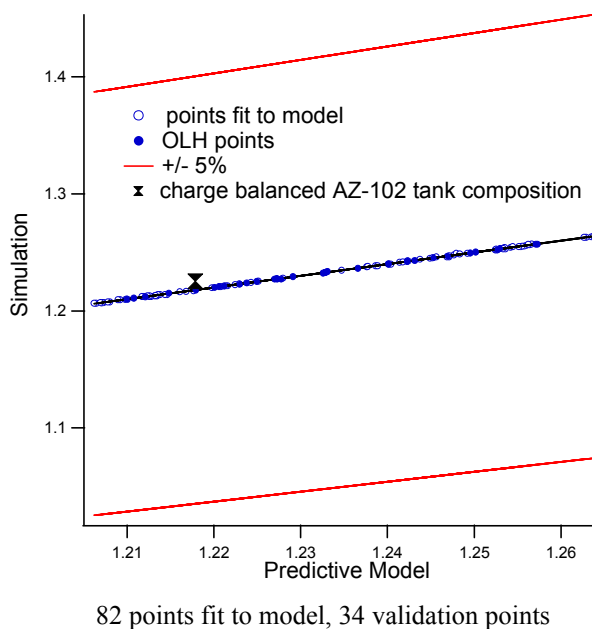
**Figure 9. Envelope B/D Supernate Viscosity (cP)**



The envelope B/D evaporator slurry density at 50°C, endpoint – steady state conditions is given as:

$$\begin{aligned} \text{density}\left(\frac{\text{g}}{\text{ml}}\right) = & 0.00243 + 1.24[\text{AlO}_2] + 1.16[\text{CO}_3] + 1.34[\text{Fe}] + 1.19[\text{NO}_3] \\ & + 1.144[\text{OH}] + 1.19[\text{SO}_4] - 0.000117[\text{Na}] + 0.000418[\text{SBS}] \\ & + 0.000839[\text{Temp}] - 0.000442[\text{AlO}_2][\text{Temp}] \\ & + 0.000310[\text{CO}_3][\text{Temp}] + 0.00140[\text{Fe}][\text{Temp}] - 0.00102[\text{OH}][\text{Temp}] \end{aligned} \quad (8)$$

**Figure 10. Envelope B/D Evaporator Bottoms Slurry Density**



#### 2.6.1.3 Envelope C Predictive Models

All concentrations are in terms of molarity. The concentrations of the mixture variables (all species except Na) are expressed relative to a stream at a 5M Na concentration. (e.g. an  $[AlO_2]$  concentration of 2M in an 8M Na stream is first adjusted to an equivalent concentration in a 5M stream:  $2M AlO_2 * (5M Na / 8M Na) = 1.25M AlO_2$ ) and then applied to the equation. [Na] is then used as a process variable to, in effect, adjust the water content of the feed stream while keeping the amount of solids relative to each other constant. An example calculation is given in Appendix A. Temperature is in °C, and the SBS/Feed ratio is a volumetric flow ratio of the HLW SBS relative to the waste feed.

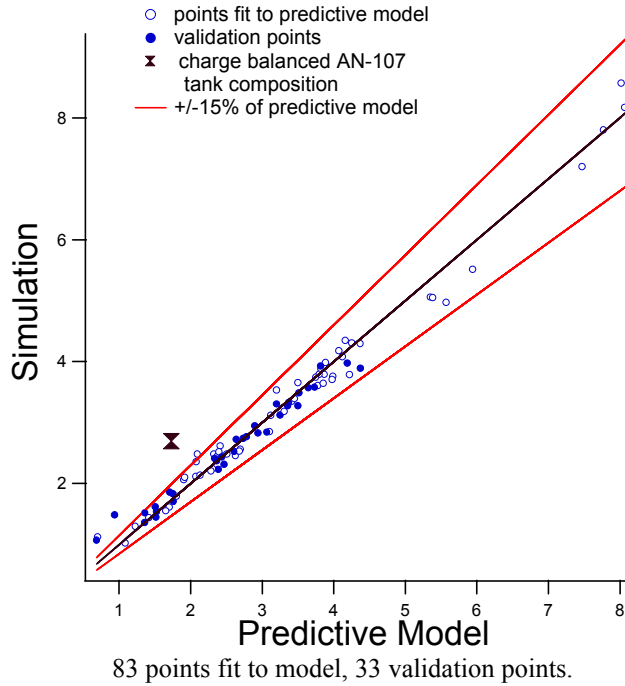
**Table 7 Valid Variable Ranges for Envelope C Models**

| Variable | Mixture Variable Molar Ranges<br>Normalized to equivalent molarity at 5M Na |                                 |                                 |                                 |                               |                                 | Process Variables |                            |              |
|----------|---|---------------------------------|---------------------------------|---------------------------------|-------------------------------|---------------------------------|-------------------|----------------------------|--------------|
|          | $[AlO_2]$<br>(molar at<br>5M Na)  | $[CO_3]$<br>(molar at<br>5M Na) | $[NO_2]$<br>(molar at<br>5M Na) | $[NO_3]$<br>(molar at<br>5M Na) | $[OH]$<br>(molar at<br>5M Na) | $[SO_4]$<br>(molar at<br>5M Na) | $[Na]$<br>(molar) | SBS / Feed<br>(volumetric) | Temp<br>(°C) |
| minimum  | 0.015   | 0.560                           | 0.780                           | 1.50                            | 0.138                         | 0.051                           | 7.0               | 0.0                        | 20           |
| maximum  | 0.290   | 0.940                           | 1.19                            | 2.30                            | 0.295                         | 0.112                           | 8.5               | 2.0                        | 70           |

The envelope C volume reduction factor (VRF: volume of total evaporator feed / volume of evaporator bottoms) at endpoint – steady state conditions is given as:

$$\begin{aligned} \text{VRF} = & -22.2 + 1.24[\text{AlO}_2] + 3.79[\text{CO}_3] + 2.07[\text{NO}_2] + 1.50[\text{NO}_3] \\ & + 14.4[\text{OH}] + 1.98[\text{SO}_4] + 1.81[\text{Na}] - 7.44[\text{SBS}] + 0.264[\text{Temp}] \\ & - 1.41[\text{Na}][\text{OH}] - 0.852[\text{Na}][\text{SBS}] - 0.0336[\text{Na}][\text{Temp}] + 0.0285[\text{SBS}][\text{Temp}] \end{aligned} \quad (9)$$

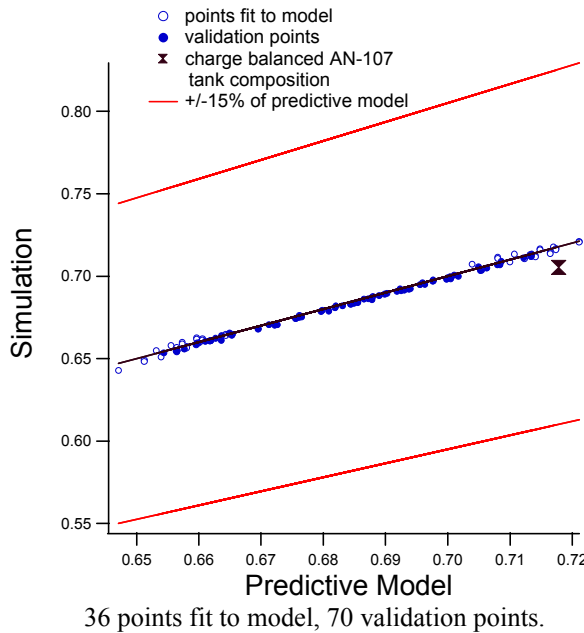
**Figure 11. Envelope C Volume Reduction Factor**



The envelope C slurry heat capacity at endpoint – steady state conditions is given as:

$$\begin{aligned} \text{Cp}\left(\frac{\text{cal}}{\text{gram } ^\circ\text{C}}\right) = & 0.187[\text{AlO}_2] + 0.319[\text{CO}_3] + 0.146[\text{NO}_2] + 0.160[\text{NO}_3] \\ & + 0.164[\text{OH}] + 0.335[\text{SO}_4] + 0.00207[\text{SBS}] - 0.00114[\text{Temp}] \end{aligned} \quad (10)$$

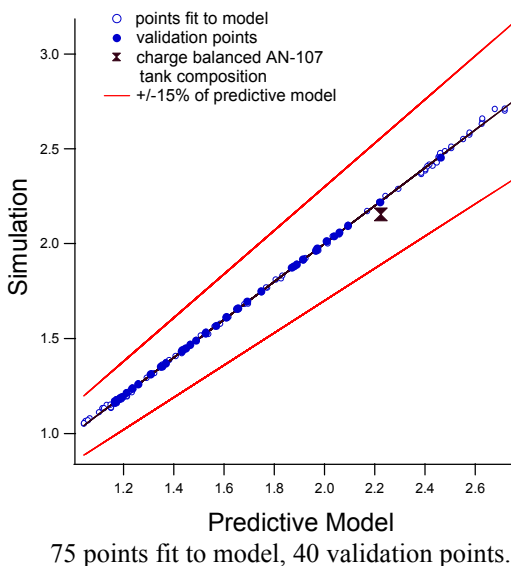
**Figure 12. Envelope C Slurry Heat Capacity (cal/(gram °C))**



The envelope C supernate viscosity at endpoint – steady state conditions is given as:

$$\text{viscosity(cP)} = -0.0454[\text{NO}_3] + 0.00451[\text{SBS}] \\ + \exp\left(\frac{312}{98.7 + [\text{Temp}]} - 1.83 + 0.134[\text{AlO}_2]\right) \\ + 0.220[\text{CO}_3] - 0.0109[\text{SBS}] \quad (11)$$

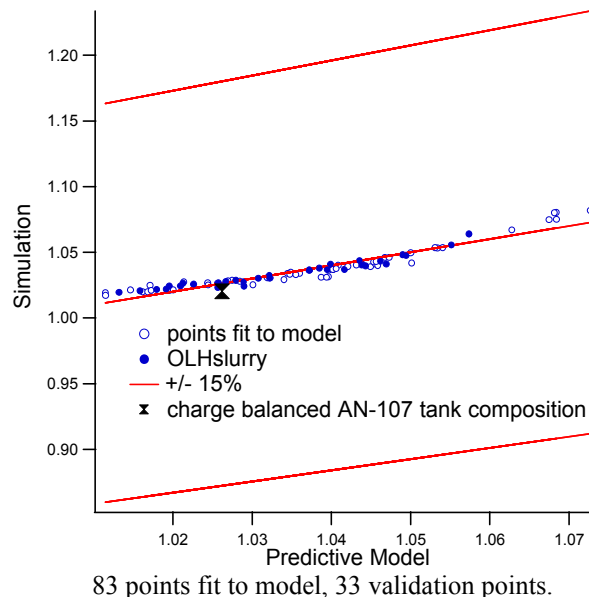
**Figure 13. Envelope C Supernate Viscosity (cP)**



The envelope C evaporator slurry density at 50°C, endpoint – steady state conditions is given as:

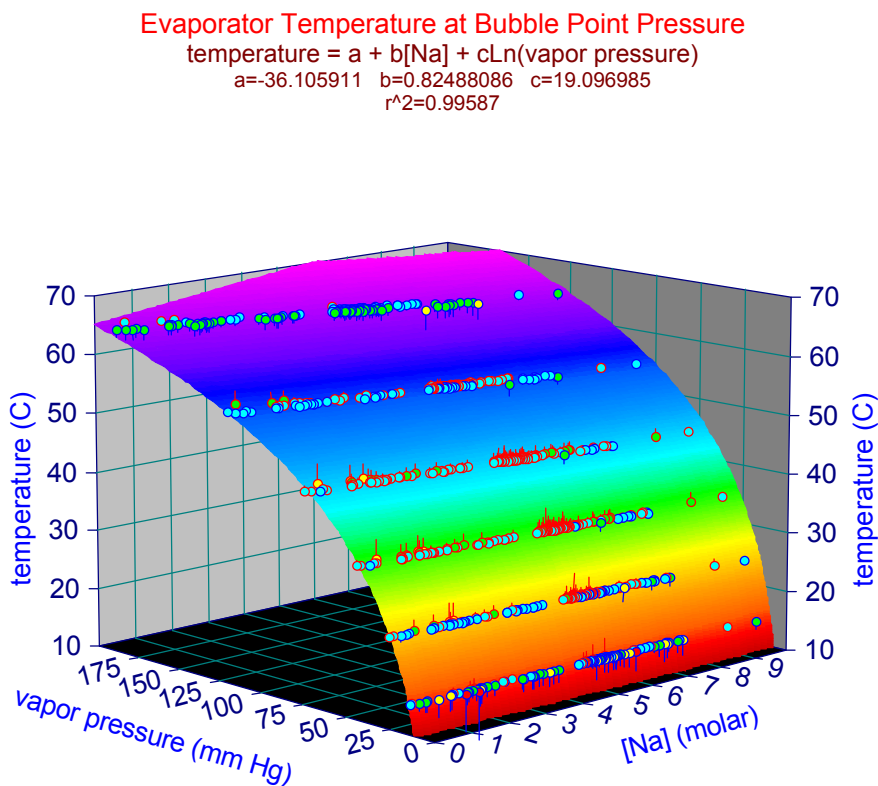
$$\text{density} \left( \frac{g}{ml} \right) = 0.000243[ALO_3] + 0.000481[CO_3] + 0.000243[NO_2] \\ + 0.000234[NO_3] + 0.000262[OH] + 0.000462[SO_4] - 0.0147[Na] + 0.00931[SBS] + 0.000576[Temp] \quad (12)$$

**Figure 14. Envelope C Evaporator Bottoms Slurry Density**



**The data used to fit the evaporator temperature shown in Figure 15 was not derived from this work.** The fit was done using results from the experimental simulant<sup>[26]</sup> over a broad range of compositions over all three envelopes. The plot gives the evaporator temperature as a function of the evaporator vapor pressure and bottoms sodium molarity. Not shown is a similar plot expressing the vapor pressure as a function of evaporator temperature and bottoms sodium molarity<sup>[26]</sup>.

**Figure 15. Evaporator Temperature at Bubble Point Pressure**



### 2.6.2 Comparison of Simulation with Experimental Results

Simulants were made of 13 envelope A-a design points based on the slurry composition of the first ultra-filtration feed stream as predicted by OLI/ESP. The compositions and physical properties of these simulants were compared with those predicted by the simulation as a method of validating the OLI/ESP chemistry.

The experimental and simulation supernate compositions listed in Table 8 show good agreement, though OLI/ESP slightly under predicts the solubility of aluminum. (GCWB predicted an even lower aluminum solubility than OLI/ESP, where OLI/ESP predicted the precipitation of 98 moles of gibbsite and 0.12 moles of NAS gel, and GCWB predicted the precipitation of 184 moles of gibbsite and 0.54 moles of NAS gel for the same system).

**Table 8. Comparison of Experimental with Simulation Supernate Compositions**

| run | Al (molar) |            |              | Ca (molar) |            |              | Fe (molar) |            |              |
|-----|------------|------------|--------------|------------|------------|--------------|------------|------------|--------------|
|     | analytical | simulation | % difference | analytical | simulation | % difference | analytical | simulation | % difference |
| 5   | 0.253      | 0.216      | 17.011       | 1.10E-05   | -          | N/A          | 4.98E-05   | 2.74E-05   | N/A          |
| 10  | 1.197      | 0.989      | 20.994       | 3.29E-05   | -          | N/A          | 1.59E-04   | 5.10E-04   | N/A          |
| 11  | 0.261      | 0.224      | 16.399       | 4.47E-06   | -          | N/A          | 1.38E-04   | 1.90E-04   | N/A          |
| 13  | 0.238      | 0.205      | 16.082       | 8.30E-06   | -          | N/A          | 4.14E-05   | 1.96E-05   | N/A          |
| 20  | 1.225      | 0.989      | 23.757       | 3.61E-05   | -          | N/A          | 1.63E-04   | 5.10E-04   | N/A          |
| 21  | 0.246      | 0.211      | 16.784       | 9.98E-06   | 9.82E-05   | N/A          | 1.24E-04   | 8.64E-04   | N/A          |
| 25  | 0.232      | 0.204      | 13.331       | 1.09E-05   | 1.57E-06   | N/A          | 8.93E-05   | 7.57E-04   | N/A          |
| 26  | 0.222      | 0.199      | 11.923       | 2.41E-05   | 1.35E-06   | N/A          | 4.07E-05   | 7.22E-04   | N/A          |
| 30  | 1.132      | 0.926      | 22.317       | 3.37E-05   | 6.08E-07   | N/A          | 1.18E-04   | 1.11E-03   | N/A          |
| 33  | 0.227      | 0.200      | 13.216       | 7.86E-06   | 6.64E-05   | N/A          | 3.93E-05   | 5.93E-04   | N/A          |
| 35  | 0.244      | 0.207      | 18.111       | 1.13E-05   | 1.52E-06   | N/A          | 8.49E-05   | 6.09E-04   | N/A          |
| 53  | 0.283      | 0.237      | 19.479       | 3.44E-06   | -          | N/A          | 4.28E-05   | 2.57E-06   | N/A          |
| 61  | 0.285      | 0.243      | 17.223       | 7.76E-06   | 4.85E-05   | N/A          | 1.91E-04   | 7.58E-04   | N/A          |

| run | P (molar)  |            |              | Si (molar) |            |              | S (molar)  |            |              |
|-----|------------|------------|--------------|------------|------------|--------------|------------|------------|--------------|
|     | analytical | simulation | % difference | analytical | simulation | % difference | analytical | simulation | % difference |
| 5   | 0.0106     | 0.0350     | -69.69       | 0.00533    | 0.00665    | -19.85       | 0.0526     | 0.0568     | -7.383       |
| 10  | 0.0049     | 0.0060     | -18.37       | 0.00431    | 0.00600    | -28.078      | 0.0414     | 0.0513     | -19.41       |
| 11  | 0.0233     | 0.0279     | -16.68       | 0.00611    | 0.00686    | -10.85       | 0.0559     | 0.0583     | -4.083       |
| 13  | 0.0055     | 0.0062     | -10.07       | 0.00310    | 0.00288    | 7.764        | 0.0485     | 0.0531     | -8.624       |
| 20  | 0.0045     | 0.0060     | -24.01       | 0.00342    | 0.00600    | -43.016      | 0.0438     | 0.0513     | -14.75       |
| 21  | 0.0267     | 0.0290     | -8.014       | 0.01399    | 0.01532    | -8.699       | 0.0525     | 0.0566     | -7.194       |
| 25  | 0.0124     | 0.0324     | -61.72       | 0.00714    | 0.00624    | 14.40        | 0.0520     | 0.0554     | -6.067       |
| 26  | 0.0200     | 0.0303     | -33.96       | 0.00615    | 0.00256    | 140.73       | 0.0482     | 0.0520     | -7.245       |
| 30  | 0.0046     | 0.0055     | -16.15       | 0.00763    | 0.00552    | 38.10        | 0.0476     | 0.0507     | -6.124       |
| 33  | 0.0053     | 0.0032     | 64.60        | 0.00420    | 0.00273    | 54.00        | 0.0484     | 0.0523     | -7.381       |
| 35  | 0.0123     | 0.0330     | -62.81       | 0.00493    | 0.00632    | -21.92       | 0.0517     | 0.0557     | -7.172       |
| 53  | 0.0068     | 0.0072     | -5.606       | 0.00292    | 0.00576    | -49.24       | 0.0611     | 0.0623     | -1.888       |
| 61  | 0.0210     | 0.0434     | -51.64       | 0.01910    | 0.01918    | -0.3799      | 0.0625     | 0.0655     | -4.616       |

N/A indicates that the values are so small that relative difference between the experimental and simulation values have little meaning.

The sodium molarity, density, and viscosity experimental and simulation results are given in Table 9. The simulants made to represent the simulation points 10, 20 and 30 overshot the target sodium concentration (defined as the composition predicted by OLI/ESP) by more than 7%, and it is expected that this will be reflected in comparisons between experimental and simulation results. This is apparent in the density and viscosity values, where the simulant values were greater than the corresponding simulation values. The remaining points generally had a difference of less than 5% in sodium molarity, 2% in density, and 9% in viscosity between the experimental and simulation results.

**Table 9. Comparison of Experimental with Simulation Na Molarity, Density and Viscosity**

| envelope A simulation design point | design point temp (°C) | Supernate Na Molarity |                     |              | Density (g/ml) (target = 1.22) |              | Viscosity (cP) |                     |                      |
|------------------------------------|------------------------|-----------------------|---------------------|--------------|--------------------------------|--------------|----------------|---------------------|----------------------|
|                                    |                        | analytical            | target (simulation) | % difference | analytical                     | % difference | analytical     | model (correlation) | simulation (OLI/ESP) |
| 5                                  | 20                     | 5.34                  | 5.210               | 2.493        | 1.229                          | 0.713        | 2.86           | 2.727               | 2.745                |
| 10                                 | 20                     | 5.62                  | 5.246               | 7.125        | 1.272                          | 4.252        | 4.82           | 3.048               | 3.162                |
| 11                                 | 20                     | 5.72                  | 5.419               | 5.560        | 1.241                          | 1.707        | 3.46           | 3.099               | 3.170                |
| 13                                 | 20                     | 4.95                  | 4.905               | 0.915        | 1.233                          | 1.102        | 2.41           | 2.190               | 2.205                |
| 20                                 | 20                     | 5.72                  | 5.246               | 9.026        | 1.272                          | 4.257        | 4.82           | 3.043               | 3.162                |
| 21                                 | 20                     | 5.48                  | 5.273               | 3.934        | 1.238                          | 1.503        | 3.38           | 3.099               | 3.021                |
| 25                                 | 20                     | 5.23                  | 5.111               | 2.319        | 1.228                          | 0.617        | 2.77           | 2.727               | 2.654                |
| 26                                 | 20                     | 4.85                  | 4.835               | 0.316        | 1.228                          | 0.695        | 3.05           | 2.940               | 2.842                |
| 30                                 | 20                     | 5.56                  | 5.146               | 8.041        | 1.267                          | 3.867        | 4.52           | 3.048               | 3.039                |
| 33                                 | 20                     | 4.99                  | 4.860               | 2.682        | 1.235                          | 1.189        | 2.45           | 2.190               | 2.183                |
| 35                                 | 20                     | 5.17                  | 5.132               | 0.738        | 1.227                          | 0.572        | 2.74           | 2.727               | 2.674                |
| 53                                 | 70                     | 6.21                  | 5.727               | 8.435        | 1.244                          | 1.932        | 1.12           | 1.049               | 1.018                |
| 61                                 | 70                     | 6.32                  | 6.045               | 4.558        | 1.240                          | 1.680        | 1.47           | 1.291               | 1.251                |
|                                    |                        |                       |                     |              |                                |              |                |                     | 17.680               |

OLI/ESP generally predicted a somewhat lower heat capacity (13.8% on average) than measured experimentally (Table 10). The experimental heat capacities given are for the supernate, while those calculated by the simulation are for the slurry. Although a supernate would in general be expected to have a higher heat capacity than a slurry, the small amount of undissolved solids is likely to make the difference in heat capacity trivial. Points 10, 20, and 30 show less of a difference between the simulation and experimental values, but this is due to the higher sodium concentration in the simulant, which reduces the heat capacity. Simulations of simple NaNO<sub>3</sub>-H<sub>2</sub>O and NaOH-H<sub>2</sub>O systems also showed OLI/ESP to under predict the heat capacity by 2-4% for solutions in the neighborhood of 5M Na as compared to published values (see Appendix D).

The experimental values for thermal conductivity (Table 10) showed a standard deviation about the value of water of 6.5%. No trend was found in the experimental values as a function of sodium concentration, and it is believed the variation is due largely to variability in the measurement. The mean in the percent difference between the experiment results and water is 1.7% with an error of 1.9%, so it is not possible to distinguish the experimental results from the value of water, as was true for the simulation results.

**Table 10. Comparison of Experimental with Simulation Heat Capacity and Thermal Conductivity**

| envelope A design point | temp (°C) | Heat Capacity (cal/(g °C)) |                      |                     |   | Thermal Conductivity (cal/(cm s K)) |            |  |
|-------------------------|-----------|----------------------------|----------------------|---------------------|---|-------------------------------------|------------|--|
|                         |           | analytical                 | simulation (OLI/ESP) | model (correlation) | % difference (analytical vs. simulation ) | analytical                          | simulation | % difference from that of water (0.63) |
| 5                       | 20        | 0.796                      | 0.699                | .6993               | 13.80                                     | 0.687                               | 0.630      | 9.002                                  |
| 10                      | 20        | 0.804                      | 0.761                | .7607               | 5.73                                      | 0.678                               | 0.630      | 7.660                                  |
| 11                      | 20        | 0.850                      | 0.703                | .7041               | 20.93                                     | 0.728                               | 0.630      | 15.498                                 |
| 13                      | 20        | 0.786                      | 0.702                | .7020               | 11.90                                     | 0.594                               | 0.630      | -5.658                                 |
| 20                      | 20        | 0.807                      | 0.761                | .7608               | 6.07                                      | 0.621                               | 0.630      | -1.405                                 |
| 21                      | 20        | 0.807                      | 0.701                | .7007               | 15.17                                     | 0.640                               | 0.630      | 1.526                                  |
| 25                      | 20        | 0.798                      | 0.696                | .6964               | 14.65                                     | 0.603                               | 0.630      | -4.273                                 |
| 26                      | 20        | 0.812                      | 0.713                | .7127               | 13.95                                     | 0.662                               | 0.630      | 5.066                                  |
| 30                      | 20        | 0.793                      | 0.753                | .7532               | 5.27                                      | 0.658                               | 0.630      | 4.430                                  |
| 33                      | 20        | 0.790                      | 0.698                | .6976               | 13.21                                     | 0.625                               | 0.630      | -0.775                                 |
| 35                      | 20        | 0.808                      | 0.697                | .6970               | 15.86                                     | 0.603                               | 0.630      | -4.343                                 |
| 53                      | 70        | 0.767                      | 0.640                | .6401               | 19.79                                     | 0.590                               | 0.630      | -6.329                                 |
| 61                      | 70        | 0.797                      | 0.648                | .6477               | 23.01                                     | 0.644                               | 0.630      | 2.235                                  |

Table 11 shows good agreement in the total weight percent solids between the experimental and simulation results (as there should be given the simulant recipes were defined by the simulation composition), with the high sodium simulants (points 10, 20, and 30) having a somewhat higher experimental value. The weight percent insoluble solids show more variation between the experimental and simulation values, but are of the same order of magnitude; measuring such small amounts of insoluble solids experimentally can be very difficult.

**Table 11. Comparison of Experimental with Simulation Dissolved and Undissolved Solids**

| envelope A simulation design point | design point temp (°C) | wt% Total Solids |            |              | wt% Insoluble Solids |            |
|------------------------------------|------------------------|------------------|------------|--------------|----------------------|------------|
|                                    |                        | analytical       | simulation | % difference | analytical           | simulation |
| 5                                  | 20                     | 27.51            | 27.07      | 1.62         | 0.694                | 0.239      |
| 10                                 | 20                     | 30.82            | 29.34      | 5.05         | 1.147                | 3.737      |
| 11                                 | 20                     | 26.59            | 26.95      | -1.34        | 0.086                | 1.494      |
| 13                                 | 20                     | 28.93            | 28.47      | 1.64         | 0.092                | 0.168      |
| 20                                 | 20                     | 30.66            | 29.34      | 4.52         | 0.823                | 3.737      |
| 21                                 | 20                     | 26.88            | 26.84      | 0.15         | 0.378                | 1.007      |
| 25                                 | 20                     | 27.64            | 27.32      | 1.17         | 0.850                | 0.313      |
| 26                                 | 20                     | 26.11            | 25.80      | 1.21         | 0.340                | 0.338      |
| 30                                 | 20                     | 30.19            | 29.22      | 3.33         | 0.477                | 3.319      |
| 33                                 | 20                     | 29.14            | 28.69      | 1.58         | 0.000                | 0.308      |
| 35                                 | 20                     | 27.44            | 27.26      | 0.67         | 0.614                | 0.275      |
| 53                                 | 70                     | 33.86            | 33.30      | 1.67         | 0.106                | 0.021      |
| 61                                 | 70                     | 30.44            | 29.92      | 1.75         | 0.444                | 0.068      |

Table 12 compares the forms of precipitated solids. OLI/ESP predicted calcium precipitates, where none was measured by XRD. However, the experimental slurry composition given in

Table 13 shows calcium to be present, whereas the experimental supernate composition (Table 8) shows essentially no calcium, therefore it is believed that calcium did precipitate in the experimental simulants but was not picked up by XRD. There is fairly close agreement on the predictions of sodium oxalate and sodium fluoride. The simulation predicts a greater frequency in the precipitation of gibbsite and NAS gel which is consistent with its lower aluminum solubility prediction (Table 8). The precise form in which the fluorides and phosphates precipitate is often different, but both occur in the simulation and experiment, where the simulation often predicts a calcium form and the experimental XRD results show a sodium form. XRD showed sodium carbonate precipitation occurring in 4 of the 13 points, but this was never predicted by the simulation.

**Table 12. Comparison of Experimental with Simulation Precipitated Solid Species**

| envelope A simulation design point | design point temp | Predicted/Measured Precipitated Solids            |                   |                                  |       |   |        |  |                           |                                   |                  |
|------------------------------------|-------------------|---|-------------------|----------------------------------|-------|---|--------|--|---------------------------|-----------------------------------|------------------|
|                                    |                   | Na <sub>2</sub> CO <sub>3</sub> xH <sub>2</sub> O | AlOH <sub>3</sub> | Na <sub>3</sub> FSO <sub>4</sub> | NaF   | Na <sub>2</sub> C <sub>2</sub> O <sub>4</sub> | NASGel | Na <sub>7</sub> FPO <sub>42</sub> 19H <sub>2</sub> O | NaPHOH 12H <sub>2</sub> O | Ca <sub>3</sub> PO <sub>4</sub> 2 | CaF <sub>2</sub> |
| 5                                  | 20                | -   | -                 | -                                | E - S | E - S   | -      | E - S  | -                         | -                                 | -                |
| 10                                 | 20                | -   | S                 | E                                | E - S | E - S   | S      | E  | -                         | -                                 | -                |
| 11                                 | 20                | -   | -                 | -                                | -     | E - S   | -      | -  | S                         | -                                 | -                |
| 13                                 | 20                | E   | E - S             | -                                | -     | E   | S      | -  | -                         | -                                 | -                |
| 20                                 | 20                | -   | S                 | E                                | E - S | E - S   | S      | E  | -                         | -                                 | -                |
| 21                                 | 20                | -   | -                 | -                                | -     | E - S   | S      | E  | S                         | S                                 | -                |
| 25                                 | 20                | -   | -                 | -                                | -     | E - S   | E - S  | E  | -                         | -                                 | S                |
| 26                                 | 20                | E   | S                 | -                                | -     | S   | S      | E  | -                         | -                                 | S                |
| 30                                 | 20                | -   | S                 | -                                | E - S | E - S   | E - S  | E  | -                         | -                                 | S                |
| 33                                 | 20                | E   | S                 | -                                | -     | E   | S      | -  | -                         | S                                 | S                |
| 35                                 | 20                | -   | -                 | -                                | E     | E - S   | S      | E  | -                         | -                                 | S                |
| 53                                 | 70                | E   | -                 | -                                | -     | E   | S      | -  | -                         | -                                 | -                |
| 61                                 | 70                | -   | -                 | -                                | -     | E   | E      | E  | -                         | S                                 | -                |

An "E" indicates the solid was observed experimentally by XRD, "S" indicates the solid was predicted by the simulation.

**Table 13. Experimental Slurry Composition**

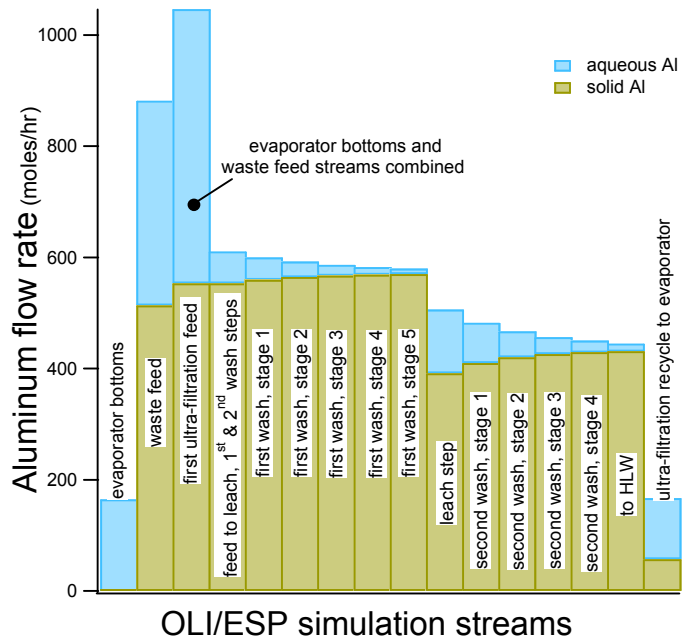
| run | Al (molar) | B (molar) | Ca (molar) | Mg (molar) | Na (molar) | P (molar) | Si (molar) | V (molar) | Zn (molar) | Zr (molar) | K (molar) | S (molar) |
|-----|------------|-----------|------------|------------|------------|-----------|------------|-----------|------------|------------|-----------|-----------|
| 5   | 1.69E-01   | 1.04E+01  | -          | -          | 3.79E+00   | 2.02E-02  | 3.88E-02   | -         | -          | 9.09E-05   | 4.80E-03  | 4.01E-02  |
| 10  | 7.47E-01   | 1.00E+01  | -          | -          | 3.90E+00   | 2.74E-03  | 2.19E-02   | -         | -          | 1.42E-04   | 1.66E-03  | 3.31E-02  |
| 11  | 1.74E-01   | 9.84E+00  | -          | -          | 3.66E+00   | 1.56E-02  | 3.97E-02   | -         | -          | 7.93E-05   | 3.43E-03  | 4.08E-02  |
| 13  | 1.60E-01   | 1.05E+01  | -          | -          | 3.56E+00   | 3.71E-03  | 3.20E-02   | -         | -          | -          | 2.98E-03  | 3.62E-02  |
| 20  | 1.63E-01   | 1.01E+01  | 4.52E-03   | 1.41E-03   | 3.80E+00   | 1.83E-02  | 2.33E-02   | 2.56E-04  | 2.47E-03   | 1.06E-04   | 8.72E-02  | 3.81E-02  |
| 21  | 1.60E-01   | 1.04E+01  | 4.39E-03   | 1.36E-03   | 3.83E+00   | 1.96E-02  | 3.39E-02   | -         | 2.51E-03   | 9.32E-05   | 9.03E-02  | 3.93E-02  |
| 25  | 1.57E-01   | 9.85E+00  | 4.18E-03   | 1.34E-03   | 3.52E+00   | 1.57E-02  | 3.00E-02   | -         | 2.46E-03   | 1.08E-04   | 8.94E-02  | 3.93E-02  |
| 26  | 6.91E-01   | 9.23E+00  | -          | -          | 3.63E+00   | 2.74E-03  | 1.96E-02   | 2.58E-04  | -          | 1.96E-04   | -         | 3.06E-02  |
| 30  | 7.10E-01   | 1.02E+01  | 3.40E-03   | 1.06E-03   | 3.79E+00   | 2.73E-03  | 8.87E-02   | -         | 2.18E-03   | 1.77E-04   | 7.72E-02  | 3.31E-02  |
| 33  | 1.53E-01   | 1.02E+01  | 3.21E-03   | 1.06E-03   | 3.34E+00   | 3.33E-03  | 2.34E-02   | 3.20E-04  | 1.91E-03   | 5.85E-05   | 6.71E-02  | 3.55E-02  |
| 35  | 1.59E-01   | 1.03E+01  | 3.28E-03   | 1.06E-03   | 3.50E+00   | 1.05E-02  | 2.71E-02   | -         | 1.95E-03   | 1.11E-04   | 7.23E-02  | 3.84E-02  |
| 53  | 1.78E-01   | 1.03E+01  | -          | -          | 3.94E+00   | 3.69E-03  | 2.11E-02   | -         | -          | 1.16E-04   | 3.29E-03  | 3.98E-02  |
| 61  | 1.84E-01   | 1.08E+01  | 4.55E-03   | 1.38E-03   | 4.25E+00   | 2.22E-02  | 3.02E-02   | -         | 2.47E-03   | -          | 8.50E-02  | 4.42E-02  |

### 2.6.3 Fate of Aluminum, Strontium, Sodium and NAS gel Through the Pre-Treatment Process for Three Waste Feed Compositions

Figure 16, Figure 17, and Figure 18 track aluminum through each stage of the pre-treatment process for waste feed from envelopes A (tank AN-104), B/D (tank AZ-102), and C (tank AN-107) respectively.

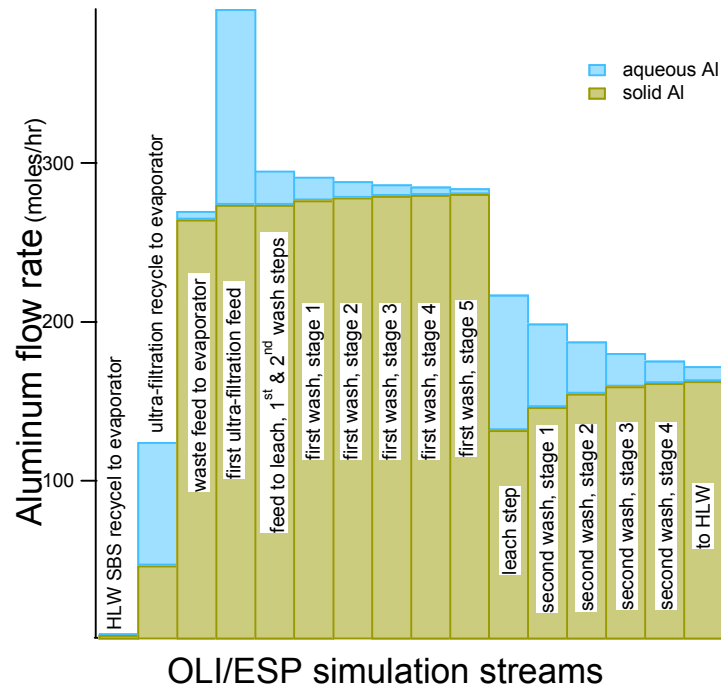
Figure 16 shows that the reduction of aluminum to HLW due to leaching for envelope A is minimal, with approximately 73% of the total aluminum fed to the wash and leach steps being sent to HLW. Most of this reduction occurs immediately following the leach step where a volume of supernate equal to that added as NaOH and steam is decanted from the slurry.

**Figure 16. Fate of Aluminum Through Pre-Treatment Process for AN-104**



The reduction of aluminum to HLW due to leaching is somewhat greater for envelope B/D (than for A) due to its higher aluminum solids content. Approximately 58% of the total aluminum fed to the wash and leach steps is sent to HLW, as shown in Figure 17.

**Figure 17. Fate of Aluminum Through Pre-Treatment Process for AZ-102**



Aluminum is not an issue for envelope C tanks and the leach step is not part of the pre-treatment process. Figure 18 is included only for comparison to the other envelopes.

**Figure 18. Fate of Aluminum Through Pre-Treatment Process for AN-107**

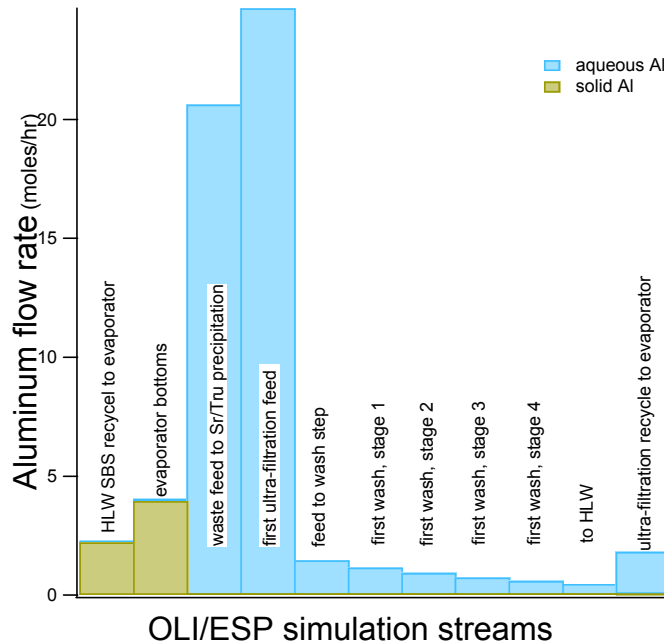
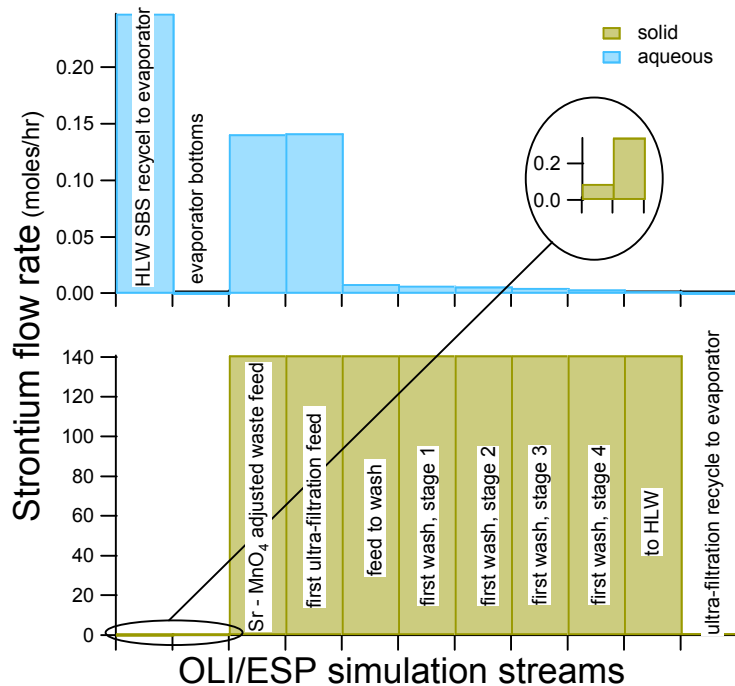


Figure 19 shows strontium in the pre-treatment process for envelope C; not surprisingly, essentially all the strontium remains as a precipitated solid and is sent to HLW.

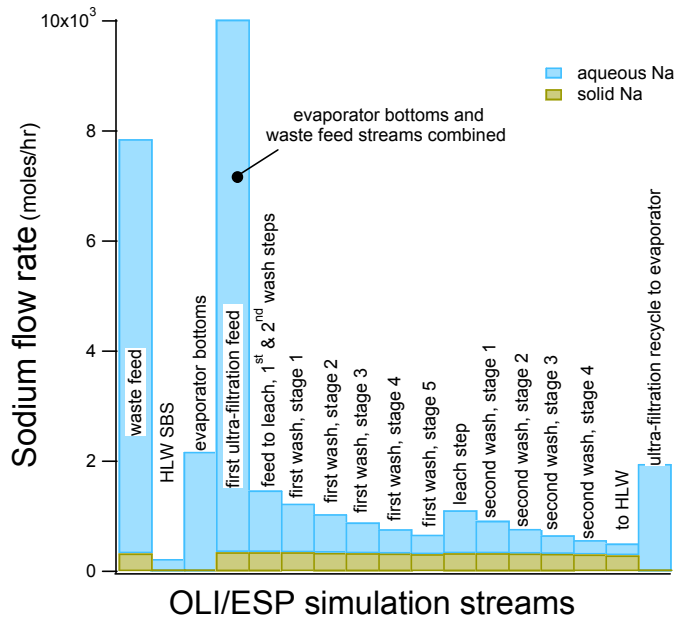
**Figure 19. Fate of Strontium Through Pre-Treatment Process for AN-107**



Note the difference in scale between the aqueous and solid phases.

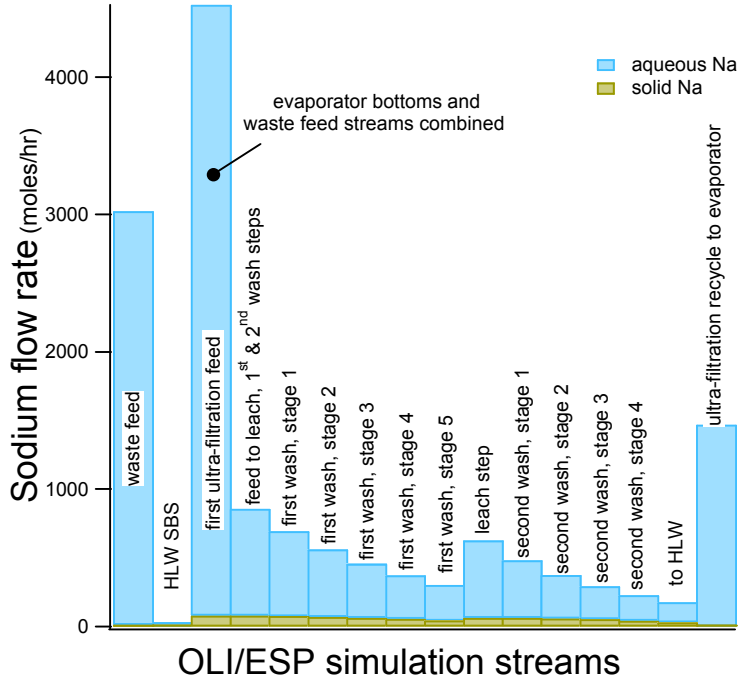
Figure 20, Figure 21, and Figure 22 track sodium through each stage of the pre-treatment process for waste feed from envelopes A (tank AN-104), B/D (tank AZ-102), and C (tank AN-107) respectively. The plots show the sodium is reduced by diluting the supernate, while the amount of sodium in the solids remains relatively constant. 34% of the sodium fed to the leach and wash step for envelope A (tank AN-104) is sent to HLW, as shown in Figure 20.

**Figure 20. Fate of Sodium Through Pre-Treatment Process for AN-104**



21% of Sodium fed to the leach and wash steps for envelope B/D are sent to HLW, as shown in Figure 21.

**Figure 21. Fate of Sodium Through Pre-Treatment Process for AZ-102**



32% of Na fed to the leach and wash steps for envelope C is sent to HLW, as shown in Figure 22.

**Figure 22. Fate of Sodium Through Pre-Treatment Process for AN-107**

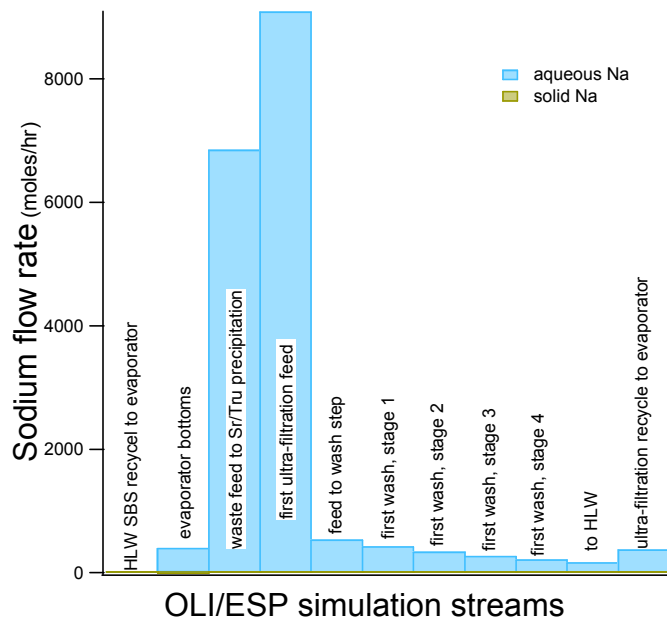
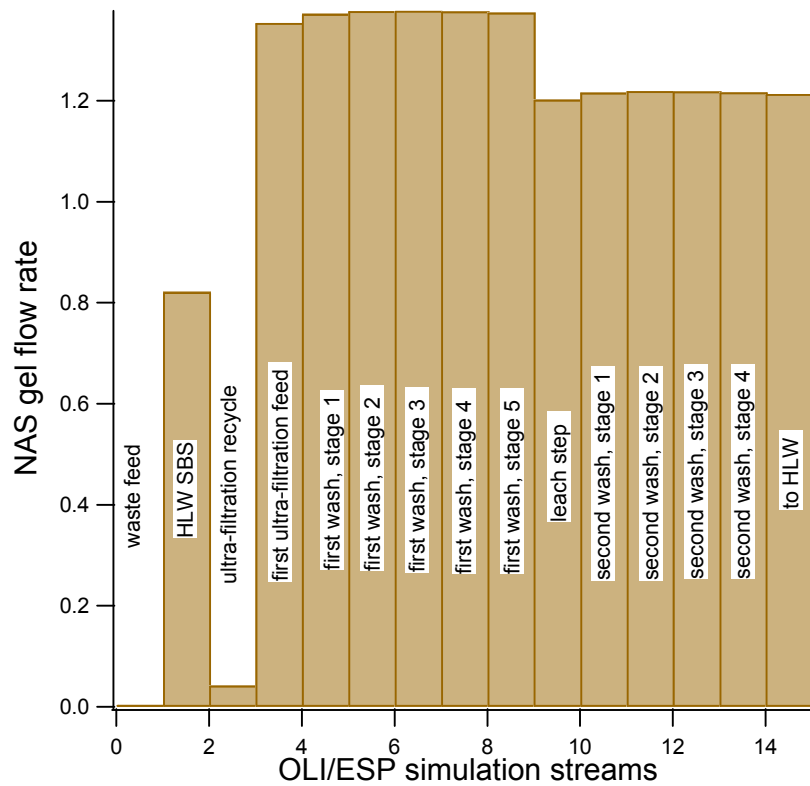
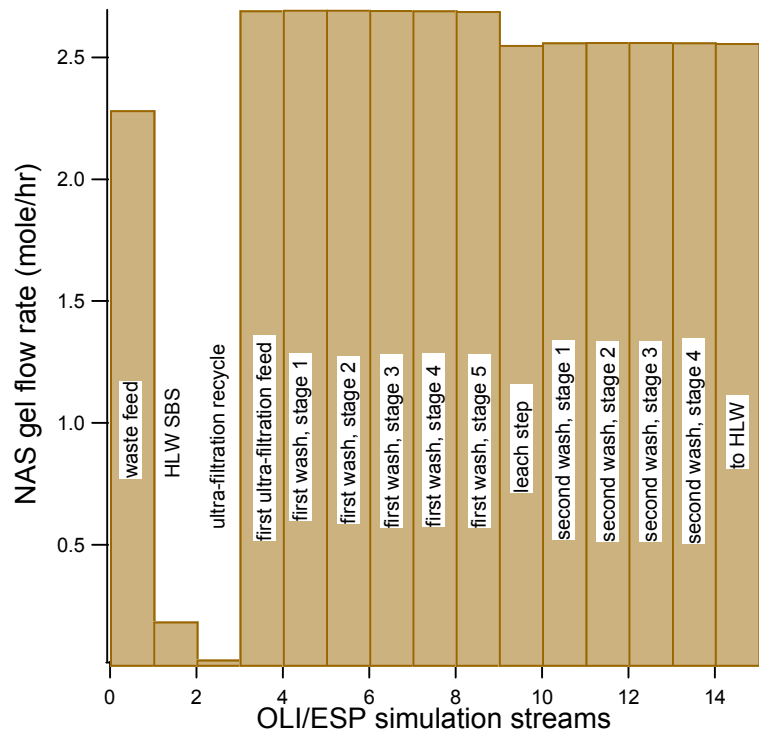


Figure 23 and Figure 24 show the progression of NAS gel through the pre-treatment process for wastes from envelope A and B/D respectively. Envelope C showed a small amount of NAS gel in the evaporator bottoms (0.34 moles/hr), and an insignificant amount in the ultra-filtration recycle (0.008moles/hr), but no NAS gel was present in the streams following the Sr/TRU precipitation step.

**Figure 23. Fate of NAS gel Through Pre-Treatment Process for AN-104**



**Figure 24. Fate of NAS gel Through Pre-Treatment Process for AZ-102**



### **3.0 FUTURE WORK**

Development of physical property models for AY-102 (C106) will be done in conjunction with the integrated pilot testing.

SrNaPO<sub>4</sub>.H<sub>2</sub>O solids which formed in experimental simulation work for envelope C are not included the OLI databases. This should be included in order to model its behavior in the pre-treatment process.

Blending of envelope A with envelope B/D wastes prior to the pre-treatment process are being considered as a method of generating continuous feed to both the HLW and LAW melters and minimize the HLW melter idle time. Modeling and experimental work could be performed to predict the compositions and solids precipitation of these blended feed streams, and the behavior of the blended streams through the pre-treatment process.

## 4.0 REFERENCES

1. Longwell, R.L. *Waste Feed Evaporation and Physical Properties Modeling*. 24590-PTF-TSP-RT-01-006, Rev. 0, Washington Group International, Richland, WA (2002)
2. Laurinat, J.E. and Choi, A.S. *Task Technical and Quality Assurance Plan for Waste Feed Evaporation and Physical Properties Modeling*. WSRC-TR-2002-00083, SRT-RPP-2002-00036, Rev. 0, Westinghouse Savannah River Co., Aiken, SC (2002)
3. SAS Institute, Inc., *JMP® Statistics and Graphics Guide*, SAS Institute Inc., Cary, NC, (2002)
4. Ye, K.Q., "Orthogonal Column Latin Hypercubes and Their Application in Computer Experiments". *J. American Statistical Association*. **93**: p. 1430-1439 ((1998)).
5. Choi, A.S. *Software Quality Assurance Plan for Hanford RPP-WTP Evaporator Modeling*. WSRC-RP-2001-00337, Westinghouse Savannah River Co., Aiken, SC 29808 (2001)
6. Ejaz, T., Jones, A.G., and Graham, P., "Solubility of Zeolite A and Its Amorphous Precursor under Synthesis Conditions". *J. Chem. Eng. Data*. **44**: p. 574-576 (1999).
7. Barnes, M.C., Addai-Mensah, J., and Gerson, A.R., "The Solubility of Sodalite and Cancrinite in Synthetic Spent Bayer Liquor". *Colloids Surfaces A: Physicochem. Eng. Aspects*. **157**: p. 101-116 (1999).
8. Kinrade, S.D. and Swaddle, T.W., "Direct Detection of Aluminosilicate Species in Aqueous Solution by Silicon-29 and Aluminum-27 NMR Spectroscopy". *Inorg. Chem.* **28**: p. 1952 - (1989).
9. Swaddle, T.W., Salerno, J., and Tregloan, P.A., "Aqueous Aluminates, Silicates, and Aluminosilicates". *Chem. Soc. Rev.*: p. 319-325 (1994).
10. Gout, R., *et al.*, "Raman Spectroscopic Study of Aluminum Silicate Complexes at 20 °C in Basic Solutions". *J. Solution Chem.* **29**: p. 1173-1186 (2000).
11. Helgeson, H.C., Kirkham, D.H., and Flowers, G.C., "Theoretical Prediction of the Thermodynamic Behavior of Aqueous Electrolytes at High Pressures and Temperatures. IV. Calculation of Activity Coefficients, Osmotic Coefficients, and Apparent Molal and Standard and Relative Partial Molal Properties to 5 kb and 600 C". *Am. J. Sci.* **281**: p. 1241-1516 (1981).
12. Diakanov, I., *et al.*, "An experimental and computational study of sodium-aluminum complexing in crustal fluids". *Geochim. Cosmochim. Acta*. **60**: p. 197-211 (1996).
13. Stefansson, A., "Dissolution of primary minerals of basalt in natural waters. I. Calculation of mineral solubilities from 0°C to 350°C". *Chem. Geol.* **172**: p. 225-250 (2000).
14. Bromley, L.A., "Thermodynamic Properties of Strong Electrolytes in Aqueous Solutions". *AICHE J.* **19**(2): p. 313-320 (1973).
15. Laurinat, J.E. *Re: Verification of Preliminary OLI Database for Aluminosilicate Solubilities*. SRT-ATS-2002-00057, Rev. 3, Savannah River Site, Aiken, SC 29808 (2002)
16. Breuer, R.G., Barsotti, L.R., and Kelly, A.C., "Behavior of Silica in Sodium Aluminate Solutions". *Extractive Metallurgy of Aluminum*. **1**: p. 133-157 (1963).
17. Park, H. and Englezos, P., "Sodium Aluminosilicate Crystal Formation in Alkaline Solutions Relevant to Closed Cycle Kraft Pulp Mills". *Can. J. Chem. Eng.* **76**: p. 915-920 (1998).

18. Bergman, I.M., *et al. WTP Material Balance and Process Flowsheet Bases, Requirements, and Results.* 24590-wtp-rpt-eng-01-004, Rev. 0, Bechtel, Richland, WA 99352 (2001)
19. Perry, R.H. and Green, D.W., *Perry's Chemical Engineer's Handbook.* 6th ed. p. 13-25, 13-26, McGraw-Hill Book Company, New York (1984)
20. Krikbride, R.A., *et al. Tank Farm Contractor Operation and Utilization Plan.* HNF-SD-WM-SP-012 Rev. 3, Numatec Hanford Corp. and CH2MHill Hanford Group, Inc, Richland, WA. (2001)
21. Edwards, T.B. *A Statistically Designed Test Matrix for a Computer Study of Waste Feed Evaporation for Envelope A (U).* SRT-SCS-2002-00065, Savannah River Site, Aiken, SC 29808 (2002)
22. Edwards, T.B. *A Statistically Designed Test Matrix for a Computer Study of Waste Feed Evaporation for Envelope B (U).* SRT-SCS-2003-00002, Savannah River Site, Aiken, SC 29808 (2003)
23. Edwards, T.B. *A Statistically Designed Test Matrix for a Computer Study of Waste Feed Evaporation for Envelope C (U).* SRT-SCS-2003-00010, Savannah River Site, Aiken, SC 29808 (2003)
24. Ye, K.Q., "Orthogonal Column Latin Hypercubes and Their Application in Computer Experiments." *J. American Statistical Association.* **93:** p. 1430-1439 (1998).
25. Edwards, T.B. *A Statistical Design to Support RPP LAW Feed Simulant Testing (U).* SRT-SCS-2002-00027, Savannah River Site, Aiken, SC 29808 (2002)
26. Stone, M.E., *et al. Waste Feed Evaporation: Physical Properties and Solubility Determination.* WSRC-TR-2003-00212 Rev 0, SRT-RPP-2003-00094 Rev. 0, Savannah River Site, Aiken, SC 29808 (2003)
27. Urie, M.W., *et al. Chemical Analysis and Physical Property Testing of 241-AZ-101 Tank Waste - Supernate and Centrifuged Solids.* WTP-RPT-048, Rev. A, Pacific Northwest National Laboratory, Richland, Washington 99352 (2002)
28. Brooks, K.P., *et al. Characterization, Washing, Leaching and Filtration of AZ-102 Sludge.* PNWD-3045, BNFL-RPT-038 Rev. 0, Pacific Northwest National Laboratory, Richland, Washington 99352 (2000)
29. Hay, M.S., *et al. Chemical Characterization of an Envelope C Sample from Hanford Tank 241-AN-102.* BNF-003-98-0250, Savannah River Site, Aiken, SC 29808 (2000)
30. Urie, M.W., *et al. Chemical Analysis and Physical Property Testing of 241-AN-102 Tank Waste - Supernate and Centrifuged Solids.* WTP-RPT-020 Rev. 0, Pacific Northwest National Laboratory, Richland, Washington 99352 (2001)
31. Urie, M.W., *et al. Inorganic and Radiochemical Analysis of AW-101 and AN-107 Tank Waste.* PNWD-2462, BNFL-RTP-008, Rev. 0, Pacific Northwest National Laboratory, Richland, Washington 99352 (1999)
32. Esch, R.A. *Tank Waste Remediation System Privatization Private Contractor Samples Waste Envelope C Material Tank 241-AN-107.* HNF-SD-WM-DP-205, Rev. 1, Pacific Northwest National Laboratory, Richland, Washington 99352 (1997)
33. Lokken, R.O., *et al. Complex Concentrate Pretreatment FY 1986 Progress Report.* PNL-7687-AD-940, Pacific Northwest National Laboratory, Richland, Washington 99352 (1986)
34. *International Critical Tables of Numerical Data, Physics, Chemistry and Technology,* ed. C.J. West, McGraw-Hill for the National Research Council, New York (1933)

## **APPENDIX A. EXAMPLE MODEL CALCULATION**

Example calculations are shown for envelopes A and B/D. Calculations for envelope C models are done the same as for envelope A.

### Envelope A Sample Calculation

The mixture variables used for envelope A and C models are expressed in molar concentrations relative to a 5M Na stream, as shown below.

Below are example analytical molar concentrations for mixture variables of the waste feed stream:

$\text{AlO}_2 = 0.9408\text{M}$ ,  $\text{CO}_3 = 0.2506\text{M}$ ,  $\text{F} = 0.0322\text{M}$ ,  $\text{NO}_2 = 1.246\text{M}$ ,  $\text{NO}_3 = 2.2078\text{M}$ ,  
 $\text{OH} = 1.5904\text{M}$ ,  $\text{PO}_4 = 0.03696\text{M}$

Below are example values for the process variables:

sodium of waste feed stream = 7M Na,

Temp. of feed stream to 1<sup>st</sup> ultra-filtration = 28°C

waste feed volumetric flow rate = 1,171 L/hr., HLW SBS volumetric flow rate = 1885 L/hr.

- 1) Normalize mixture variables to a 5M Na stream by multiplying the molar concentration by 5 and dividing by the analytical sodium molar concentration, in this case 7.

$$\begin{aligned} [\text{AlO}_2] &= 0.9408\text{M} \times 5 / 7 = 0.672\text{M}, \\ [\text{CO}_3] &= 0.2506\text{M} \times 5 / 7 = 0.179\text{M}, \\ [\text{F}] &= 0.0322\text{M} \times 5 / 7 = 0.23\text{M}, \\ [\text{NO}_2] &= 1.246\text{M} \times 5 / 7 = 0.89\text{M}, \\ [\text{NO}_3] &= 2.2078\text{M} \times 5 / 7 = 1.577\text{M}, \\ [\text{OH}] &= 1.5904\text{M} \times 5 / 7 = 1.136\text{M}, \\ [\text{PO}_4] &= 0.03696\text{M} \times 5 / 7 = 0.0264, \end{aligned}$$

- 2) Calculate the waste feed to HLW SBS volumetric ratio:

$$[\text{SBS}] = (\text{HLW SBS flow}) / (\text{waste feed flow}) = 1885(\text{L/hr.}) / 1,171(\text{L/hr.}) = 1.61$$

3) Input values into model equation:

$$\begin{aligned}
 \text{viscosity(cP)} &= 0.0544[NO_2] + 0.0608[NO_3] - 0.149[OH] \\
 &\quad + \exp\left(\frac{219}{77.4+[Temp]} - 0.947 - 0.0678[NO_2] - 0.134[NO_3]\right) \\
 &\quad \left. + 0.0611[OH] - 0.0826[NO_3][NO_2]\right) \\
 &= 0.0544(0.89) + 0.0608(1.577) - 0.149(1.136) \\
 &\quad + \exp\left(\frac{219}{77.4+(28)} - 0.947 - 0.0678(0.89) - 0.134(1.577)\right) \\
 &\quad \left. + 0.0611(1.136) - 0.0826(0.89)(1.577)\right) \\
 &= 2.229(cP)
 \end{aligned}$$

Although the process variables [SBS] and [Na] were not used in this example, the values applied to the model equations would be 1.16 and 7 respectively.

#### Envelope B/D Sample Calculation

The mixture variables used for envelope B/D models are expressed in term of their mass fraction relative to the total mass of the mixture variables, as shown below.

Below are example analytical masses given for mixture variables of the waste feed stream based on the *total solids* of the waste stream:

$\text{AlO}_2 = 0.42825\text{g}$ ,  $\text{CO}_3 = 0.9555\text{g}$ ,  $\text{Fe} = 0.17526\text{g}$ ,  $\text{NO}_3 = 0.87771\text{g}$ ,  $\text{OH} = 0.2529\text{g}$ ,  
 $\text{SO}_4 = 0.31038\text{g}$

(all aluminum and sulfur are treated as  $\text{AlO}_2$  and  $\text{SO}_4$  and should be assigned be molecular weight of these anions, i.e. grams of  $\text{AlO}_2$  = moles of Al  $\times$  59)

Below are example values for the process variables:

sodium of waste feed stream = 2.5M Na,

Temp. of feed stream to 1<sup>st</sup> ultra-filtration = 68°C

waste feed volumetric flow rate = 1,171 L/hr., HLW SBS volumetric flow rate = 1464 L/hr.

- 1) Normalize mixture variables to a mass fraction by dividing by the total mass of the mixture variables:

$$\begin{aligned}
 \text{Total mixture variable mass} &= 0.42825\text{g} + 0.9555\text{g} + 0.17526\text{g} + 0.87771\text{g} + 0.2529\text{g} \\
 &\quad + 0.31038\text{g} \\
 &= 3\text{g}
 \end{aligned}$$

$$[\text{AlO}_2] = 0.42825\text{g} / 3\text{g} = 0.14275,$$

$$[\text{CO}_3] = 0.9555\text{g} / 3\text{g} = .3185,$$

$$[\text{Fe}] = 0.17526\text{g} / 3\text{g} = 0.05842,$$

$$\begin{aligned} [\text{NO}_3] &= 0.87771 \text{g} / 3\text{g} = 0.29257, \\ [\text{OH}] &= 0.2529 \text{g} / 3\text{g} = 0.0843, \\ [\text{SO}_4] &= 0.31038 \text{g} / 3\text{g} = 0.10346, \end{aligned}$$

2) Calculate the waste feed to HLW SBS volumetric ratio:

$$[\text{SBS}] = (\text{HLW SBS flow}) / (\text{waste feed flow}) = 1464(\text{L/hr.}) / 1,171(\text{L/hr.}) = 1.25$$

3) Input values into model equation:

$$\begin{aligned} \text{viscosity(cP)} &= -0.0454[\text{NO}_3] + 0.0045[\text{SBS}] \\ &\quad + \exp \left( \frac{312}{98.7 + [\text{Temp}]} - 1.83 + 0.134[\text{AlO}_2] \right) \\ &\quad + 0.22[\text{CO}_3] - 0.0109[\text{SBS}] \\ &= -0.0454(0.29257) + 0.0045(1.25) \\ &\quad + \exp \left( \frac{312}{98.7 + (68)} - 1.83 + 0.134(0.14275) \right) \\ &\quad + 0.22(0.3185) - 0.0109(1.25) \\ &= 1.117(\text{cP}) \end{aligned}$$

Although the process variable [Na] was not used in this example, the value applied to the model equation would be 2.5.

## APPENDIX B. DESIGN MATRICES FOR ENVELOPES A, B/D, AND C

The following tables list the compositions of the waste feed stream, SBS/Feed volumetric flow ratio, and filtration feed stream temperature used in the OLI/ESP computer simulations. The mixture variables for envelopes A-a and C are given in terms of 5M Na stream, and in terms of the mass fraction to the total mass of the mixture variables for envelope B/D. The sodium concentration represents a “dilution factor” of the waste feed stream, water is added or removed to a waste feed stream of a given mixture variable concentration to achieve the target sodium molarity. The Test ID describes the type of design point. MPV indicates a model design point used in the property model fit and are derived using only the minimum and maximum values of the factor space. OLH indicates a design point used to validate the model (though some were occasionally used in the model fits as described in the results section), and were generated to be uniformly distributed over the factor space (as opposed to only the extreme vertices of the MPV points).

**Table 14. Sub-envelope A-a Computer Simulation Design Matrix**

| Test ID | Type | [AlO <sub>2</sub> ]<br>(molar at<br>5M Na) | [CO <sub>3</sub> ]<br>(molar at<br>5M Na) | [F]<br>(molar at<br>5M Na) | [NO <sub>2</sub> ]<br>(molar at<br>5M Na) | [NO <sub>3</sub> ]<br>(molar at<br>5M Na) | [OH]<br>(molar at<br>5M Na) | [PO <sub>4</sub> ]<br>(molar at<br>5M Na) | SBS/Feed | [Na]<br>(molar) | Temp (°C) |
|---------|------|--|---|----------------------------|---|---|-----------------------------|---|----------|-----------------|-----------|
| 1       | MPV  | 0.206984                                   | 0.032611                                  | 0.009284                   | 0.73098                                   | 0.991014                                  | 2.606201                    | 0.042265                                  | 0        | 5.6             | 20        |
| 2       | MPV  | 0.206984                                   | 0.032611                                  | 0.009284                   | 0.730981                                  | 0.991014                                  | 2.71405                     | 0.006315                                  | 0        | 5.6             | 20        |
| 3       | MPV  | 0.206984                                   | 0.032611                                  | 0.009284                   | 1.541582                                  | 1.911454                                  | 0.983009                    | 0.006315                                  | 0        | 5.6             | 20        |
| 4       | MPV  | 0.206984                                   | 0.032611                                  | 0.228819                   | 0.730982                                  | 2.016651                                  | 1.468877                    | 0.006315                                  | 0        | 5.6             | 20        |
| 5       | MPV  | 0.206984                                   | 0.032611                                  | 0.228819                   | 1.541581                                  | 0.991014                                  | 1.600911                    | 0.033983                                  | 0        | 5.6             | 20        |
| 6       | MPV  | 0.206984                                   | 0.665097                                  | 0.228819                   | 0.73098                                   | 1.154545                                  | 0.983009                    | 0.033983                                  | 0        | 5.6             | 20        |
| 7       | MPV  | 0.673054                                   | 0.665097                                  | 0.009284                   | 0.73098                                   | 0.991014                                  | 0.983009                    | 0.006315                                  | 0        | 5.6             | 20        |
| 8       | MPV  | 0.736049                                   | 0.032611                                  | 0.009284                   | 0.73098                                   | 2.016651                                  | 1.051499                    | 0.042265                                  | 0        | 5.6             | 20        |
| 9       | MPV  | 0.824593                                   | 0.032611                                  | 0.009284                   | 1.541582                                  | 0.991014                                  | 1.17799                     | 0.042265                                  | 0        | 5.6             | 20        |
| 10      | MPV  | 1.085885                                   | 0.032611                                  | 0.228819                   | 0.730982                                  | 0.991014                                  | 1.615613                    | 0.006315                                  | 0        | 5.6             | 20        |
| 11      | MPV  | 0.206984                                   | 0.032611                                  | 0.009284                   | 0.73098                                   | 0.991014                                  | 2.606201                    | 0.042265                                  | 0        | 7               | 20        |
| 12      | MPV  | 0.206984                                   | 0.032611                                  | 0.009284                   | 0.730981                                  | 0.991014                                  | 2.71405                     | 0.006315                                  | 0        | 7               | 20        |
| 13      | MPV  | 0.206984                                   | 0.032611                                  | 0.009284                   | 1.541582                                  | 1.911454                                  | 0.983009                    | 0.006315                                  | 0        | 7               | 20        |
| 14      | MPV  | 0.206984                                   | 0.032611                                  | 0.228819                   | 0.730982                                  | 2.016651                                  | 1.468877                    | 0.006315                                  | 0        | 7               | 20        |
| 15      | MPV  | 0.206984                                   | 0.032611                                  | 0.228819                   | 1.541581                                  | 0.991014                                  | 1.600911                    | 0.033983                                  | 0        | 7               | 20        |
| 16      | MPV  | 0.206984                                   | 0.665097                                  | 0.228819                   | 0.73098                                   | 1.154545                                  | 0.983009                    | 0.033983                                  | 0        | 7               | 20        |
| 17      | MPV  | 0.673054                                   | 0.665097                                  | 0.009284                   | 0.73098                                   | 0.991014                                  | 0.983009                    | 0.006315                                  | 0        | 7               | 20        |
| 18      | MPV  | 0.736049                                   | 0.032611                                  | 0.009284                   | 0.73098                                   | 2.016651                                  | 1.051499                    | 0.042265                                  | 0        | 7               | 20        |
| 19      | MPV  | 0.824593                                   | 0.032611                                  | 0.009284                   | 1.541582                                  | 0.991014                                  | 1.17799                     | 0.042265                                  | 0        | 7               | 20        |
| 20      | MPV  | 1.085885                                   | 0.032611                                  | 0.228819                   | 0.730982                                  | 0.991014                                  | 1.615613                    | 0.006315                                  | 0        | 7               | 20        |
| 21      | MPV  | 0.206984                                   | 0.032611                                  | 0.009284                   | 0.73098                                   | 0.991014                                  | 2.606201                    | 0.042265                                  | 2        | 5.6             | 20        |
| 22      | MPV  | 0.206984                                   | 0.032611                                  | 0.009284                   | 0.730981                                  | 0.991014                                  | 2.71405                     | 0.006315                                  | 2        | 5.6             | 20        |
| 23      | MPV  | 0.206984                                   | 0.032611                                  | 0.009284                   | 1.541582                                  | 1.911454                                  | 0.983009                    | 0.006315                                  | 2        | 5.6             | 20        |
| 24      | MPV  | 0.206984                                   | 0.032611                                  | 0.228819                   | 0.730982                                  | 2.016651                                  | 1.468877                    | 0.006315                                  | 2        | 5.6             | 20        |
| 25      | MPV  | 0.206984                                   | 0.032611                                  | 0.228819                   | 1.541581                                  | 0.991014                                  | 1.600911                    | 0.033983                                  | 2        | 5.6             | 20        |
| 26      | MPV  | 0.206984                                   | 0.665097                                  | 0.228819                   | 0.73098                                   | 1.154545                                  | 0.983009                    | 0.033983                                  | 2        | 5.6             | 20        |
| 27      | MPV  | 0.673054                                   | 0.665097                                  | 0.009284                   | 0.73098                                   | 0.991014                                  | 0.983009                    | 0.006315                                  | 2        | 5.6             | 20        |
| 28      | MPV  | 0.736049                                   | 0.032611                                  | 0.009284                   | 0.73098                                   | 2.016651                                  | 1.051499                    | 0.042265                                  | 2        | 5.6             | 20        |
| 29      | MPV  | 0.824593                                   | 0.032611                                  | 0.009284                   | 1.541582                                  | 0.991014                                  | 1.17799                     | 0.042265                                  | 2        | 5.6             | 20        |
| 30      | MPV  | 1.085885                                   | 0.032611                                  | 0.228819                   | 0.730982                                  | 0.991014                                  | 1.615613                    | 0.006315                                  | 2        | 5.6             | 20        |











**Table 16. Envelope C Computer Simulation Design Matrix**

| Test ID | Type | [AlO2]<br>(molar at<br>5M Na) | [CO3]<br>(molar at<br>5M Na) | [NO2]<br>(molar at<br>5M Na) | [NO3]<br>(molar at<br>5M Na) | [OH]<br>(molar at<br>5M Na) | [SO4]<br>(molar at<br>5M Na) | SBS/Feed | [Na]<br>(molar) | Temp (oC) |
|---------|------|-------------------------------|------------------------------|------------------------------|------------------------------|-----------------------------|------------------------------|----------|-----------------|-----------|
| 1       | MPV  | 0.015                         | 0.94                         | 0.78                         | 1.5                          | 0.2438                      | 0.112                        | 0        | 7               | 20        |
| 2       | MPV  | 0.015                         | 0.94                         | 0.78                         | 1.5                          | 0.2438                      | 0.112                        | 0        | 8.5             | 20        |
| 3       | MPV  | 0.015                         | 0.94                         | 0.78                         | 1.5                          | 0.2438                      | 0.112                        | 2        | 7               | 20        |
| 4       | MPV  | 0.015                         | 0.94                         | 0.78                         | 1.5                          | 0.2438                      | 0.112                        | 2        | 8.5             | 20        |
| 5       | MPV  | 0.015                         | 0.94                         | 0.78                         | 1.5                          | 0.2438                      | 0.112                        | 0        | 7               | 70        |
| 6       | MPV  | 0.015                         | 0.94                         | 0.78                         | 1.5                          | 0.2438                      | 0.112                        | 0        | 8.5             | 70        |
| 7       | MPV  | 0.015                         | 0.94                         | 0.78                         | 1.5                          | 0.2438                      | 0.112                        | 2        | 7               | 70        |
| 8       | MPV  | 0.015                         | 0.94                         | 0.78                         | 1.5                          | 0.2438                      | 0.112                        | 2        | 8.5             | 70        |
| 9       | MPV  | 0.0888                        | 0.56                         | 0.78                         | 2.3                          | 0.13                        | 0.112                        | 0        | 7               | 20        |
| 10      | MPV  | 0.0888                        | 0.56                         | 0.78                         | 2.3                          | 0.13                        | 0.112                        | 0        | 8.5             | 20        |
| 11      | MPV  | 0.0888                        | 0.56                         | 0.78                         | 2.3                          | 0.13                        | 0.112                        | 2        | 7               | 20        |
| 12      | MPV  | 0.0888                        | 0.56                         | 0.78                         | 2.3                          | 0.13                        | 0.112                        | 2        | 8.5             | 20        |
| 13      | MPV  | 0.0888                        | 0.56                         | 0.78                         | 2.3                          | 0.13                        | 0.112                        | 0        | 7               | 70        |
| 14      | MPV  | 0.0888                        | 0.56                         | 0.78                         | 2.3                          | 0.13                        | 0.112                        | 0        | 8.5             | 70        |
| 15      | MPV  | 0.0888                        | 0.56                         | 0.78                         | 2.3                          | 0.13                        | 0.112                        | 2        | 7               | 70        |
| 16      | MPV  | 0.0888                        | 0.56                         | 0.78                         | 2.3                          | 0.13                        | 0.112                        | 2        | 8.5             | 70        |
| 17      | MPV  | 0.015                         | 0.5754                       | 0.78                         | 2.3                          | 0.295                       | 0.051                        | 0        | 7               | 20        |
| 18      | MPV  | 0.015                         | 0.5754                       | 0.78                         | 2.3                          | 0.295                       | 0.051                        | 0        | 8.5             | 20        |
| 19      | MPV  | 0.015                         | 0.5754                       | 0.78                         | 2.3                          | 0.295                       | 0.051                        | 2        | 7               | 20        |
| 20      | MPV  | 0.015                         | 0.5754                       | 0.78                         | 2.3                          | 0.295                       | 0.051                        | 2        | 8.5             | 20        |
| 21      | MPV  | 0.015                         | 0.5754                       | 0.78                         | 2.3                          | 0.295                       | 0.051                        | 0        | 7               | 70        |
| 22      | MPV  | 0.015                         | 0.5754                       | 0.78                         | 2.3                          | 0.295                       | 0.051                        | 0        | 8.5             | 70        |
| 23      | MPV  | 0.015                         | 0.5754                       | 0.78                         | 2.3                          | 0.295                       | 0.051                        | 2        | 7               | 70        |
| 24      | MPV  | 0.015                         | 0.5754                       | 0.78                         | 2.3                          | 0.295                       | 0.051                        | 2        | 8.5             | 70        |
| 25      | MPV  | 0.015                         | 0.8529                       | 1.19                         | 1.5                          | 0.13                        | 0.051                        | 0        | 7               | 20        |
| 26      | MPV  | 0.015                         | 0.8529                       | 1.19                         | 1.5                          | 0.13                        | 0.051                        | 0        | 8.5             | 20        |
| 27      | MPV  | 0.015                         | 0.8529                       | 1.19                         | 1.5                          | 0.13                        | 0.051                        | 2        | 7               | 20        |
| 28      | MPV  | 0.015                         | 0.8529                       | 1.19                         | 1.5                          | 0.13                        | 0.051                        | 2        | 8.5             | 20        |
| 29      | MPV  | 0.015                         | 0.8529                       | 1.19                         | 1.5                          | 0.13                        | 0.051                        | 0        | 7               | 70        |
| 30      | MPV  | 0.015                         | 0.8529                       | 1.19                         | 1.5                          | 0.13                        | 0.051                        | 0        | 8.5             | 70        |
| 31      | MPV  | 0.015                         | 0.8529                       | 1.19                         | 1.5                          | 0.13                        | 0.051                        | 2        | 7               | 70        |
| 32      | MPV  | 0.015                         | 0.8529                       | 1.19                         | 1.5                          | 0.13                        | 0.051                        | 2        | 8.5             | 70        |
| 33      | MPV  | 0.29                          | 0.9204                       | 0.78                         | 1.5                          | 0.13                        | 0.051                        | 0        | 7               | 20        |
| 34      | MPV  | 0.29                          | 0.9204                       | 0.78                         | 1.5                          | 0.13                        | 0.051                        | 0        | 8.5             | 20        |
| 35      | MPV  | 0.29                          | 0.9204                       | 0.78                         | 1.5                          | 0.13                        | 0.051                        | 2        | 7               | 20        |
| 36      | MPV  | 0.29                          | 0.9204                       | 0.78                         | 1.5                          | 0.13                        | 0.051                        | 2        | 8.5             | 20        |
| 37      | MPV  | 0.29                          | 0.9204                       | 0.78                         | 1.5                          | 0.13                        | 0.051                        | 0        | 7               | 70        |
| 38      | MPV  | 0.29                          | 0.9204                       | 0.78                         | 1.5                          | 0.13                        | 0.051                        | 0        | 8.5             | 70        |
| 39      | MPV  | 0.29                          | 0.9204                       | 0.78                         | 1.5                          | 0.13                        | 0.051                        | 2        | 7               | 70        |
| 40      | MPV  | 0.29                          | 0.9204                       | 0.78                         | 1.5                          | 0.13                        | 0.051                        | 2        | 8.5             | 70        |
| 41      | MPV  | 0.29                          | 0.56                         | 1.19                         | 1.5238                       | 0.295                       | 0.112                        | 0        | 7               | 20        |
| 42      | MPV  | 0.29                          | 0.56                         | 1.19                         | 1.5238                       | 0.295                       | 0.112                        | 0        | 8.5             | 20        |
| 43      | MPV  | 0.29                          | 0.56                         | 1.19                         | 1.5238                       | 0.295                       | 0.112                        | 2        | 7               | 20        |
| 44      | MPV  | 0.29                          | 0.56                         | 1.19                         | 1.5238                       | 0.295                       | 0.112                        | 2        | 8.5             | 20        |
| 45      | MPV  | 0.29                          | 0.56                         | 1.19                         | 1.5238                       | 0.295                       | 0.112                        | 0        | 7               | 70        |
| 46      | MPV  | 0.29                          | 0.56                         | 1.19                         | 1.5238                       | 0.295                       | 0.112                        | 0        | 8.5             | 70        |
| 47      | MPV  | 0.29                          | 0.56                         | 1.19                         | 1.5238                       | 0.295                       | 0.112                        | 2        | 7               | 70        |
| 48      | MPV  | 0.29                          | 0.56                         | 1.19                         | 1.5238                       | 0.295                       | 0.112                        | 2        | 8.5             | 70        |
| 49      | OLH  | 0.015                         | 0.68172                      | 0.8825                       | 2.05674                      | 0.13258                     | 0.09627                      | 1.75     | 8.32            | 42.66     |
| 50      | OLH  | 0.02145                       | 0.83313                      | 0.79281                      | 1.79107                      | 0.2473                      | 0.061955                     | 1.17     | 7.81            | 52.42     |
| 51      | OLH  | 0.02359                       | 0.65797                      | 1.18039                      | 1.70871                      | 0.27309                     | 0.07054                      | 1.08     | 7.62            | 64.92     |



**WSRC-TR-2003-00172, REV. 0**  
**SRT-RPP-2003-00073. REV. 0**

| Test ID | Type | [AlO2]<br>(molar at<br>5M Na) | [CO3]<br>(molar at<br>5M Na) | [NO2]<br>(molar at<br>5M Na) | [NO3]<br>(molar at<br>5M Na) | [OH]<br>(molar at<br>5M Na) | [SO4]<br>(molar at<br>5M Na) | SBS/Feed | [Na]<br>(molar) | Temp (oC) |
|---------|------|-------------------------------|------------------------------|------------------------------|------------------------------|-----------------------------|------------------------------|----------|-----------------|-----------|
| 105     | OLH  | 0.19332                       | 0.71734                      | 0.82164                      | 1.84502                      | 0.23184                     | 0.05815                      | 1.44     | 8.11            | 68.83     |
| 106     | OLH  | 0.19547                       | 0.87766                      | 0.87289                      | 1.55114                      | 0.15836                     | 0.05481                      | 0.08     | 7.59            | 44.61     |
| 107     | OLH  | 0.20191                       | 0.56                         | 1.11633                      | 1.83984                      | 0.25891                     | 0.052905                     | 0.91     | 8.05            | 26.25     |
| 108     | OLH  | 0.20836                       | 0.60453                      | 1.00422                      | 1.87385                      | 0.17383                     | 0.08674                      | 1.64     | 7.48            | 32.5      |
| 109     | OLH  | 0.21051                       | 0.76188                      | 0.83445                      | 1.6171                       | 0.29113                     | 0.082925                     | 0.14     | 7.64            | 39.14     |
| 110     | OLH  | 0.2148                        | 0.58969                      | 1.14516                      | 1.69866                      | 0.26277                     | 0.071015                     | 1.39     | 7.61            | 20.39     |
| 111     | OLH  | 0.21695                       | 0.75594                      | 0.93375                      | 1.51878                      | 0.24602                     | 0.10771                      | 1.05     | 7.33            | 22.73     |
| 112     | OLH  | 0.2191                        | 0.57188                      | 0.89531                      | 1.97907                      | 0.18156                     | 0.112                        | 0.2      | 7.53            | 46.95     |
| 113     | OLH  | 0.22125                       | 0.62828                      | 0.78                         | 1.9627                       | 0.28598                     | 0.068155                     | 0.23     | 8.31            | 55.16     |
| 114     | OLH  | 0.2234                        | 0.80344                      | 0.85047                      | 1.55288                      | 0.25762                     | 0.075775                     | 0.84     | 8.01            | 27.81     |
| 115     | OLH  | 0.22555                       | 0.68469                      | 0.84406                      | 1.77814                      | 0.21121                     | 0.10723                      | 1.33     | 7.96            | 61.41     |
| 116     | OLH  | 0.2277                        | 0.64016                      | 1.04906                      | 1.76516                      | 0.16996                     | 0.0753                       | 0.78     | 8.44            | 38.36     |
| 117     | OLH  | 0.23414                       | 0.60156                      | 0.81203                      | 2.00838                      | 0.26406                     | 0.060535                     | 1.72     | 7.01            | 49.69     |
| 118     | OLH  | 0.24273                       | 0.68766                      | 1.0907                       | 1.5566                       | 0.23828                     | 0.069585                     | 0.66     | 7.63            | 31.72     |
| 119     | OLH  | 0.24488                       | 0.69063                      | 0.86648                      | 1.80938                      | 0.18543                     | 0.077685                     | 0.98     | 7.95            | 68.05     |
| 120     | OLH  | 0.25563                       | 0.73219                      | 0.82805                      | 1.72865                      | 0.15449                     | 0.1058                       | 2        | 7.38            | 53.98     |
| 121     | OLH  | 0.26422                       | 0.63125                      | 1.10992                      | 1.70846                      | 0.14805                     | 0.074825                     | 1.2      | 8.41            | 22.34     |
| 122     | OLH  | 0.26637                       | 0.63422                      | 0.85688                      | 1.94618                      | 0.14289                     | 0.08102                      | 1.13     | 8.43            | 66.88     |
| 123     | OLH  | 0.27066                       | 0.70547                      | 1.01383                      | 1.61464                      | 0.19832                     | 0.067205                     | 1.42     | 7.2             | 43.44     |
| 124     | OLH  | 0.27711                       | 0.71141                      | 0.95938                      | 1.51344                      | 0.2718                      | 0.099125                     | 0.38     | 7.13            | 65.31     |
| 125     | OLH  | 0.28141                       | 0.84203                      | 0.78961                      | 1.55089                      | 0.15191                     | 0.09246                      | 0.92     | 7.88            | 25.08     |
| 126     | OLH  | 0.2857                        | 0.64313                      | 0.80242                      | 1.9983                       | 0.13                        | 0.07006                      | 0.3      | 7.73            | 51.25     |
| 127     | OLH  | 0.28785                       | 0.67578                      | 0.83766                      | 1.78053                      | 0.20219                     | 0.091505                     | 0.16     | 8.2             | 56.33     |

## APPENDIX C. UNDISSOLVED SOLIDS PREDICTED BY OLI/ESP FOR ENVELOPES A-a, B/D, AND C

The following tables list the solids present in the feed to the 1<sup>st</sup> ultra-filtration step as the mass fraction of the total undissolved (insoluble) solids. NAS gel was the only form of sodium aluminosilicate turned on during the simulations as it is the precursor to all other forms (i.e. cancrinite). The last row of each table lists the number of simulations for which the solids was present.

**Table 17. Sub-Envelope A-a Solids**

| Run# | MGOH2    | NASGEL   | CAF2     | ALOH3    | NIOH2    | NA2C2O4  | CA3PO42  | NAF      | NAPHOH<br>.12H2O | CAOH2    | CACO3    | NAFPO4<br>.19H2O | sum      |
|------|----------|----------|----------|----------|----------|----------|----------|----------|------------------|----------|----------|------------------|----------|
| 1    | 4.11E-05 | -        | -        | -        | -        | 1.67E-01 | -        | -        | 8.33E-01         | -        | -        | -                | 1.00E+00 |
| 2    | 4.11E-05 | -        | -        | -        | -        | 1.00E+00 | -        | -        | -                | -        | -        | -                | 1.00E+00 |
| 3    | 4.74E-05 | 2.69E-01 | -        | 7.31E-01 | -        | -        | -        | -        | -                | -        | -        | -                | 1.00E+00 |
| 4    | 4.51E-05 | 4.29E-01 | -        | -        | -        | 5.71E-01 | -        | -        | -                | -        | -        | -                | 1.00E+00 |
| 5    | 4.26E-05 | -        | -        | -        | -        | 5.13E-01 | -        | 3.26E-01 | -                | -        | -        | 1.61E-01         | 1.00E+00 |
| 6    | 4.69E-05 | 2.60E-01 | -        | 6.65E-01 | -        | 7.49E-02 | -        | -        | -                | -        | -        | -                | 1.00E+00 |
| 7    | 4.60E-05 | 1.13E-02 | -        | 9.32E-01 | 6.38E-05 | 5.61E-02 | -        | -        | -                | -        | -        | -                | 1.00E+00 |
| 8    | 4.61E-05 | 8.59E-03 | -        | 9.53E-01 | 7.50E-05 | 3.79E-02 | -        | -        | -                | -        | -        | -                | 1.00E+00 |
| 9    | 4.59E-05 | 6.88E-03 | -        | 9.29E-01 | 5.96E-05 | 6.39E-02 | -        | -        | -                | -        | -        | -                | 1.00E+00 |
| 10   | 4.59E-05 | 1.23E-03 | -        | 8.16E-01 | 6.87E-05 | 5.68E-02 | -        | 1.26E-01 | -                | -        | -        | -                | 1.00E+00 |
| 11   | 4.11E-05 | -        | -        | -        | -        | 1.67E-01 | -        | -        | 8.33E-01         | -        | -        | -                | 1.00E+00 |
| 12   | 4.11E-05 | -        | -        | -        | -        | 1.00E+00 | -        | -        | -                | -        | -        | -                | 1.00E+00 |
| 13   | 4.74E-05 | 2.69E-01 | -        | 7.31E-01 | -        | -        | -        | -        | -                | -        | -        | -                | 1.00E+00 |
| 14   | 4.51E-05 | 4.29E-01 | -        | -        | -        | 5.71E-01 | -        | -        | -                | -        | -        | -                | 1.00E+00 |
| 15   | 4.26E-05 | -        | -        | -        | -        | 5.25E-01 | -        | 3.33E-01 | -                | -        | -        | 1.42E-01         | 1.00E+00 |
| 16   | 4.69E-05 | 2.60E-01 | -        | 6.65E-01 | -        | 7.49E-02 | -        | -        | -                | -        | -        | -                | 1.00E+00 |
| 17   | 4.60E-05 | 1.13E-02 | -        | 9.32E-01 | 6.38E-05 | 5.61E-02 | -        | -        | -                | -        | -        | -                | 1.00E+00 |
| 18   | 4.61E-05 | 8.59E-03 | -        | 9.53E-01 | 7.50E-05 | 3.78E-02 | -        | -        | -                | -        | -        | -                | 1.00E+00 |
| 19   | 4.59E-05 | 6.88E-03 | -        | 9.29E-01 | 5.97E-05 | 6.39E-02 | -        | -        | -                | -        | -        | -                | 1.00E+00 |
| 20   | 4.59E-05 | 1.23E-03 | -        | 8.16E-01 | 6.86E-05 | 5.68E-02 | -        | 1.26E-01 | -                | -        | -        | -                | 1.00E+00 |
| 21   | 1.19E-02 | 5.30E-02 | -        | -        | -        | 1.98E-01 | 6.86E-02 | -        | 6.69E-01         | -        | -        | -                | 1.00E+00 |
| 22   | 4.23E-02 | 1.25E-01 | -        | -        | -        | 6.57E-01 | -        | -        | -                | 1.76E-01 | -        | -                | 1.00E+00 |
| 23   | 2.66E-02 | 5.50E-01 | 3.80E-02 | 2.82E-01 | -        | -        | 1.04E-01 | -        | -                | -        | -        | -                | 1.00E+00 |
| 24   | 3.82E-02 | 6.89E-01 | 1.68E-01 | -        | -        | 1.05E-01 | -        | -        | -                | -        | -        | -                | 1.00E+00 |
| 25   | 3.05E-02 | 4.92E-01 | 1.35E-01 | -        | -        | 3.43E-01 | -        | -        | -                | -        | -        | -                | 1.00E+00 |
| 26   | 2.66E-02 | 5.56E-01 | 1.17E-01 | 2.55E-01 | -        | 4.55E-02 | -        | -        | -                | -        | -        | -                | 1.00E+00 |
| 27   | 3.53E-03 | 6.68E-02 | -        | 8.63E-01 | 6.99E-05 | 4.72E-02 | -        | -        | -                | -        | 1.97E-02 | -                | 1.00E+00 |
| 28   | 3.17E-03 | 5.84E-02 | -        | 8.88E-01 | 8.00E-05 | 3.22E-02 | 1.81E-02 | -        | -                | -        | -        | -                | 1.00E+00 |
| 29   | 3.01E-03 | 5.43E-02 | -        | 8.65E-01 | 6.59E-05 | 6.05E-02 | 1.71E-02 | -        | -                | -        | -        | -                | 1.00E+00 |
| 30   | 2.31E-03 | 3.80E-02 | 1.00E-02 | 8.64E-01 | 6.22E-05 | 5.90E-02 | -        | 2.65E-02 | -                | -        | -        | -                | 1.00E+00 |
| 31   | 9.53E-03 | 1.50E-02 | -        | -        | -        | 1.99E-01 | 5.46E-02 | -        | 7.22E-01         | -        | -        | -                | 1.00E+00 |
| 32   | 4.05E-02 | -        | -        | -        | -        | 7.91E-01 | -        | -        | -                | 1.69E-01 | -        | -                | 1.00E+00 |
| 33   | 2.39E-02 | 5.20E-01 | 2.54E-02 | 3.26E-01 | -        | -        | 1.04E-01 | -        | -                | -        | -        | -                | 1.00E+00 |
| 34   | 3.65E-02 | 6.77E-01 | 1.61E-01 | -        | -        | 1.25E-01 | -        | -        | -                | -        | -        | -                | 1.00E+00 |
| 35   | 2.79E-02 | 4.51E-01 | 1.23E-01 | -        | -        | 3.98E-01 | -        | -        | -                | -        | -        | -                | 1.00E+00 |
| 36   | 2.36E-02 | 5.21E-01 | 1.04E-01 | 3.01E-01 | -        | 5.04E-02 | -        | -        | -                | -        | -        | -                | 1.00E+00 |
| 37   | 2.87E-03 | 5.63E-02 | -        | 8.76E-01 | 6.86E-05 | 4.84E-02 | -        | -        | -                | -        | 1.60E-02 | -                | 1.00E+00 |
| 38   | 2.58E-03 | 4.90E-02 | -        | 9.00E-01 | 7.91E-05 | 3.33E-02 | 1.46E-02 | -        | -                | -        | -        | -                | 1.00E+00 |
| 39   | 2.45E-03 | 4.53E-02 | -        | 8.77E-01 | 6.47E-05 | 6.12E-02 | 1.38E-02 | -        | -                | -        | -        | -                | 1.00E+00 |
| 40   | 1.75E-03 | 2.88E-02 | 7.54E-03 | 8.31E-01 | 6.62E-05 | 5.84E-02 | -        | 7.22E-02 | -                | -        | -        | -                | 1.00E+00 |





**WSRC-TR-2003-00172, REV. 0**  
**SRT-RPP-2003-00073. REV. 0**

| Run#                  | MGOH2    | NASGEL   | CAF2     | ALOH3    | NIOH2    | NA2C2O4 | CA3PO42  | NAF | NAPHOH<br>.12H2O | CAOH2 | CACO3 | NAFPO4<br>.19H2O | sum      |
|-----------------------|----------|----------|----------|----------|----------|---------|----------|-----|------------------|-------|-------|------------------|----------|
| 149                   | 3.81E-02 | 7.95E-01 | 1.67E-01 | -        | -        | -       | -        | -   | -                | -     | -     | -                | 1.00E+00 |
| 150                   | 5.68E-03 | 1.37E-01 | 2.48E-02 | 8.32E-01 | 1.32E-04 | -       | -        | -   | -                | -     | -     | -                | 1.00E+00 |
| 151                   | 9.56E-03 | 3.36E-01 | 4.15E-02 | 6.13E-01 | 2.18E-05 | -       | -        | -   | -                | -     | -     | -                | 1.00E+00 |
| 152                   | 8.50E-05 | 4.39E-02 | 1.64E-04 | 9.56E-01 | 1.34E-04 | -       | -        | -   | -                | -     | -     | -                | 1.00E+00 |
| 153                   | 3.71E-02 | 8.00E-01 | 1.63E-01 | -        | -        | -       | -        | -   | -                | -     | -     | -                | 1.00E+00 |
| 154                   | 3.57E-02 | 8.09E-01 | 1.55E-01 | -        | -        | -       | -        | -   | -                | -     | -     | -                | 1.00E+00 |
| 155                   | 4.95E-02 | 7.32E-01 | 2.18E-01 | -        | -        | -       | -        | -   | -                | -     | -     | -                | 1.00E+00 |
| 156                   | 3.03E-02 | 7.95E-01 | -        | -        | -        | -       | 1.75E-01 | -   | -                | -     | -     | -                | 1.00E+00 |
| 157                   | 8.63E-03 | 1.84E-01 | 3.78E-02 | 7.69E-01 | 1.42E-04 | -       | -        | -   | -                | -     | -     | -                | 1.00E+00 |
| 158                   | 3.23E-02 | 7.81E-01 | -        | -        | -        | -       | 1.86E-01 | -   | -                | -     | -     | -                | 1.00E+00 |
| 159                   | 3.51E-02 | 8.11E-01 | 1.54E-01 | -        | -        | -       | -        | -   | -                | -     | -     | -                | 1.00E+00 |
| 160                   | 4.42E-02 | 7.61E-01 | 1.95E-01 | -        | -        | -       | -        | -   | -                | -     | -     | -                | 1.00E+00 |
| 161                   | 5.34E-02 | 6.91E-01 | 1.64E-01 | -        | -        | -       | 9.19E-02 | -   | -                | -     | -     | -                | 1.00E+00 |
| 162                   | 7.95E-03 | 9.57E-01 | -        | -        | -        | -       | 3.51E-02 | -   | -                | -     | -     | -                | 1.00E+00 |
| 163                   | 3.73E-02 | 7.99E-01 | 1.64E-01 | -        | -        | -       | -        | -   | -                | -     | -     | -                | 1.00E+00 |
| 164                   | 1.16E-02 | 2.57E-01 | 5.03E-02 | 6.81E-01 | 1.15E-04 | -       | -        | -   | -                | -     | -     | -                | 1.00E+00 |
| 165                   | 6.11E-03 | 2.58E-01 | -        | 7.02E-01 | 9.72E-05 | -       | 3.45E-02 | -   | -                | -     | -     | -                | 1.00E+00 |
| 166                   | 1.16E-02 | 2.90E-01 | -        | 6.32E-01 | 1.24E-04 | -       | 6.66E-02 | -   | -                | -     | -     | -                | 1.00E+00 |
| 167                   | 4.03E-02 | 7.82E-01 | 1.77E-01 | -        | -        | -       | -        | -   | -                | -     | -     | -                | 1.00E+00 |
| 168                   | 3.08E-02 | 8.34E-01 | 1.35E-01 | -        | -        | -       | -        | -   | -                | -     | -     | -                | 1.00E+00 |
| 169                   | 4.04E-02 | 7.71E-01 | 1.37E-01 | -        | -        | -       | 5.22E-02 | -   | -                | -     | -     | -                | 1.00E+00 |
| 170                   | 1.71E-02 | 3.48E-01 | -        | 5.36E-01 | 1.19E-04 | -       | 9.92E-02 | -   | -                | -     | -     | -                | 1.00E+00 |
| 171                   | 4.60E-02 | 7.03E-01 | -        | -        | -        | -       | 2.51E-01 | -   | -                | -     | -     | -                | 1.00E+00 |
| 172                   | 3.69E-02 | 7.49E-01 | -        | -        | 6.54E-05 | -       | 2.14E-01 | -   | -                | -     | -     | -                | 1.00E+00 |
| 173                   | 1.06E-01 | 4.30E-01 | 4.65E-01 | -        | -        | -       | -        | -   | -                | -     | -     | -                | 1.00E+00 |
| 174                   | 3.68E-02 | 7.51E-01 | -        | -        | -        | -       | 2.12E-01 | -   | -                | -     | -     | -                | 1.00E+00 |
| 175                   | 2.85E-02 | 6.75E-01 | -        | 1.31E-01 | 1.15E-04 | -       | 1.65E-01 | -   | -                | -     | -     | -                | 1.00E+00 |
| 176                   | 2.42E-02 | 5.26E-01 | 1.05E-01 | 3.44E-01 | 5.55E-05 | -       | -        | -   | -                | -     | -     | -                | 1.00E+00 |
| 177                   | 4.03E-02 | 7.82E-01 | 1.78E-01 | -        | 7.61E-05 | -       | -        | -   | -                | -     | -     | -                | 1.00E+00 |
| 178                   | 3.62E-02 | 8.04E-01 | 1.59E-01 | -        | 1.05E-04 | -       | -        | -   | -                | -     | -     | -                | 1.00E+00 |
| 179                   | 1.70E-02 | 9.10E-01 | 7.34E-02 | -        | -        | -       | -        | -   | -                | -     | -     | -                | 1.00E+00 |
| 180                   | 2.34E-02 | 8.75E-01 | 1.02E-01 | -        | -        | -       | -        | -   | -                | -     | -     | -                | 1.00E+00 |
| 181                   | 3.40E-02 | 8.17E-01 | 1.49E-01 | -        | -        | -       | -        | -   | -                | -     | -     | -                | 1.00E+00 |
| 182                   | 6.45E-02 | 5.62E-01 | -        | -        | -        | -       | 3.73E-01 | -   | -                | -     | -     | -                | 1.00E+00 |
| 183                   | 2.62E-02 | 8.60E-01 | 1.13E-01 | -        | -        | -       | -        | -   | -                | -     | -     | -                | 1.00E+00 |
| 184                   | 1.59E-02 | 9.15E-01 | 6.91E-02 | -        | -        | -       | -        | -   | -                | -     | -     | -                | 1.00E+00 |
| 185                   | 3.93E-02 | 7.87E-01 | 1.73E-01 | -        | 8.34E-05 | -       | -        | -   | -                | -     | -     | -                | 1.00E+00 |
| 186                   | 2.16E-02 | 8.84E-01 | 9.40E-02 | -        | -        | -       | -        | -   | -                | -     | -     | -                | 1.00E+00 |
| 187                   | 3.66E-02 | 8.02E-01 | 1.61E-01 | -        | 1.03E-04 | -       | -        | -   | -                | -     | -     | -                | 1.00E+00 |
| 188                   | 3.61E-02 | 8.05E-01 | 1.59E-01 | -        | -        | -       | -        | -   | -                | -     | -     | -                | 1.00E+00 |
| number of occurrences | 178      | 166      | 108      | 87       | 83       | 60      | 38       | 6   | 4                | 4     | 4     | 2                |          |

Mass fraction of total undissolved solids present in 1<sup>st</sup> ultra filtration slurry. The last row lists the number of simulations for which the particular solid was present. The right-hand most column is a sum of the mass fractions as a check.

**Table 18. Envelope B/D Solids**

| Run# | FEIIIOH3 | ZRO2     | NASGEL   | MGOH2    | NIOH2    | ALOH3    | SRCO3    | CAF2     | NA2C2O4  | MNOH2 | CACO3 | sum      |
|------|----------|----------|----------|----------|----------|----------|----------|----------|----------|-------|-------|----------|
| 1    | 3.97E-01 | 5.53E-02 | 9.55E-02 | 4.55E-05 | 1.49E-04 | 3.59E-01 | 5.00E-03 | 1.59E-03 | 8.65E-02 | -     | -     | 1.00E+00 |
| 2    | 2.65E-01 | 6.33E-02 | 1.07E-01 | 4.57E-05 | 1.34E-04 | 4.67E-01 | 5.73E-03 | 1.82E-03 | 8.94E-02 | -     | -     | 1.00E+00 |





**WSRC-TR-2003-00172, REV. 0**  
**SRT-RPP-2003-00073. REV. 0**

| Run#                  | FEIII OH3 | ZRO2     | NASGEL   | MGOH2    | NIOH2    | ALOH3    | SRCO3    | CAF2     | NA2C2O4  | MNOH2 | CACO3 | sum      |
|-----------------------|-----------|----------|----------|----------|----------|----------|----------|----------|----------|-------|-------|----------|
| 111                   | 4.53E-01  | 7.40E-02 | 8.00E-02 | 4.56E-05 | 1.80E-04 | 3.80E-01 | 2.48E-04 | 9.00E-05 | 1.22E-02 | -     | -     | 1.00E+00 |
| 112                   | 4.24E-01  | 5.58E-02 | 6.67E-02 | 4.54E-05 | 1.69E-04 | 3.87E-01 | 1.12E-03 | 3.64E-04 | 6.51E-02 | -     | -     | 1.00E+00 |
| 113                   | 3.29E-01  | 5.75E-02 | 7.46E-02 | 4.55E-05 | 1.57E-04 | 4.59E-01 | 1.91E-03 | 6.17E-04 | 7.79E-02 | -     | -     | 1.00E+00 |
| 114                   | 3.83E-01  | 5.78E-02 | 6.68E-02 | 4.55E-05 | 1.71E-04 | 4.32E-01 | 8.04E-04 | 2.65E-04 | 5.92E-02 | -     | -     | 1.00E+00 |
| 115                   | 3.82E-01  | 6.65E-02 | 7.04E-02 | 4.55E-05 | 1.64E-04 | 4.23E-01 | 3.23E-04 | 1.15E-04 | 5.80E-02 | -     | -     | 1.00E+00 |
| 116                   | 4.22E-01  | 7.20E-02 | 8.12E-02 | 4.55E-05 | 1.74E-04 | 3.65E-01 | 7.06E-04 | 2.33E-04 | 5.87E-02 | -     | -     | 1.00E+00 |
| number of occurrences | 116       | 116      | 116      | 116      | 116      | 107      | 92       | 89       | 70       | 14    | 3     |          |

Mass fraction of total undissolved solids present in 1<sup>st</sup> ultra filtration slurry. The last row lists the number of simulations for which the particular solid was present. The right-hand most column is a sum of the mass fractions as a check.

**Table 19. Envelope C Solids**

| Run# | MNOH2    | MGOH2    | SRCO3    | FEIII OH3 | ZRO2     | NASGEL   | ALOH3    | sum      |
|------|----------|----------|----------|-----------|----------|----------|----------|----------|
| 1    | 1.28E-02 | 6.14E-05 | 9.40E-01 | 4.73E-02  | -        | -        | -        | 1.00E+00 |
| 3    | 1.23E-02 | 6.14E-05 | 9.28E-01 | 6.01E-02  | -        | -        | -        | 1.00E+00 |
| 4    | 1.24E-02 | 6.14E-05 | 9.30E-01 | 5.79E-02  | -        | -        | -        | 1.00E+00 |
| 5    | 1.23E-02 | 5.69E-05 | 9.87E-01 | -         | 3.22E-04 | -        | -        | 1.00E+00 |
| 7    | 1.25E-02 | 5.73E-05 | 9.87E-01 | -         | 3.22E-04 | -        | -        | 1.00E+00 |
| 8    | 1.25E-02 | 5.72E-05 | 9.87E-01 | -         | 3.22E-04 | -        | -        | 1.00E+00 |
| 9    | 1.24E-02 | 6.13E-05 | 9.41E-01 | 4.61E-02  | -        | -        | -        | 1.00E+00 |
| 11   | 1.19E-02 | 6.14E-05 | 9.30E-01 | 5.85E-02  | -        | -        | -        | 1.00E+00 |
| 12   | 1.19E-02 | 6.14E-05 | 9.32E-01 | 5.64E-02  | -        | -        | -        | 1.00E+00 |
| 13   | 1.02E-02 | 5.63E-05 | 9.89E-01 | -         | 3.22E-04 | -        | -        | 1.00E+00 |
| 15   | 1.06E-02 | 5.68E-05 | 9.89E-01 | -         | 3.23E-04 | -        | -        | 1.00E+00 |
| 16   | 1.05E-02 | 5.67E-05 | 9.89E-01 | -         | 3.23E-04 | -        | -        | 1.00E+00 |
| 17   | 1.29E-02 | 6.13E-05 | 9.39E-01 | 4.82E-02  | -        | -        | -        | 1.00E+00 |
| 19   | 1.23E-02 | 6.14E-05 | 9.27E-01 | 6.09E-02  | -        | -        | -        | 1.00E+00 |
| 20   | 1.25E-02 | 6.14E-05 | 9.29E-01 | 5.88E-02  | -        | -        | -        | 1.00E+00 |
| 21   | 1.04E-02 | 5.60E-05 | 9.89E-01 | -         | 3.23E-04 | -        | -        | 1.00E+00 |
| 23   | 1.09E-02 | 5.65E-05 | 9.89E-01 | -         | 3.23E-04 | -        | -        | 1.00E+00 |
| 24   | 1.08E-02 | 5.64E-05 | 9.89E-01 | -         | 3.23E-04 | -        | -        | 1.00E+00 |
| 25   | 1.26E-02 | 6.14E-05 | 9.41E-01 | 4.65E-02  | -        | -        | -        | 1.00E+00 |
| 27   | 1.20E-02 | 6.14E-05 | 9.29E-01 | 5.93E-02  | -        | -        | -        | 1.00E+00 |
| 28   | 1.21E-02 | 6.14E-05 | 9.31E-01 | 5.71E-02  | -        | -        | -        | 1.00E+00 |
| 29   | 1.20E-02 | 5.49E-05 | 9.88E-01 | -         | 3.22E-04 | -        | -        | 1.00E+00 |
| 31   | 1.22E-02 | 5.73E-05 | 9.87E-01 | -         | 3.23E-04 | -        | -        | 1.00E+00 |
| 32   | 1.22E-02 | 5.72E-05 | 9.87E-01 | -         | 3.23E-04 | -        | -        | 1.00E+00 |
| 33   | 1.02E-02 | 6.18E-05 | 7.68E-01 | 3.73E-02  | -        | -        | 1.84E-01 | 1.00E+00 |
| 35   | 9.75E-03 | 6.18E-05 | 7.64E-01 | 4.77E-02  | -        | 1.93E-02 | 1.59E-01 | 1.00E+00 |
| 36   | 9.83E-03 | 6.18E-05 | 7.66E-01 | 4.60E-02  | -        | 1.38E-02 | 1.64E-01 | 1.00E+00 |
| 37   | 1.17E-02 | 5.70E-05 | 9.88E-01 | -         | 3.28E-04 | -        | -        | 1.00E+00 |
| 39   | 1.16E-02 | 5.76E-05 | 9.69E-01 | -         | 3.33E-04 | 1.91E-02 | -        | 1.00E+00 |
| 40   | 1.17E-02 | 5.75E-05 | 9.77E-01 | -         | 3.31E-04 | 1.08E-02 | -        | 1.00E+00 |
| 41   | 1.03E-02 | 6.19E-05 | 7.35E-01 | 3.79E-02  | -        | -        | 2.16E-01 | 1.00E+00 |
| 43   | 9.87E-03 | 6.19E-05 | 7.29E-01 | 4.81E-02  | -        | 2.06E-02 | 1.92E-01 | 1.00E+00 |
| 44   | 9.95E-03 | 6.19E-05 | 7.32E-01 | 4.65E-02  | -        | 1.51E-02 | 1.96E-01 | 1.00E+00 |
| 45   | 1.17E-02 | 5.66E-05 | 9.88E-01 | -         | 3.28E-04 | -        | -        | 1.00E+00 |
| 47   | 1.18E-02 | 5.74E-05 | 9.67E-01 | -         | 3.34E-04 | 2.11E-02 | -        | 1.00E+00 |
| 48   | 1.18E-02 | 5.72E-05 | 9.75E-01 | -         | 3.31E-04 | 1.27E-02 | -        | 1.00E+00 |
| 49   | 1.41E-02 | 6.04E-05 | 9.77E-01 | 8.67E-03  | -        | -        | -        | 1.00E+00 |
| 50   | 1.43E-02 | 5.96E-05 | 9.86E-01 | -         | 8.51E-05 | -        | -        | 1.00E+00 |
| 51   | 1.28E-02 | 5.77E-05 | 9.87E-01 | -         | 2.77E-04 | -        | -        | 1.00E+00 |

**WSRC-TR-2003-00172, REV. 0**  
**SRT-RPP-2003-00073. REV. 0**

| Run# | MNOH2    | MGOH2    | SRCO3    | FEIIIOH3 | ZRO2     | NASGEL   | ALOH3 | sum      |
|------|----------|----------|----------|----------|----------|----------|-------|----------|
| 52   | 1.28E-02 | 5.83E-05 | 9.87E-01 | -        | 2.43E-04 | -        | -     | 1.00E+00 |
| 53   | 1.30E-02 | 6.13E-05 | 9.36E-01 | 5.07E-02 | -        | -        | -     | 1.00E+00 |
| 54   | 1.42E-02 | 6.10E-05 | 9.51E-01 | 3.52E-02 | -        | -        | -     | 1.00E+00 |
| 55   | 1.23E-02 | 5.77E-05 | 9.87E-01 | -        | 2.85E-04 | -        | -     | 1.00E+00 |
| 56   | 1.48E-02 | 6.02E-05 | 9.85E-01 | -        | -        | -        | -     | 1.00E+00 |
| 57   | 1.42E-02 | 6.08E-05 | 9.63E-01 | 2.23E-02 | -        | -        | -     | 1.00E+00 |
| 58   | 1.27E-02 | 5.74E-05 | 9.87E-01 | -        | 3.02E-04 | -        | -     | 1.00E+00 |
| 59   | 1.28E-02 | 6.13E-05 | 9.39E-01 | 4.85E-02 | -        | -        | -     | 1.00E+00 |
| 60   | 1.23E-02 | 5.80E-05 | 9.87E-01 | -        | 2.57E-04 | -        | -     | 1.00E+00 |
| 61   | 1.38E-02 | 6.11E-05 | 9.47E-01 | 3.96E-02 | -        | -        | -     | 1.00E+00 |
| 62   | 1.51E-02 | 6.09E-05 | 9.64E-01 | 2.09E-02 | -        | -        | -     | 1.00E+00 |
| 63   | 1.43E-02 | 6.01E-05 | 9.86E-01 | -        | -        | -        | -     | 1.00E+00 |
| 64   | 1.34E-02 | 6.12E-05 | 9.35E-01 | 5.11E-02 | -        | -        | -     | 1.00E+00 |
| 65   | 1.40E-02 | 6.11E-05 | 9.54E-01 | 3.20E-02 | -        | -        | -     | 1.00E+00 |
| 66   | 1.41E-02 | 6.10E-05 | 9.51E-01 | 3.48E-02 | -        | -        | -     | 1.00E+00 |
| 67   | 1.35E-02 | 5.90E-05 | 9.86E-01 | -        | 1.97E-04 | -        | -     | 1.00E+00 |
| 68   | 1.26E-02 | 5.80E-05 | 9.87E-01 | -        | 2.69E-04 | -        | -     | 1.00E+00 |
| 69   | 1.46E-02 | 6.05E-05 | 9.75E-01 | 1.01E-02 | -        | -        | -     | 1.00E+00 |
| 70   | 1.47E-02 | 5.99E-05 | 9.85E-01 | -        | -        | -        | -     | 1.00E+00 |
| 71   | 1.43E-02 | 6.06E-05 | 9.67E-01 | 1.89E-02 | -        | -        | -     | 1.00E+00 |
| 72   | 1.25E-02 | 5.81E-05 | 9.87E-01 | -        | 2.53E-04 | -        | -     | 1.00E+00 |
| 73   | 1.29E-02 | 5.83E-05 | 9.87E-01 | -        | 2.48E-04 | -        | -     | 1.00E+00 |
| 74   | 1.20E-02 | 5.74E-05 | 9.88E-01 | -        | 2.99E-04 | -        | -     | 1.00E+00 |
| 75   | 1.20E-02 | 5.71E-05 | 9.88E-01 | -        | 3.19E-04 | -        | -     | 1.00E+00 |
| 76   | 1.41E-02 | 6.05E-05 | 9.70E-01 | 1.59E-02 | -        | -        | -     | 1.00E+00 |
| 77   | 1.41E-02 | 5.99E-05 | 9.86E-01 | -        | 4.25E-05 | -        | -     | 1.00E+00 |
| 78   | 1.19E-02 | 5.74E-05 | 9.88E-01 | -        | 2.89E-04 | -        | -     | 1.00E+00 |
| 79   | 1.42E-02 | 6.05E-05 | 9.76E-01 | 9.84E-03 | -        | -        | -     | 1.00E+00 |
| 80   | 1.42E-02 | 5.94E-05 | 9.86E-01 | -        | 1.16E-04 | -        | -     | 1.00E+00 |
| 81   | 1.39E-02 | 6.08E-05 | 9.56E-01 | 2.97E-02 | -        | -        | -     | 1.00E+00 |
| 82   | 1.47E-02 | 6.03E-05 | 9.85E-01 | -        | -        | -        | -     | 1.00E+00 |
| 83   | 1.40E-02 | 6.11E-05 | 9.53E-01 | 3.32E-02 | -        | -        | -     | 1.00E+00 |
| 84   | 1.22E-02 | 5.71E-05 | 9.87E-01 | -        | 3.16E-04 | -        | -     | 1.00E+00 |
| 85   | 1.41E-02 | 6.09E-05 | 9.54E-01 | 3.15E-02 | -        | -        | -     | 1.00E+00 |
| 86   | 1.35E-02 | 5.87E-05 | 9.86E-01 | -        | 2.14E-04 | -        | -     | 1.00E+00 |
| 87   | 1.28E-02 | 5.85E-05 | 9.87E-01 | -        | 2.31E-04 | -        | -     | 1.00E+00 |
| 88   | 1.35E-02 | 5.91E-05 | 9.86E-01 | -        | 1.62E-04 | -        | -     | 1.00E+00 |
| 89   | 1.31E-02 | 6.11E-05 | 9.41E-01 | 4.55E-02 | -        | -        | -     | 1.00E+00 |
| 90   | 1.12E-02 | 5.66E-05 | 9.88E-01 | -        | 3.22E-04 | -        | -     | 1.00E+00 |
| 91   | 1.41E-02 | 6.07E-05 | 9.67E-01 | 1.91E-02 | -        | -        | -     | 1.00E+00 |
| 92   | 1.47E-02 | 6.03E-05 | 9.85E-01 | -        | -        | -        | -     | 1.00E+00 |
| 93   | 1.44E-02 | 6.02E-05 | 9.86E-01 | -        | -        | -        | -     | 1.00E+00 |
| 94   | 1.43E-02 | 6.03E-05 | 9.86E-01 | -        | -        | -        | -     | 1.00E+00 |
| 95   | 1.21E-02 | 5.75E-05 | 9.88E-01 | -        | 2.92E-04 | -        | -     | 1.00E+00 |
| 96   | 1.38E-02 | 6.10E-05 | 9.46E-01 | 3.99E-02 | -        | -        | -     | 1.00E+00 |
| 97   | 1.23E-02 | 5.82E-05 | 9.87E-01 | -        | 2.62E-04 | -        | -     | 1.00E+00 |
| 98   | 1.40E-02 | 6.09E-05 | 9.54E-01 | 3.20E-02 | -        | -        | -     | 1.00E+00 |
| 99   | 1.42E-02 | 6.08E-05 | 9.62E-01 | 2.40E-02 | -        | -        | -     | 1.00E+00 |
| 100  | 1.40E-02 | 6.11E-05 | 9.51E-01 | 3.52E-02 | -        | -        | -     | 1.00E+00 |
| 101  | 1.37E-02 | 6.11E-05 | 9.44E-01 | 4.22E-02 | -        | -        | -     | 1.00E+00 |
| 102  | 1.24E-02 | 6.14E-05 | 9.28E-01 | 5.53E-02 | -        | 4.18E-03 | -     | 1.00E+00 |
| 103  | 1.36E-02 | 5.90E-05 | 9.86E-01 | -        | 2.04E-04 | -        | -     | 1.00E+00 |
| 104  | 1.43E-02 | 5.99E-05 | 9.86E-01 | -        | -        | -        | -     | 1.00E+00 |
| 105  | 1.15E-02 | 5.71E-05 | 9.88E-01 | -        | 3.14E-04 | -        | -     | 1.00E+00 |

**WSRC-TR-2003-00172, REV. 0**  
**SRT-RPP-2003-00073. REV. 0**

| Run#                  | MNOH2    | MGOH2    | SRCO3    | FEIIIOH3 | ZRO2     | NASGEL   | ALOH3    | sum      |
|-----------------------|----------|----------|----------|----------|----------|----------|----------|----------|
| 106                   | 1.47E-02 | 6.04E-05 | 9.85E-01 | -        | -        | -        | -        | 1.00E+00 |
| 107                   | 1.35E-02 | 6.12E-05 | 9.40E-01 | 4.61E-02 | -        | -        | -        | 1.00E+00 |
| 108                   | 1.36E-02 | 6.10E-05 | 9.41E-01 | 3.92E-02 | -        | 5.76E-03 | -        | 1.00E+00 |
| 109                   | 1.49E-02 | 6.07E-05 | 9.73E-01 | 1.25E-02 | -        | -        | -        | 1.00E+00 |
| 110                   | 1.25E-02 | 6.14E-05 | 9.25E-01 | 5.52E-02 | -        | 7.23E-03 | -        | 1.00E+00 |
| 111                   | 1.29E-02 | 6.13E-05 | 9.35E-01 | 5.09E-02 | -        | 8.34E-04 | -        | 1.00E+00 |
| 112                   | 1.41E-02 | 6.00E-05 | 9.86E-01 | -        | -        | -        | -        | 1.00E+00 |
| 113                   | 1.35E-02 | 5.91E-05 | 9.86E-01 | -        | 1.54E-04 | -        | -        | 1.00E+00 |
| 114                   | 1.37E-02 | 6.12E-05 | 9.43E-01 | 4.28E-02 | -        | -        | -        | 1.00E+00 |
| 115                   | 1.27E-02 | 5.85E-05 | 9.87E-01 | -        | 2.41E-04 | -        | -        | 1.00E+00 |
| 116                   | 1.42E-02 | 6.07E-05 | 9.68E-01 | 1.74E-02 | -        | -        | -        | 1.00E+00 |
| 117                   | 1.37E-02 | 5.99E-05 | 9.75E-01 | -        | 7.35E-06 | 1.16E-02 | -        | 1.00E+00 |
| 118                   | 1.41E-02 | 6.10E-05 | 9.51E-01 | 3.50E-02 | -        | -        | -        | 1.00E+00 |
| 119                   | 1.15E-02 | 5.72E-05 | 9.88E-01 | -        | 3.09E-04 | -        | -        | 1.00E+00 |
| 120                   | 1.33E-02 | 5.97E-05 | 9.70E-01 | -        | 1.41E-04 | 1.61E-02 | -        | 1.00E+00 |
| 121                   | 1.21E-02 | 6.14E-05 | 9.03E-01 | 4.86E-02 | -        | 4.84E-03 | 3.11E-02 | 1.00E+00 |
| 122                   | 1.13E-02 | 5.74E-05 | 9.88E-01 | -        | 3.00E-04 | -        | -        | 1.00E+00 |
| 123                   | 1.42E-02 | 6.05E-05 | 9.72E-01 | 4.21E-03 | -        | 9.79E-03 | -        | 1.00E+00 |
| 124                   | 1.26E-02 | 5.78E-05 | 9.87E-01 | -        | 2.86E-04 | -        | -        | 1.00E+00 |
| 125                   | 1.25E-02 | 6.14E-05 | 9.09E-01 | 4.41E-02 | -        | 2.48E-03 | 3.14E-02 | 1.00E+00 |
| 126                   | 1.34E-02 | 5.96E-05 | 9.86E-01 | -        | 4.94E-05 | -        | -        | 1.00E+00 |
| 127                   | 1.33E-02 | 5.91E-05 | 9.86E-01 | -        | 1.75E-04 | -        | -        | 1.00E+00 |
| number of occurrences | 115      | 115      | 115      | 54       | 51       | 17       | 8        |          |

Mass fraction of total undissolved solids present in 1<sup>st</sup> ultra-filtration slurry. The last row lists the number of simulations for which the particular solid was present. The right-hand most column is a sum of the mass fractions as a check.

## APPENDIX D. OLI PREDICTION OF HEAT CAPACITY FOR SIMPLE NAOH-H<sub>2</sub>O AND NANO<sub>3</sub>-H<sub>2</sub>O SYSTEMS

OLI/ESP prediction of Cp was consistently below the value measured experimentally of simulants. Simulations of simple binary systems were run and compared with data published in the “International Critical Tables”<sup>[34]</sup>, Vol. 5, pp 115 and 125. These results indicate the OLI/ESP under-predicts the Cp by 2-4% for a 5M Na solution.

**Figure 25. OLI/ESP Prediction of Cp Compared to Published Values for NaNO<sub>3</sub>-H<sub>2</sub>O System at 20°C and Various Concentrations**

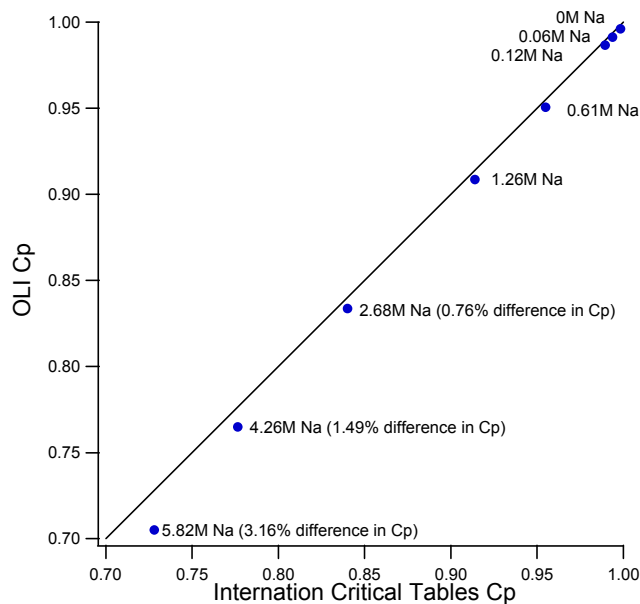
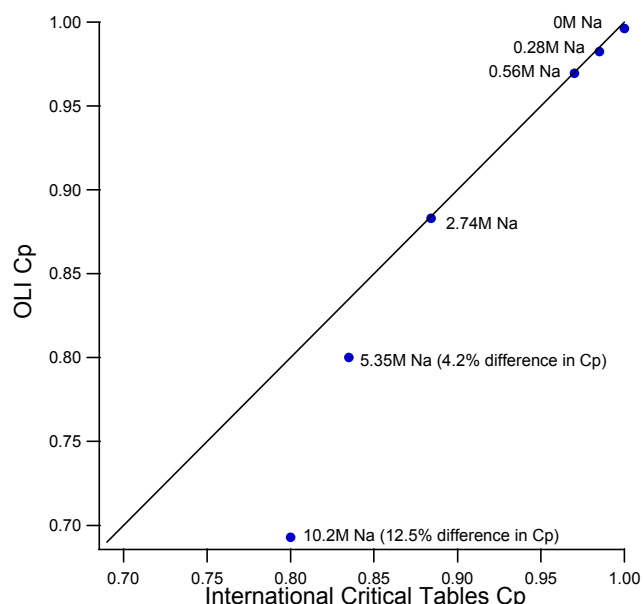


**Figure 26. OLI/ESP Prediction of Cp Compared to Published Values for NaOH-H<sub>2</sub>O System at 20°C and Various Concentrations**



## APPENDIX E. RESULTS OF TRIAL SIMULATIONS FOR WHICH THE NUMBER OF WASH STAGES WAS VARIED

The RPP pre-treatment flow-sheet calls for the concentrated slurry to be washed in 22 stages (for each wash step) with 0.01M NaOH. Simulating this many stages would take a tremendous amount of time with little comparative gain in the accuracy of the simulations. A series of trial simulations were run in which the number of wash stages was varied (1, 3, 5, 8, 10, 12, 15, 18, 20, and 22). The plots below show the results of selected streams as a function of the number of wash stages. The left axis of all the plots is the percent difference of the stream property at the given number of stages (x-axis) and the full 22 stages. Based on these trial simulations, 5 wash stages were used in simulation flow-sheet to approximate the 22 stages of the actual process.

**Figure 27. UF1 Slurry**

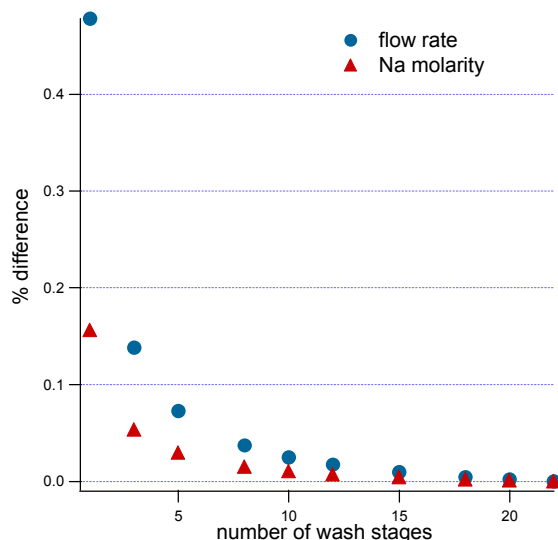


**Figure 28. UF Recycle**

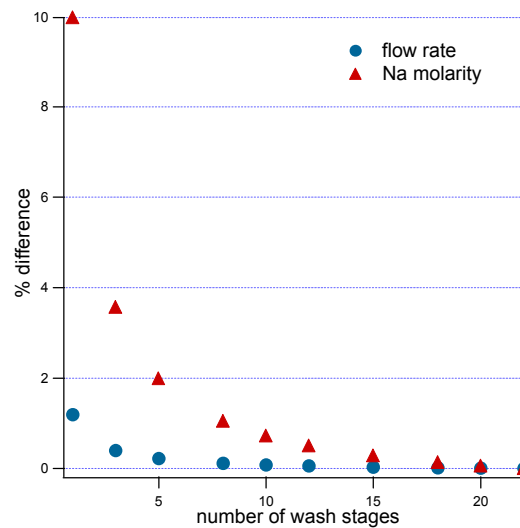


**Figure 29. UF2 Slurry**

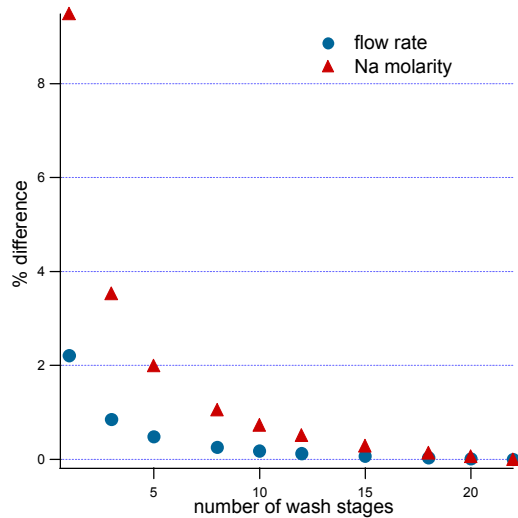


**Figure 30. Slurry to HLW**

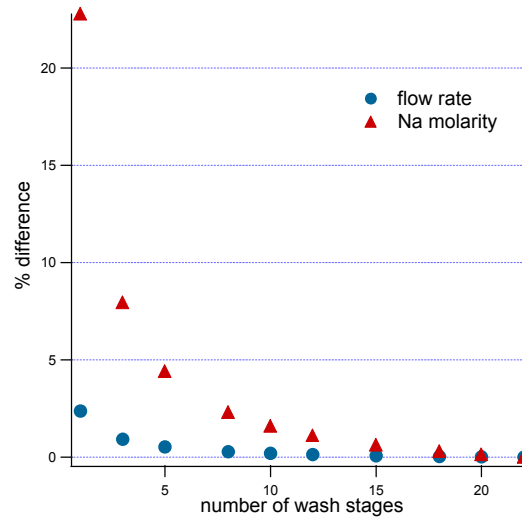


**Figure 31. Evaporator Overhead**

